Assessment of a Regenerative Therapy Strategy for Chondral Defects in Articular Cartilage

by

Andrew Carroll

A thesis submitted to the Department of Chemical Engineering

in conformity with the requirements for

the degree of Master of Applied Science

Queen's University

Kingston, Ontario, Canada
August, 2015

Abstract

Osteoarthritis is one of the leading causes of disability in adults over the age of 40 years, and there is currently no curative measure for the disease. As a result, there is a critical need for a strategy that can promote cartilage regeneration. Of particular interest is an injectable, *in situ* gelling hydrogel for cell encapsulation that can be delivered with low cytotoxicity to native chondrocytes and encapsulated cells. Adipose-derived stem cells are an attractive cell population for delivery because they secrete a wide array of soluble factors and they have the ability to differentiate down the chondrogenic lineage.

Chemotaxis of passage 0 and passage 2 bovine chondrocytes toward bovine ASCs was measured using a modified Boyden chamber assay. Passage 0 chondrocyte migration was less than 3% of seeded cells for all conditions investigated with no significant differences between groups. Passage 2 chondrocytes exhibited significantly higher migration than P0 chondrocytes, but migration towards bASCs was actually lower than media controls. PDGF-BB and IGF-I promoted chemotaxis of passage 2 chondrocytes at 5 ng/mL and up to 100 ng/mL.

Acrylate-poly(trimethylene carbonate)-*block*-poly(ethylene glycol)-*block*-poly(trimethylene carbonate)-acrylate (A-PTMC-PEG-PTMC-A) tri-block copolymers were synthesized from 3.4 and 20 kg/mol PEG-diol initiators. Methacrylate chondroitin sulphate (MCS) modified with collagen integrin peptides RGD, GLOGEN, and GVOGEA was blended with A-PTMC-PEG-PTMC-A to form hydrogels for ASC encapsulation. Conjugation of peptides onto MCS resulted in higher ASC viability in A-PTMC-PEG-PTMC-A/MCS hydrogels as assessed by LIVE/DEAD stain. The 20k/MCS hydrogels exhibited higher equilibrium water content, ultimate strain, and toughness, but lower equilibrium moduli than MCS and

3.4k/MCS hydrogels. In addition, 3.4k/MCS hydrogels were tougher than MCS hydrogels but had a comparable equilibrium modulus.

The present work showed that ASCs do not encourage chemotaxis of bovine chondrocytes in 2-D culture. This finding provides early evidence that ASCs may be unsuitable for promoting chondrocyte migration in a cartilage defect model. The viability and mechanical measurements demonstrate that A-PTMC-PEG-PTMC-A/MCS hydrogels modified with integrin peptides can maintain ASC viability following encapsulation. However, further experiments are necessary to assess the suitability of peptide-modified A-PTMC-PEG-PTMC-A/MCS hydrogels as a viable cartilage regeneration strategy.

Acknowledgments

First, I would like to thank my supervisors Dr. Lauren Flynn and Dr. Brian Amsden for their limitless guidance, support, and patience throughout this project. Their knowledge and experience were critical in guiding my research and overcoming obstacles along the way. It has been a privilege to work for and learn from them during my time as their student, and I am very grateful for the experience. I would also like to thank Drs. Lauren Flynn, Evelyn Morin, Brian Amsden, and Tim Bryant for their invaluable teaching and instruction during my graduate studies. The material covered in their courses was a huge benefit to my understanding of my research topic and the greater biomedical engineering field. In addition, I would like to thank the Amsden and Flynn lab groups for their support and friendship throughout my project. In particular, Dr. Dale Marecak, Stuart Young, Valerio Russo, Claire Yu, Bryen Turco, Cody Brown, Lydia Fütterer, James Hayami, Moira Vyner, Julian Chesterman, Dr. Fei Chen, Bowen Yang, and Ming Gong were always available to help with my research or simply to talk.

A special thank you to all my friends during my time at Queen's University, both within the lab and outside. And another special thank you to my parents and sisters for their unwavering encouragement and motivation. Their support and understanding gave me the confidence and enthusiasm to pursue graduate research and I will always be grateful.

Table of Contents

List of Figures

List of Tables

Common Abbreviations

AC	Acryloyl chloride
(M)ACI-(P)	(matrix)Autologous chondrocyte implantation (periosteal)
APS	ammonium persulfate
(b)ASC	(bovine)Adipose-derived stem cell
bFGF	Basic fibroblast growth factor
BMP	Bone morphogenetic protein
BSA	Bovine serum albumin
DCM	Dichloromethane
DMAP	4-Dimethylaminopyridine
DOS	Degree of substitution
ECM	Extracellular matrix
EDC	1-Ethyl-3-(3-dimethylaminopropyl)carbodiimide
EDTA	Ethylenediaminetetraacetic acid
EGF	Epidermal growth factor
FBS	Fetal bovine serum
GAG	Glycosaminoglycans
GMA	Glycidyl methacrylate
HEPES	4-(2-hydroxyethyl)-1-piperazineethanesulfonic acid
HGF	Hepatocyte growth factor
IGF-I	Insulin-like growth factor
MCS	Methacrylated chondroitin sulphate
MES	2-(N-morpholino)ethanesulfonic acid
MMP	Matrix metalloproteinase
MSC	Mesenchymal stem cell
MTT	3-(4,5-dimethylthiazol-2-yl)-2,5-diphenyltetrazolium bromide
MWCO	Molecular weight cut-off
NHS	N-Hydroxysuccinimide
OA	Osteoarthritis
P0, P2	Passage 0, 2
PDGF	Platelet-derived growth factor
PEG	Poly(ethylene glycol)
PGA	Poly(glycolic acid)
PLA	Poly(lactic acid)
PTMC	Poly(trimethylene carbonate)
PVA	Poly(vinyl alcohol)
SZP	Superficial zone protein
TCPS	Tissue culture polystyrene
TEA	Triethylamine
TEMED	N,N,N',N'-tetramethylethylenediamine
TGF-β	Transforming growth factor-β
TMC	Trimethylene carbonate
TNF-α	Tumor necrosis factor-α

Chapter 1

Introduction

Osteoarthritis (OA) is a degenerative joint disease that results in the loss of articular cartilage from the interface of diarthrodial joints. The Global Burden of Disease 2010 study found that knee and hip osteoarthritis ranked as the 11th highest contributor to global disability out of 291 conditions (Cross et al. 2014). Osteoarthritis is also the leading cause of disability in adults in the United States and is estimated to have a total annual healthcare cost of $185.5 billion, based on data from 2005 (Kotlarz et al. 2009). Furthermore, the number of people suffering from OA in the United States is projected to grow from 27 million in 2009 to 67 million by 2030 with increasingly obese and elderly populations (Murphy & Helmick 2012; Bitton 2009). The increase in prevalence highlights the need for an affordable, long-term treatment option for those suffering from OA.

Articular cartilage has a very limited capacity for self-repair due to its avascular nature. Current treatment options, such as microfracture and autologous chondrocyte implantation (ACI), provide short-term relief from pain but result in inferior repair tissue. Defects are typically filled with fibrocartilage that fails after several years and total joint replacements are the inevitable course for most patients (Oussedik et al. 2015). As a result, significant interest has been placed in tissue engineering approaches to cartilage regeneration. The combination of stem cells, chondrocytes, and polymer scaffolds may provide a cheaper and more effective means of regenerating articular cartilage than current surgical interventions.

Adipose-derived stem cells have potential for cartilage tissue engineering due to their chondrogenic differentiation capacity and paracrine effects *in vivo* (Bosnakovski et al. 2006; Perdisa et al. 2015). An *in-situ* forming hydrogel for delivery of ASCs to cartilage lesions holds promise as a cartilage regeneration strategy (Figure 1.1). However, promoting stable chondrogenesis of ASCs *in situ* can be challenging due to the complex biological environment. Co-cultures of ASCs and articular chondrocytes have demonstrated a chondroinductive effect of chondrocytes on ASCs (Zhao et al. 2013). For this reason, promoting chondrocyte migration into the hydrogel from the periphery of the lesion may encourage the chondrogenic differentiation of encapsulated ASCs. Therefore, migration of chondrocytes into the defect site could promote cartilage regeneration through tissue remodeling by native chondrocytes and differentiated ASCs. The migration of chondrocytes may be promoted by soluble factors secreted by ASCs, some of which have been individually confirmed as chondrocyte chemoattractants (Skalnikova et al. 2011; Morales 2007). Chemotaxis of articular chondrocytes towards ASCs was investigated in the present study to determine the effects of secreted factors on chondrocyte migration.

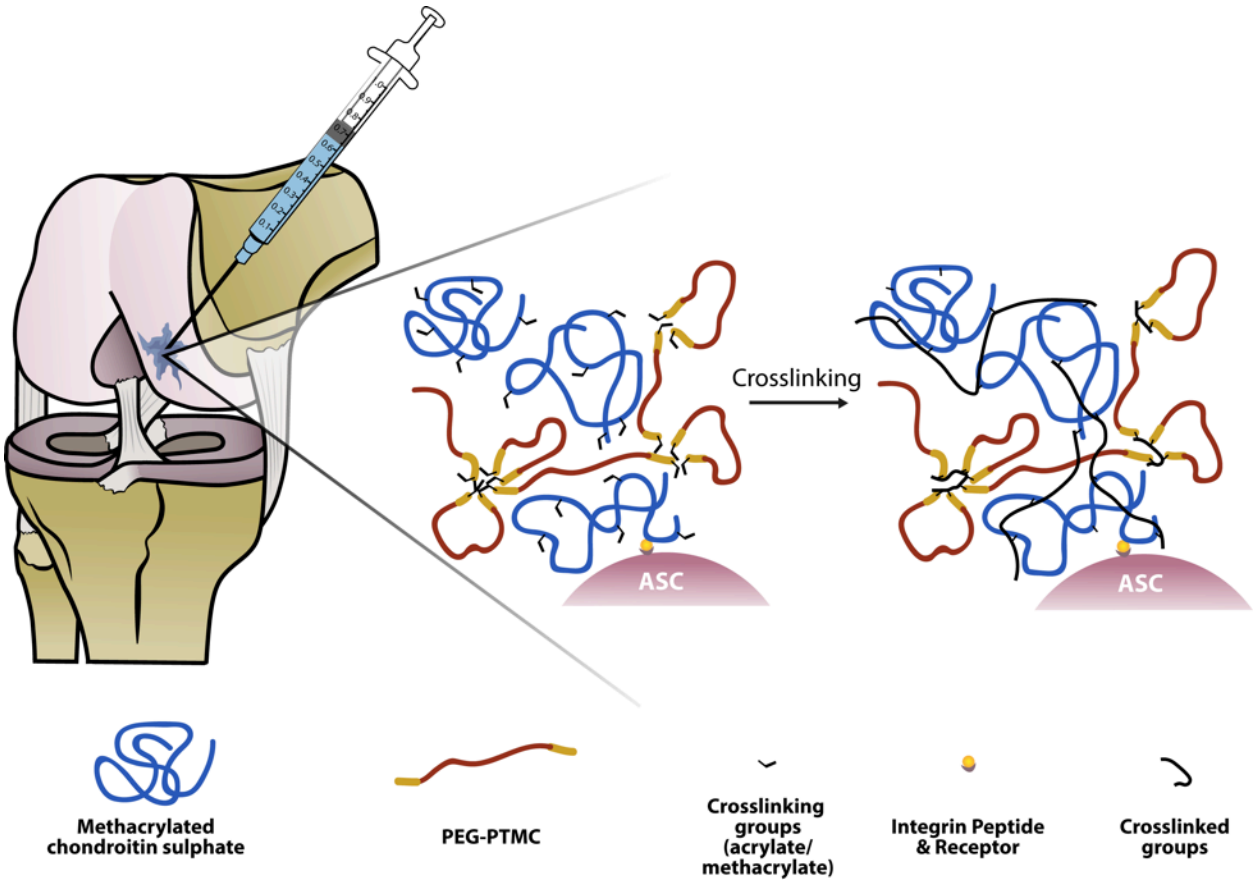

Figure 1.1: Adipose-derived stem cell delivery approach for cartilage regeneration.

Chondroitin sulphate is a natural component of articular cartilage and has a chondroinductive effect on ASCs and chondrocytes (Varghese et al. 2008). These properties make it an attractive basis for a cell delivery vehicle for cartilage tissue engineering. However, chondroitin sulphate is highly negatively charged and swells considerably after crosslinking. To address this challenge in the present work, a copolymer of poly(ethylene glycol) (PEG) and poly(trimethylene carbonate) (PTMC) was incorporated in the hydrogel to control swelling and improve mechanical properties with the long-term goal of facilitating integration with the native cartilage (Sims et al. 1996). The hydrophobic PTMC block was chosen to reduce swelling of the hydrogel and provide elasticity through the coiling and uncoiling of hydrophobic domains. Enzymatic degradation of the PTMC domain

also helps facilitate the *in vivo* degradation necessary to accommodate matrix secretion, cell infiltration and constructive tissue remodeling (Zhu et al. 1991). The PEG domain increases the water solubility of the polymer to facilitate cell encapsulation and results in a more homogeneous hydrogel. As a further refinement of the tissue-specific delivery vehicle, it was postulated that the incorporation of the integrin binding peptides GLOGEN and GVOGEA, derived from collagen III and II respectively, onto chondroitin sulphate may help to support ASC viability and chondrogenic differentiation following encapsulation. These peptides may also promote chondrocyte interaction with the hydrogel matrix to encourage migration.

Initial polymer studies in the present work were conducted with methacrylate-PEG-PTMC-acrylate (MA-PEG-PTMC-A) di-block copolymers. The relatively low molecular weight (<2,000 g/mol) copolymers were used to provide hydrogels with a high compressive modulus. However, cytotoxicity and encapsulation experiments showed significant cell death with the MA-PEG-PTMC-A copolymers in solution and following crosslinking. To address this problem, higher molecular weight (>5,000 g/mol) A-PTMC-*block*-PEG-*block*-PTMC-A tri-block copolymers were made and mixed with methacrylated chondroitin sulphate (MCS) to form two-component hydrogels.

1.1 Project Hypotheses:

Chondrocyte chemotaxis towards ASCs and ASC encapsulation in MCS/PEG-PTMC hydrogels were investigated to determine the efficacy of the cartilage regeneration strategy outlined in Figure 1.1. The two hypotheses investigated in the present work are as follows:

1. Soluble factors secreted by ASCs can promote the migration of chondrocytes.

2. A hydrogel prepared from methacrylated chondroitin sulphate (MCS) bearing integrin binding sites derived from collagen and crosslinked with (meth)acrylated PEG-PTMC block copolymers will support encapsulated ASC viability and will have mechanical properties matching that of the native articular cartilage.

1.2 Specific Aims:

1. Measure the migration of bovine articular chondrocytes towards bovine ASCs in a modified Boyden chamber assay.
2. Prepare and assess (meth)acrylated PEG-PTMC copolymers that can be blended with methacrylated chondroitin sulphate to form injectable, *in situ* gelling hydrogels for encapsulation of ASCs. The hydrogels need a low degree of swelling, a toughness similar to articular cartilage, and ASC viability greater than 80% following crosslinking.

Chapter 2

Literature Review

2.1 Cartilage Structure and Function

Hyaline articular cartilage is one of three types of cartilage in the human body, in addition to fibrocartilage and elastic cartilage (Stockwell 1979). Articular cartilage is found covering the articulating surface of the long bones in synovial joints. The unique structure and composition of the tissue allows for low-friction articulation and the distribution of joint contact forces over a larger area (Buckwalter & Mankin 1997; Mow et al. 1992). This protective layer of cartilage is separated from the underlying bone by an impermeable tidemark, so nutrients and oxygen reach the tissue through diffusion from the synovial fluid at the articulating surface (Harty 1978). Therefore, the thickness of the tissue is important in determining nutrient diffusion and oxygen tension at various depths. The thickness of articular cartilage varies depending on the joint, location within the joint, and between species, but generally ranges between 1 – 5 mm in humans (Athanasiou et al. 1991). The resident cells are termed chondrocytes, and are responsible for production and maintenance of the extracellular matrix (ECM) (Mankin et al. 1994). The tissue itself is composed of a solid phase, including collagen and proteoglycans, and a liquid phase of water and electrolytes (Cohen et al. 1998). The interaction of the liquid phase with the solid ECM phase gives cartilage its compressive strength and wear properties.

2.1.1 Extracellular Matrix

2.1.1.1 Overview

The solid matrix of articular cartilage is composed of collagen, proteoglycans, and various glycoproteins. The proportions of these extracellular molecules vary with distance from the articular surface, but collagens, proteoglycans, and water account for 10-30%, 3-10%, and 60-85% of cartilage wet weight respectively. Collagen II accounts for 90-95% of collagens in the matrix, although collagens III, VI, IX, X, and XI are also found to a smaller degree (Eyre et al. 2006; Buckwalter et al. 2005; Cohen et al. 1998). Proteoglycans are composed of a core protein with bound glycosaminoglycan (GAG) chains, which are formed by repeating disaccharides. Chondroitin sulphate, keratan sulphate, and dermatan sulphate are the GAGs present in articular cartilage, and the repeating sulphate and carboxylic acid groups result in proteoglycans being highly negatively charged. These proteoglycans take the form of either large aggregating proteoglycans, large non-aggregating proteoglycans, or smaller non-aggregating proteoglycans such as biglycan, fibromodulin, and decorin (Roughley & Lee 1994; Anderson 1962; Poole et al. 1996). The large aggregates are formed by spontaneous assembly of core protein, keratin sulphate, and chondroitin sulphate to form aggrecan. Subsequent association of aggrecan with link protein and hyaluronic acid results in aggregates as large as 10 μm, which become trapped in the dense collagen network (Figure 1.2) (Buckwalter & Rosenberg 1983; Pottenger et al. 1982).

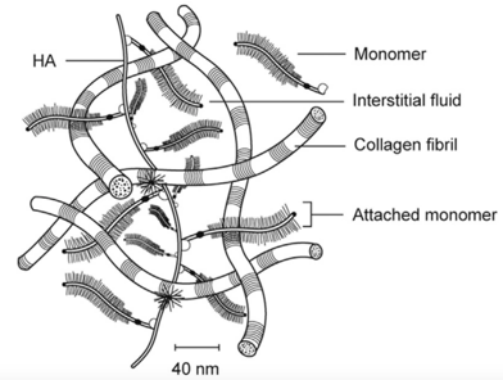

Figure 1.2: Collagen II fibrils entrap the hyaluronic acid (HA) and aggrecan (monomer) proteoglycans. Reprinted with permission from Brody, 2014.

The entrapped negatively charged proteoglycans create a very high fixed charge density that attracts cations, resulting in a Donnan effect. The water content of articular cartilage is 60-85% of the wet weight as a result of water influx from Donnan osmotic pressure (Gu et al. 1993). The crosslinked collagen network resists swelling of the proteoglycan aggregates, and puts the collagen fibrils under tension. Movement of water through the dense ECM during loading results in significant drag and gives cartilage its characteristic poroviscoelastic behaviour (Setton et al. 1993). This effect is compounded at higher loads due to the compression of the matrix and pores, which increases the drag force of fluid flow.

2.1.1.2 Zonal Architecture

The exact proportion and organization of collagens and proteoglycans in articular cartilage varies from the articulating surface to the underlying bone, creating four distinct zones. The specific zones, starting from the articular surface, are the superficial, middle, deep, and calcified zones (Figure 1.3). Chondrocyte morphology and metabolism also vary between zones, and matrix production in each zone is specific to its respective structure (Buckwalter & Mankin 1997; Buckwalter et al. 2005; Mow et al. 1992).

The superficial zone comprises the top 10-20% of the cartilage thickness and contains a dense mesh of collagen fibres aligned parallel to the articulating surface (Clark 1985; Poole et al. 1984). The structure of the superficial zone plays an important role in cartilage biomechanics by decreasing tissue permeability and possibly preventing loss of extracellular molecules (Setton et al. 1993; Buckwalter & Mankin 1997). Chondrocytes have a slightly flattened morphology and produce superficial zone protein (SZP, or lubricin) (Swann et al. 1981; Schumacher et al. 1994). The proteoglycan content of the superficial zone is the lowest of the four zones and instead has the highest collagen content.

Collagen content decreases slightly in the middle zone and the parallel fibrils of the superficial zone become thicker fibres with a more random orientation. These fibres form arches near the boundary with the superficial zone and help to anchor the superficial zone to the deep zone (Becerra et al. 2010). The chondrocytes in the middle zone become more spheroid and have larger endoplasmic reticulum and Golgi bodies for increased ECM synthesis (Buckwalter & Mankin 1997).

Chondrocytes in the deep zone are stacked into columns, perpendicular to the articulating surface. Synthetic activity of chondrocytes in the deep zone is much higher than those found in the superficial zone (Wong et al. 1996). The collagen synthesized by chondrocytes is arranged into large-diameter fibres aligned perpendicular to the articular surface and tidemark (Mow et al. 1992). The tidemark itself is the boundary between calcified and uncalcified cartilage (Buckwalter & Mankin 1997).

The calcified zone continues from the tidemark to the sub-chondral bone, and delineates the transition from articular cartilage to bone. Chondrocytes have very low synthetic activity and can be entirely surrounded by calcified cartilage (Temenoff & Mikos

2000). Collagen fibres from the deep zone are anchored in the calcified cartilage to integrate the articular cartilage with the underlying bone (Mow et al. 1992). In addition to collagen II, collagen X is also present in the calcified zone and is associated with chondrocyte hypertrophy and matrix mineralization. Chondrocyte hypertrophy is the terminal differentiation of chondrocytes during endochondral ossification and results in chondrocyte apoptosis, vascular invasion, and bone formation (Hidaka & Goldring 2008).

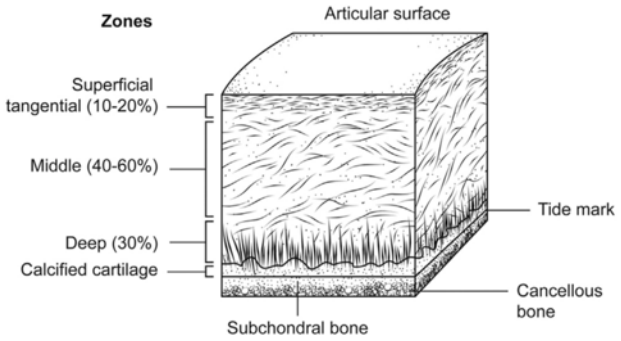

Figure 1.3: The collagen fibrils are oriented differently in each of the four zones of articular cartilage with fibrils parallel to the surface in the superficial zone and gradually transitioning to perpendicular in the deep zone. Reprinted with permission from Brody, 2014.

2.1.1.3 Chondrons and Radial Architecture

The cartilage ECM composition and organization also varies radially from the chondrocyte membrane out into the surrounding matrix. The pericellular region consists of the matrix molecules immediately surrounding chondrocytes, which together with the chondrocytes form the functional units of cartilage known as chondrons (Poole 1997). The territorial region is short transition between the pericellular region and the surrounding inter-territorial region. The pericellular and territorial regions are responsible for cell-matrix interactions and protect chondrocytes during deformation. Guilak *et al.* have demonstrated that the presence of the pericellular matrix can significantly alter the stress and strain on chondrocytes within tissue, and this effect appears to vary with cartilage zone

(Guilak et al. 1995; Guilak & Mow 2000). The much larger inter-territorial region contains the largest fraction of ECM in which the zonal architecture of articular cartilage is evident and is responsible for the mechanical properties of the tissue (Buckwalter et al. 2005).

Link protein, laminin, fibronectin, and collagen VI are concentrated in the pericellular environment (Chang et al. 1997). Fibronectin and collagen VI are thought to have a role in molecular assembly of the pericellular matrix and cell interactions through integrin receptors. Collagen IX is also found preferentially in the pericellular matrix where it is hypothesized to stabilize the small collagen II fibrils that form the pericellular capsule (Poole 1997). The pericellular environment is rich in aggrecan, keratan sulphate, hyaluronic acid, and link protein, which indicate a role in proteoglycan assembly.

The territorial region contains a higher proportion of collagen fibrils that form a basket around and bind the pericellular matrix (Buckwalter et al. 2005). The fibrillar network likely plays a role in protecting chondrocytes from mechanical loading. The territorial region transitions into thicker collagen fibrils and fibres with the characteristic macromolecular structure of articular cartilage as it transitions into the inter-territorial region (Buckwalter & Mankin 1997).

2.1.2 Chondrocytes

Chondrocytes were originally thought to be the only resident cell population of articular cartilage, although there has been recent evidence of a chondroprogenitor cell in the superficial zone (Hattori et al. 2007; Jiang & Tuan 2014). Chondrocytes account for 1-10% of the tissue volume depending on species and developmental stage (Cohen et al. 1998). Chondrocytes are solely responsible for ECM production and a careful balance of catabolic and anabolic activities maintain the tissue structure. Chondrocytes have

significant metabolic activity and prominent endoplasmic reticulum and Golgi bodies to meet matrix production demands (Kuettner et al. 1982). However, the low cellularity of articular cartilage results in low tissue metabolism and turnover (Buckwalter et al. 2005). Cilia have also been reported to extend from the chondrocyte plasma membrane into the ECM and allow mechanical sensing (Kouri et al. 1996). The ability of chondrocytes to respond to mechanical and chemical stimuli decreases with age (Buckwalter et al. 2005).

2.1.2.1 Chondrocyte Migration

The migratory capacity of chondrocytes is of particular interest in the repair of articular cartilage. The ability of cells to migrate towards the periphery of a cartilage defect and into any tissue-engineered construct may be necessary for effective tissue remodeling and integration. Cell adhesion to the ECM is necessary for migration, so the interaction between matrix molecules and cell receptors is of utmost importance. Freshly isolated chondrocytes express integrin subunits α_2, α_3, α_5, α_6, α_v, and β_1 and also express high levels of the hyaluronic acid adhesion molecule CD44 (Diaz-Romero et al. 2005; Hidaka et al. 2006; Dürr et al. 1993). Both the $\alpha_1\beta_1$ and $\alpha_2\beta_1$ integrins can serve as binding receptors for collagens II and VI, while the $\alpha_v\beta_1$ integrin is commonly associated with adhesion to fibronectin (Loeser et al. 2000).

The chemotactic and haptotactic response of chondrocytes to various soluble factors *in vitro* has been investigated through the use of Boyden chamber assays. These factors include bone morphogenetic protein-2 (BMP) (Frenkel et al. 1996), insulin-like growth factor-I (IGF-I) (Fujita et al. 2004), transforming growth factor-β (TGF-β) (Chang et al. 2003), platelet derived growth factors (PDGF-AA, AB, and BB) (Mishima & Lotz 2008), and basic fibroblast growth factor (bFGF) (Hidaka et al. 2006; Maniwa et al. 2001). Collagen

I, collagen II, and fibronectin were also shown to be haptotactic for articular chondrocytes (Shimizu et al. 1997).

Perhaps more importantly, migration of chondrocytes within 3-D scaffolds has also been confirmed (Frenkel et al. 1996; Gosiewska et al. 2001). The pore sizes of scaffolds are often much larger than those found in articular cartilage, where they are typically 2.5-6.5 nm in diameter (Balakrishnan & Banerjee 2011). Migration through the dense ECM is a far more complex process that likely requires matrix degradation or amoeboid migration (Morales 2007). Lyman *et al.* provided evidence of chondrocyte death around the periphery of a cartilage defect followed by a gradual repopulation with culture time. This effect was most prominent in the middle zone where fibrils are aligned towards the defect site, and may provide a guide for cell migration (Lyman et al. 2000). There was also evidence of cell polarization and extensions that are characteristic of a migratory phenotype. Studies involving disruption and enzymatic digestion of cartilage have also demonstrated the outgrowth of chondrocytes (Lyman et al. 2000; Qiu et al. 2000). Specifically, Qiu *et al.* noted a decrease in chondrocyte outgrowth time from 30 days to 3 days following 15 min of collagenase digestion.

2.1.3 Mechanical Properties

The mechanical properties of articular cartilage stem from the crosslinked network of collagen fibrils and the negatively charged proteoglycans trapped within it. Early experimental models attempted to describe cartilage as a single-phase material, but the significant contribution of fluid flow eventually led to biphasic models (Buckwalter et al. 2005). Most of the water within cartilage is free to flow through the tissue, but the dense matrix acts as a barrier to fluid flow. The low permeability allows cartilage to support large

stresses over short times, but still reduces the contact stresses with prolonged exposure to load. The equilibrium compressive modulus of articular cartilage is generally 0.5-1 MPa, but the tensile strength of the collagen network results in a tensile modulus of 10-50 MPa (Buckwalter et al. 2005; Athanasiou et al. 1991). The compressive modulus increases with increasing proteoglycan and collagen content, and decreases with increasing water content (Mow et al. 1984; Mow et al. 1992; Williamson et al. 2001).

2.2 Cartilage Surgical Repair Strategies

Articular cartilage regeneration remains a challenge due to its avascular, aneural nature and its limited capacity for self-repair. Lesions in the tissue can cause discomfort, joint pain, locking, and often lead to osteoarthritis of the joint (Buckwalter & Mankin 1997; Hunziker 2002). This is likely due to the relative catabolic and anabolic activities of chondrocytes following tissue damage (Poole 1995). The slow ECM turnover in cartilage means that only small, partial-thickness defects are capable of gradual repair. Tissue maturity may also have a significant impact on cartilage repair, as younger, skeletally immature individuals have shown a greater capacity for repair (Schüettler et al. 2013; Nevo et al. 1990; Newman 1998). However, larger defects fail to show signs of healing and lesions often grow until surgical interventions are required. To date, these surgical interventions include cartilage lavage, resurfacing techniques, joint re-alignment, abrasion technique, and cell-based strategies.

2.2.1 Resurfacing Techniques

Lavage and resurfacing techniques are meant to provide temporary pain relief to the patient. Lavage consists of rinsing the joint with salt solutions, and has very little biological

rationale for its effectiveness in providing pain relief. In agreement with this, some investigators have shown that lavage had no significant effect on patients' symptoms (Strachan et al. 1992). However, Livesley *et al.* reported evidence of pain relief in subjects undergoing lavage and physiotherapy as compared to those treated with physiotherapy alone (Livesley et al. 1991). Resurfacing techniques are intended to remove fibrillated matrix around the damaged area and represent a more empirical approach to create a smoother joint surface (Hunziker 2002). Shaving and debridement are the two resurfacing techniques used clinically. Shaving involves the dissection of damaged or fibrillated cartilage surrounding the lesion, but is usually limited to treatment of patellar cartilage damage. Clinical studies showed no significant improvement in pain symptoms except in groups that suffered an acute injury (Ogilvie-Harris & Jackson 1984). Studies in rabbits showed further degeneration of articular cartilage after shaving, likely due to chondrocyte death surrounding the excision site (Hunziker & Quinn 2003; McGregor et al. 2011). Debridement is a more extensive procedure that combines shaving, lavage, and partial meniscectomy. However, pain relief from the procedure varies and, as with shaving, is generally temporary (Hunziker 2002).

2.2.2 Joint Alignment and Osteotomy

Joint realignment aims to move the load-bearing area of articular cartilage to an undamaged site and is typically performed in misaligned joints. Realignment is achieved by osteotomy and often results in extended pain relief for the patient, although the procedure is usually coupled with techniques that penetrate the subchondral bone (Akizuki et al. 1997). Osteotomy alone would be expected to result in overloading of the tissue, and is therefore combined with other approaches to regenerate the damaged cartilage. These

combinations have resulted in success rates between 70-85%, although the procedures are usually reserved for deformed joints (Oussedik et al. 2015; Hunziker 2002).

2.2.3 Formation of Full-thickness Defects

Procedures that intentionally disrupt the tidemark and expose the subchondral bone include abrasion chondroplasty, Pridie drilling, and microfracture. Abrasion chondroplasty exposes large areas of bone, while Pridie drilling and microfracture involve drilling small holes to better preserve the structure of the underlying bone. Microfracture is a refinement of Pridie drilling and creates holes 0.5-1 mm in diameter at regular distances and depths as compared to the 2-2.5 mm holes made during Pridie drilling (Insall 1967; Steadman et al. 1999). These techniques allow for a spontaneous healing response through bleeding and subsequent clot formation. Mesenchymal stem cells (MSCs) are postulated to migrate from the bone into the clot and begin to remodel the tissue, but this often leads to the formation of fibrocartilage with a high proportion of collagen I (Shapiro et al. 1993; Furukawa et al. 1980). Fibrocartilage does not have the mechanical properties necessary to withstand the compressive and shear forces within diarthrodial joints and usually fails after several years (Hunziker 2002). However, animal studies have shown that microfracture technique is capable of yielding a more hyaline-like cartilage, which may be attributed to smaller changes in biomechanics due to smaller diameter holes (Hunziker 2002; Gill et al. 2005). Clinical studies with humans have also shown a decrease in pain and increase in functional movement after 5 years following microfracture surgery (Solheim et al. 2010; Steadman et al. 2003). Microfracture and Pridie drilling can alleviate pain and even produce hyaline or hyaline-like cartilage, but results vary and the procedure sometimes needs to be repeated.

2.2.4 Cell-based Approaches

The two most commonly cited cell-based approaches to cartilage repair are autologous chondrocyte implantation (ACI) and mosaic arthroplasty (Ahmed & Hincke 2010; Hunziker 2002). ACI is performed by taking a biopsy of the patient's cartilage and expanding the chondrocytes *in vitro* before injecting them into the damaged site under either a periosteal flap (ACI-P) or a collagen matrix (ACI-C or MACI). The periosteum contains progenitor cells with chondrogenic potential that can aid in cartilage repair (Nakahara et al. 1991). In one study, hyaline cartilage formation was reported in 11 of 15 patients 2 years after undergoing ACI-P surgery as assessed by biopsy and histological staining (Brittberg et al. 1994). However, another study has shown that ACI-P has a higher rate of chondrocyte hypertrophy and matrix mineralization as compared to ACI-C (Gooding et al. 2006). In place of transplanting suspensions of culture-expanded cells, mosaic arthroplasty uses small osteochondral grafts from non-load bearing areas of cartilage and reinserts them at the site of damage to restore joint congruency. Grafts are typically autologous although allogenic sources have been used, and the donor site typically heals with fibrocartilage (Ahmed & Hincke 2010). One study of over 1,000 patients demonstrated good to excellent results in 92% of patients with femoral condylar implants, and mosaicplasty had better clinical outcomes than abrasion chondroplastly, Pridie drilling, and microfracture surgery (Hangody et al. 2008).

Current surgical interventions, such as microfracture, mosaicplasty, and ACI can alleviate pain and restore functional movement for up to 5 years (Ebert et al. 2011; Oussedik et al. 2015). Oussedik *et al.* recommended either an osteotomy, microfracture, or ACI-C depending on the joint alignment and lesion size (Oussedik et al. 2015). However,

repair cartilage usually fails and joint arthroplasty remains the ultimate outcome for most OA patients.

2.3 Tissue Engineering Strategies

The lack of long-term success with surgical repair strategies has led to the investigation of polymer scaffolds, chondrocytes, and progenitor cells for tissue engineering approaches. Cell source and polymer selection are two important factors in cartilage tissue engineering, and biocompatibility, biodegradability, mechanical properties, and integration are key design considerations (Balakrishnan & Banerjee 2011; Kock et al. 2012).

2.3.1 Cell Source

Cell source is one of the first considerations when designing a tissue-engineered cartilage construct. Chondrocytes are the obvious choice since they are capable of producing all of the ECM components necessary to repair and regenerate articular cartilage. Despite the appeal of chondrocytes, biopsy is required, which results in donor site morbidity. Further, chondrocytes have been shown to dedifferentiate in a more fibroblast-like phenotype, with increased collagen I production, following monolayer expansion (Darling & Athanasiou 2005). Chondrocytes from older patients and those suffering from OA also exhibit a less differentiated phenotype and lower anabolic metabolism than those from young, healthy patients (Dehne et al. 2009; Hidaka et al. 2006; Pestka et al. 2011).

Stem cells are another promising cell source due to their differentiation potential, trophic effects, and lower potential for donor site morbidity as compared to cartilage. A

comparison of chondrocytes and MSCs from immature and mature horses showed that MSCs from mature tissue actually produced more collagen II and proteoglycans than adult chondrocytes (Kopesky et al. 2010). Contrary to this finding, several studies have shown that constructs seeded with chondrocytes have better mechanical properties due to increased collagen II and proteoglycan production (Vinardell et al. 2010; Erickson et al. 2009). Both bone marrow-derived mesenchymal stem cells and adipose-derived mesenchymal stem cells have been investigated for their chondrogenic potential. Although bone marrow MSCs (BMSCs) have shown greater expression of chondrogenic genes (Sox9) and ECM molecules (collagen II and aggrecan), ASCs from and adipose tissue are far more abundant than their BMSC counterparts (Im et al. 2005; Kisiday et al. 2008; Koga et al. 2008; Zuk et al. 2002). Chondrogenesis of BMSCs and ASCs is enhanced in the presence of TGF-β, which results in increased ECM production (Kisiday et al. 2008). Overall, BMSCs and ASCs are promising cell sources for cartilage tissue engineering due to their relative abundance and chondrogenic differentiation potential.

2.3.2 Adipose-derived Stem Cells

Adipose-derived stem cells are a source of multi-potent adult stem cells found within adipose tissue (Zuk et al. 2002). They are capable of self-renewal and have the ability to differentiate into osteoblasts, adipocytes, chondrocytes, and myocytes (Morizono et al. 2003). ASCs have been extensively investigated for cartilage tissue engineering along with bone marrow and synovium-derived mesenchymal stem cells (Mazor et al. 2014; van Osch et al. 2009). The procedure for isolation of bone marrow-derived MSCs is considered painful and results in donor-site morbidity and increased risk of infection (Khan et al. 2010). In contrast, ASCs from lipoaspirates can be harvested with limited pain, lower

donor-site morbidity, and in much higher numbers (Dragoo et al. 2003). ASCs also have a higher proliferation rate than BMSCs and can better maintain their phenotype with passaging (Strioga et al. 2012; Zuk et al. 2002). Although several groups have shown lower chondrogenic potential in ASCs as compared to BMSCs, an emerging hypothesis attributes the repair of articular cartilage to the trophic activity of ASCs instead of their capacity for chondrogenic differentiation (Koga et al. 2008; Li et al. 2011; Ude et al. 2014; Ruetze & Richter 2014).

2.3.2.1 Trophic Factors

Although ASCs are capable of differentiation into various cell types, an emerging theory is that much of their clinical function *in vivo* may be due to trophic activity and secreted factors. These secreted factors can have anti-apoptotic, angiogenic, anti-fibrotic, immunomodulatory, chemotactic, or growth and differentiation effects of the surrounding cells and tissue (da Silva Meirelles et al. 2009; Ruetze & Richter 2014). Of these, anti-apoptotic, immunomodulatory, chemotactic, and differentiation effects may be of particular importance in cartilage tissue engineering. Factors secreted by ASCs include hepatocyte growth factor (HGF), IGF-I, TGF-β, and bFGF (Chen et al. 2005; Kilroy et al. 2007; Rehman et al. 2004; Tögel et al. 2007). Many of these factors have been shown to be important in promoting and maintaining a differentiated chondrocyte phenotype and IGF-I and bFGF are also chemoattractants for cultured and freshly isolated chondrocytes (Chang et al. 2003; Hidaka et al. 2006; Maniwa et al. 2001). Exposure of ASCs to bFGF, endothelial growth factor (EGF), tumor necrosis factor-α (TNF-α), hypoxia, and apoptotic cells results in a change in their secretory profile that includes increased production of the anti-apoptotic stanniocalcin-1 (Wang et al. 2006; Lee et al. 2010; Rehman et al. 2004; Block et al. 2009).

The secretory profile and its changes during ASC differentiation and exposure to various conditions could have a dramatic impact on chondrocytes in co-culture (Chiellini et al. 2008). As an example, Wu *et al.* and Tsuchiya *et al.* have demonstrated that the trophic activity of MSCs on articular chondrocytes results in increased cartilage ECM production in co-culture models. The secretome of ASCs can have significant benefits in cartilage tissue engineering, and may be more important than their chondrogenic differentiation alone.

2.3.3 Hydrogel Scaffolds

Hydrogels are crosslinked hydrophilic networks that swell in water without dissolving (Pedley et al. 1980; Hoffman 2012), and were popularized for use in biomedical applications by Lim *et al.* in 1960 (Wichterle & Lím 1960). Hydrogels are a logical choice for articular cartilage engineering, due to the high water content of articular cartilage. Hydrogels are classified as either physical gels or chemical gels. Chemical gels are covalently crosslinked, whereas the polymer chains inphysical gels are held together by intermolecular forces such as hydrogen bonding, ionic interactions, and hydrophobic interactions (Hoffman 2012). The biocompatibility of hydrogels depends on the polymer composition, crosslinking procedure, and the degradation rate and products (Spiller et al. 2011). The polymer composition may be one of the most important factors in hydrogel design, and can include natural polymers, synthetic polymers or a combination of the two.

Naturally derived polymers are an attractive source for cartilage engineering because of their potential to support beneficial cell-matrix interactions and potential enzymatic degradation by cellular enzymes. Among the natural polymers investigated to date are alginate, agarose, collagen, hyaluronic acid, chondroitin sulphate, chitosan, and self-assembling peptides (Spiller et al. 2011; Ahmed & Hincke 2010). Collagen I hydrogels have

been used to treat cartilage defects in healthy, young rabbits with relative success through encapsulation of MSCs and chondrocytes (Wakitani et al. 1994). However, the repair tissue generated was not hyaline in nature when the hydrogels were implanted in osteoarthritic knees (Wakitani et al. 2002). Adopting a more tissue-specific approach, collagen II hydrogels were shown to display a greater chondrogenic effect on encapsulated MSCs than collagen I gels in terms of ECM synthesis (Bosnakovski et al. 2006; Lu et al. 2010). Similarly, hyaluronic acid and chondroitin sulphate GAGs have been extensively investigated for cartilage engineering as they are naturally found in articular cartilage (Muzzarelli et al. 2012). These polymers are typically modified with methacrylate groups for crosslinking through radical polymerization (Nettles et al. 2004; Wang et al. 2007). Hyaluronic acid and chondroitin sulphate are degraded by cell-secreted hyaluronidase and chondroitinase, respectively, which allows for natural matrix turnover. Incorporating either molecule into composite PEG hydrogels containing MSCs or chondrocytes increased chondrogenesis and cartilage ECM synthesis as compared to PEG controls (Chung & Burdick 2009; Varghese et al. 2008; Chen et al. 2011). One shortcoming is that methacrylated chondroitin sulphate hydrogels are brittle on their own and require a second component to add elasticity and toughness (Hayami et al. 2015). In spite of this, the chondroinductive properties of these naturally derived polymers make them appealing for cartilage tissue engineering.

Synthetic polymers lack the innate bioactivity of natural polymers, but they can provide better control over the mechanical properties through customization of molecular weight and composition. Poly(vinyl alcohol) (PVA), poly(lactic acid) (PLA), poly(glycolic acid) (PGA), and PEG have all been investigated for cartilage engineering (Spiller et al. 2011; Ahmed & Hincke 2010). PLA and PGA are hydrophobic, semi-crystalline, linear

polyesters that maintain the rounded chondrocyte phenotype and accumulate proteoglycans and collagen II in chondrocyte-seeded scaffolds (Zwingmann et al. 2007; Lu et al. 2005; Seung et al. 2008; Shin et al. 2006). Unfortunately, the acidic degradation products of PGA and PLA sometimes result in an inflammatory response *in vivo* and are cytotoxic to chondrocytes (Sittinger et al. 1996; Böstman & Pihlajamäki 2000; Hsu et al. 2006). In contrast, PEG has very limited degradation *in vivo* due to the hydrolytically stable ether linkages and has minimal interaction with proteins and other macromolecules (Sims et al. 1996). Elisseeff *et al.* were the first to use photosensitive PEG macromers, in the form of PEG-dimethacrylate, for cartilage tissue engineering (Elisseeff et al. 1999). This approach allowed for the preparation of a prepolymer solution with suspended cells that could be injected into the defect site and crosslinked *in situ* with minimally invasive techniques. Another benefit of methacrylate-functionalized PEG-based hydrogels is the relative ease with which hydrogel mechanical properties can be tailored by varying the molecular weight, concentration, and functionalization of macromers (Temenoff et al. 2002; Bryant, Chowdhury, et al. 2004; Bryant, Bender, et al. 2004). Bryant *et al.* have shown that PEG hydrogels formed with high crosslinking densities and moduli decrease encapsulated chondrocyte proliferation and matrix production (Bryant, Chowdhury, et al. 2004; Bryant, Anseth, et al. 2004). PEG macromers have also been modified with degradable blocks of PLA and PTMC to increase the biodegradation of the hydrogels (Bryant, Bender, et al. 2004; Bryant et al. 2003; Zhang et al. 2011). PTMC is a rubber-like polymer often used in soft tissue engineering that undergoes enzymatic degradation *in vivo* (Zhang et al. 2006; Zhu et al. 1991). Unlike PLA and PGA, the degradation products of PTMC are not acidic, which makes it a more appealing option for tissue engineering purposes (Albertsson & Eklund

1995). Incorporation of these degradable blocks into PEG hydrogels increases the synthetic activity of encapsulated chondrocytes (Bryant & Anseth 2002).

The degradation of engineered scaffolds is clearly an important consideration for differentiation of cells and effective tissue remodeling. In theory, scaffolds that gradually degrade can slowly transfer the mechanical load to neo-cartilage formed by the encapsulated cells and can even result in a more homogeneous distribution of ECM components (Bryant & Anseth 2002). Bhaney *et al.* incorporated a matrix metalloproteinase-7 (MMP-7)-sensitive peptide into PEG hydrogels and achieved a more homogeneous distribution of ECM components. More importantly, the MMP-sensitive hydrogels had a higher dynamic modulus than their non-degradable PEG counterparts, despite lower overall ECM accumulation (Bahney et al. 2011). Other PEG-based hydrogels have been modified with hydrolytically degradable blocks and MMP-sensitive peptides to achieve similar results in terms of matrix distribution (Park et al. 2004; Bryant & Anseth 2003).

The hydrogel crosslink density or molecular weight between crosslinks will also affect ECM distribution throughout the scaffold. A lower crosslink density will allow greater hydrogel swelling and result in a higher equilibrium water content than a tightly crosslinked gel. Several groups have shown that more loosely crosslinked hydrogels allow diffusion of ECM molecules away from the cell, which in turn results in greater ECM synthesis (Bryant, Chowdhury, et al. 2004; Park et al. 2009; Söntjens et al. 2006; Liu et al. 2010). The pore size of scaffolds may also be an important consideration for similar reasons. Two groups showed that larger pore sizes in gelatin and PGA scaffolds resulted in greater ECM production by seeded chondrocytes (Lien et al. 2009; Griffon et al. 2006).

These results indicate that carefully tuned polymer degradation, swelling properties, and crosslinking density can yield mechanically robust repair tissue from a tissue-engineered construct.

2.3.4 Crosslinking Method

Physical or chemical crosslinks are necessary to prevent the dissolution of hydrogel polymer networks. Using an *in-situ* gelling system for cell delivery can limit the crosslinking strategies available. As an example, gluteralehyde crosslinking of hydroxyl containing polymers requires low pH, temperatures as high as 80 °C, and methanol (Peppas & Benner 1980; Dai & Barbari 1999). These conditions are cytotoxic and would likely cause significant damage to the surrounding tissue. In contrast, radical polymerization of vinyl groups by exposure to a chemical initiator or UV light and a photoinitiator produces a gel under mild conditions (Hennink & van Nostrum 2012). Hydroxyethylmethacrylate, methacrylic acid, and N-isopropylacrylamide are vinyl monomers that have been used to form hydrogels, commonly with PEG-diacrylate as a crosslinker (Wichterle & Lím 1960; Bettini et al. 1995; Tuncel & Cicek 1998). Hydrophilic polymers such as chondroitin sulphate, hyaluronic acid, chitosan, dextran, and PEG can also be modified with vinyl groups by reaction with (meth)acryloyl chloride, methacrylic anhydride, or glycidyl methacrylate (Huang et al. 1997; Marsano et al. 2000; Kim & Chu 2000; Wang et al. 2003; Hayami et al. 2015; Salinas & Anseth 2008a). These polymers can be crosslinked with the ammonium persulfate/N,N,N',N'-tetramethylethylenediamine (APS/TEMED) radical initiator system, which produces free radicals at body temperature without the use of a UV probe (Gotoh et al. 1998). Despite the convenience, Mironi-Harpaz *et al.* reported less than 20% cell viability after encapsulation with APS/TEMED and Duan *et al.* reported a negative

cooperative effect on viability of using the two components together (Mironi-Harpaz et al. 2012; Duan 2005). However, Temenoff *et al.* and Park *et al.* have used the initiator system for cell encapsulation without issue (Temenoff et al. 2004; Park et al. 2009). Overall, the radical polymerization of vinyl groups is an ideal strategy for *in-situ* gelation and cell encapsulation.

2.3.5 Mimetic Peptide Conjugation

The biological response of stem cells and chondrocytes to hydrogels can be modified through the use of mimetic peptides. These modifications can take the form of enzymatically degradable linkages, cell adhesion peptides, or conjugated growth factors (Zhu 2010). Often, the biologically active component of the full protein is attributable to a much smaller sequence or mimetic peptide (Heino 2007; Nomizu et al. 1995; Luzak et al. 2003; Hamaia et al. 2012). These shorter peptides are less susceptible to denaturation or proteolytic degradation than the full proteins (Massia & Hubbell 1992). Peptides investigated for cartilage tissue engineering include the cell adhesion peptides RGD and GFOGER (Liu et al. 2010; Reyes & García 2003; Hwang et al. 2006), and the enzyme-sensitive peptides GCRDGPQGIWGQDRCG, PENFF (MMP-13 sensitive), PLELRA (MMP-7), and VPLSLTMG (MMP-7) (Salinas & Anseth 2008a; Park et al. 2004; Bahney et al. 2011). The presence of integrin peptides increases collagen II and proteoglycan production, while incorporation of MMP-sensitive peptides result in a more homogenous distribution of matrix components. A tissue-specific approach incorporating the GLOGEN and GVOGEA integrin peptides may also enhance chondrogenesis due to their presence in collagens III and II, respectively (Hamaia et al. 2012). These collagens are found in articular cartilage and the integrin-binding motifs have a high affinity for the α1β1 expressed by articular

chondrocytes (Loeser et al. 2000; Shakibaei et al. 2008). Together with an appropriate hydrogel composition, the right combination of mimetic peptides could lead to neo-cartilage formation following delivery and encapsulation.

Chapter 3

Materials and Methods

3.1.1 Materials

Kreb's Ringer Buffer, collagenase type VIII (C2139), 4-(2-hydroxyethyl)-1-piperazineethanesulfonic acid (HEPES), glucose, bovine serum albumin (BSA), ethylenediaminetetraacetic acid (EDTA), Dulbecco's Modified Eagle Medium:Ham's F12 (DMEM:F12), protease (P5147), 2-hydroxy-4-(2-hydroxyethoxy)-2-methylpropiophenone (Irgacure I2959), gelatin (G9391), collagen II (9301), paraformaldehyde, and PEG-methacrylate (MA-PEG, Mn = 500 g/mol), triethylamine (TEA), acryloyl chloride (AC), and glycidyl methacrylate (GMA), APS, and TEMED were purchased from Sigma-Aldrich Canada Co. (Oakville, Ontario). Fetal bovine serum (FBS), penicillin-streptomycin (pen-strep), 0.25% trypsin/EDTA, LIVE/DEAD stain, and 3-(4,5-dimethylthiazol-2-yl)-2,5-diphenyltetrazolium bromide (MTT reagent) were purchase from Life Technologies Inc. (Burlington, Ontario). Collagenase type II was purchased from Worthington Biochemical Corporation (Lakewood, New Jersey), GUAVA viacount reagent from Millipore Ltd. (Etobicoke, Ontario), PDGF-BB and IGF-I from Peprotech (Quebec, Canada). Chondroitin sulphate (Mn ≈ 50,000 g/mol, ≥ 90% purity) was purchased from LKT Laboratories Inc. (St. Paul, Minnesota), 12- and 24-well transwell inserts were purchased from Greiner Bio-One (Monroe, North Carolina), DAPI mounting medium was purchased from abcam (Cambridge, Massachusetts). 1-ethyl-3-(3-dimethylaminopropyl)carbodiimide (EDC) and sulfo-N-hydroxysulfosuccinimide (sulfo-NHS) were purchased from Acros Organics (New Jersey). GGGGGRGDS (661 g/mol), GLOGEN (600 g/mol), and GVOGEA (543 g/mol) were purchased from CAN Peptide (Montreal, Québec). (4-[3-(4-iodophenyl)-2-(4-nitrophenyl)-2H-5-

tetrazolio]-1,3-benzene disulfonate) (WST-1) was purchased from Roche (Mississauga, Ontario). 2-(N-morpholino)ethanesulfonic acid (MES) buffer, D_2O, DMSO-d_6, and organic solvents were purchased from Fisher Chemical (Ottawa, Ontario).

3.1.2 Bovine Adipose-Derived Stem Cell Isolation and Culture

Adipose tissue was harvested from the inter-digital fat pad of 12-18 month old calf hooves donated by Quinn's Meats abbatoir in Yarker, Ontario. Zhao *et al.* described the protocol for bovine ASC (bASC) isolation (Zhao et al. 2012), which was adapted from a protocol for human ASC isolation (Flynn et al. 2007). The adipose tissue was minced and digested in Kreb's Ringer Buffer solution containing 2mg/mL type VIII collagenase, 25 mM HEPES, 3 mM glucose, and 2% BSA. Digestion was performed in a shaker incubator at 120 rpm and 37°C for 1 h. The digestion solution was then filtered through a 250 μm stainless steel mesh to remove undigested tissue. Floating adipocytes were removed by aspiration and the remaining digest was centrifuged at 1200xg for 5 min. The cell pellet was suspended in erythrocyte lysing buffer (0.154 M NH4Cl, 10 mM KHCO3, and 0.1 mM EDTA) and gently agitated for 10 min. Remaining tissue fragments were removed by passing the solution through a 100 μm nylon filter. Cells were washed twice with growth medium (1:1 mixture of DMEM:F12 supplemented with 10% FBS, 100 U/mL penicillin, and 0.1 mg/mL streptomycin) and centrifuged at 1200xg for 5 min between washes. Cell pellets were resuspended in growth medium and plated in 75 cm^2 flasks (Corning) and cultured at 37 °C with 5% CO_2. Cells were rinsed with PBS at 24 h after plating and growth medium was replaced every 2-3 days until 90% confluent. Cells were then trypsin-released (0.25% trypsin/EDTA) and centrifuged at 1200xg for 5 min. Cells required for immediate use in culture studies were resuspended in growth medium and plated in fresh T-75 flasks.

Additional samples were frozen to establish a cell bank by resuspending the cells at $1x10^6$ cells/mL in freezing medium (80% FBS, 10% DMEM:F12, and 10% dimethyl sulfoxide (DMSO)) and freezing in cryovials using an isopropanol bath at -80 °C for 24 h. Cryovials were then transferred to a liquid nitrogen tank for long-term cell storage. Passage 2 (P2) cells were used for all experiments. Previously-frozen bASCs were used for all cell-based experiments unless otherwise stated.

3.1.3 Bovine Chondrocyte Isolation and Culture

Bovine articular chondrocytes (bACs) were isolated from the metacarpophalangeal joint of 12-18 month old calf legs donated by Quinn's Meats abbattoir in Yarker, Ontario. Cow legs were decontaminated by soaking in a 10% bleach solution for 1 h, followed by 1 h in a 70% ethanol solution. Following the protocol described by Roos *et al.*, cartilage slices were excised from the surface of the metacarpophalangeal joint and placed in 15 mL of DMEM:F12 medium with 500 µL of pen-strep during collection (Boyle et al. 1995). The cartilage slices were then incubated at 37 °C with 5% CO_2 in a 0.5% w/v solution of protease in DMEM:F12 for 2 h. The cartilage slices were then washed with DMEM:F12 and incubated for 16 h in a 0.15% w/v solution of collagenase type II in DMEM:F12 at 37 °C with 5% CO_2. The digest solution was passed through a 100 µm nylon filter to remove cartilage fragments. Chondrocytes were washed twice with growth medium (same as bASC growth medium) and counted with GUAVA viacount reagent and a Guava easyCyte 8HT flow cytometer (Millipore, 0500-4008, Etobicoke, Ontario). Chondrocytes intended for use at P0 were used immediately after counting, and chondrocytes intended for monolayer culture were resuspended in growth medium and plated at $1x10^6$ cells per T-75 flask. All

cultured chondrocytes were incubated at 37 °C with 5% CO_2 and were used at P2 for experiments.

3.2 Chondrocyte Migration

3.2.1 Boyden Chamber Migration Assay

Five migration experiments were performed to measure the chemotactic capacity of P0 and P2 chondrocytes. FBS, BSA, IGF-I, PDGF-BB, and bASCs were added to the wells of modified Boyden chamber assays (Figure 1.4) and chemotaxis was measured under various conditions (Table 1.1).

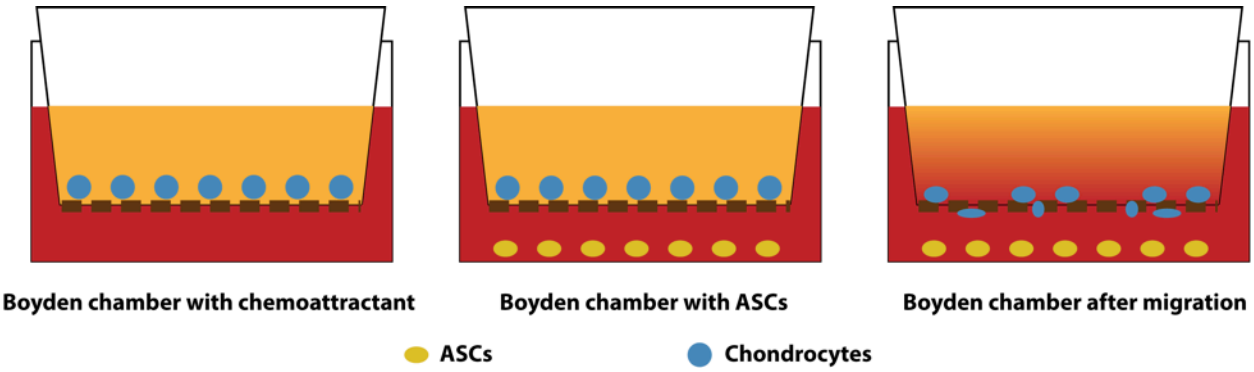

Figure 1.4: Modified Boyden chamber assay at A) the beginning of migration and at B) the end of the migration period.

Table 1.1: Summary of parameters and incubation conditions used for measuring bovine articular chondrocyte migration in Boyden Chamber assays. The experiments are presented in the order in which they were performed and the order they are presented in the results section.

	bAC Passage #	bACs /insert (coating)	Duration	Plate, (Well) & [Insert] Volume	O_2 Conc.	General Medium (insert & well)	Test Group (well only)
1	P0 P2	500,000 (gelatin)	24 h	12-well (0.5 mL) [2 mL]	21% 5% 1%	DMEM:F12 2% FBS 1% pen-strep	-medium -bASCs + medium -Cond. medium
2	P0 P2	500,000 (gelatin)	48 h	12 well (0.5 mL) [2 mL]	21%	DMEM:F12 2% FBS 1% pen-strep	-medium -bASCs + medium
3	P0	500,000 (collagen II)	24 h	12-well (0.5 mL)	21%	DMEM:F12 1% pen-strep 2% FBS	-medium -monolayer bASCs -MCS gel bASCs

		(10 μg/cm^2)		[2 mL]			
4	P0 P2	150,000 (gelatin)	24 h	24-well (0.2 mL) [1 mL]	21% 5%	DMEM:F12 1% pen-strep 0.1% BSA, 2% FBS, or 10% FBS	-0.1% BSA, 2% FBS, or 10% FBS w/ or w/o bASCs
5	P0 P2	150,000 (gelatin)	24 h	24-well (0.2 mL) [1 mL]	21%	DMEM:F12 0.1% BSA 1% pen-strep	-PDGF-BB -IGF-I (0-100 ng/mL)

Migration experiments 1-4, listed in Table 1, included monolayer bASCs in the wells of the Boyden chambers. Wells with bASCs were prepared 24 h before the start of the migration assays by seeding P2 bASCs at a density of 50,000 cells/cm^2. bASCs in experiment 3 were also encapsulated in 100 μL methacrylated chondroitin sulfate hydrogels (20 wt%) at 10x10^6 cells/mL to assess whether increasing the bASC density in the well would enhance migration. The photoinitiator, Irgacure I2959, was dissolved to 2 mg/mL in the prepolymer solution and the gels were crosslinked by exposure to 320-390 nm UV light at 15 mW/cm^2 using a Hamamatsu Lightningcure Spot light source LC8 (Hamamatsu, Skokie, Illinois). Cells in monolayer and in gels were incubated in growth medium for 24 h at 37 °C, 5% CO_2, and the O_2 concentration of conditions under investigation. Oxygen concentration was controlled with a ProOx 110 oxygen controller and subchamber system (Biospherix, Lacona, NY). The oxygen tension was varied for experiments 1 and 4, but all other migration assays were conducted at 21% O_2. Before the start of the migration assay, the growth medium was replaced with the medium conditions described in the second to last column of Table 1.1. Experiment 1 was the only exception to this protocol, in which bASCs were incubated in general medium supplemented with 2% FBS and the media was transferred to fresh wells as the conditioned media. Conditioned

media was included as a group to determine if ASC and chondrocyte co-culture was necessary for any observed effects.

To prepare the migration chamber, 8 μm pore-size inserts were incubated in a 0.25% w/v solution of gelatin in distilled water for 1 h at 37 °C. The gelatin solution was aspirated from the inserts and the inserts were dried at 37 °C for 1 h. Membranes in experiment 3 were coated with 10 $\mu g/cm^2$ of collagen II instead of gelatin, to assess whether a more tissue-specific ECM component would enhance chondrocyte migration. P0 (primary isolates) and/or P2 (cultured) chondrocyte suspensions were prepared by suspending cells in the appropriate insert media at $1x10^6$ cells/mL and $7.5x10^5$ cells/mL for 12 and 24 well-plates respectively. The chondrocyte suspensions were added to the upper chamber of the inserts, 500 μL for 12-well plates and 200 μL for 24 well-plates. Culture medium was added to the plates and the inserts were transferred to the wells. Plates were incubated at 37 °C, 5% CO_2 and the appropriate oxygen tension for 24 h (experiments 1 and 3-5) or 48 h (experiment 2). At the end of the migration period, the media was aspirated from the wells and the cells remaining on the upper surface of the insert membranes were gently removed with a cotton swab. Membranes were carefully rinsed with PBS, fixed with 4% paraformaldehyde for 25 min and then rinsed with PBS. Membranes were cut from the inserts and mounted between two coverslips in DAPI mounting medium. Images of the cells that had migrated through the membrane were captured with a Fluoview FV1000 confocal microscope (Olympus, Richmond Hill, Ontario). Image J analysis software was used to count cell nuclei in 13 images and cell numbers were averaged and extrapolated over the entire area of the membrane to determine total cell migration. Percent migration was

calculated by dividing total migrated cells by the number of chondrocytes seeded in the inserts.

3.3 Polymer Synthesis and Characterization

3.3.1 Methacrylation of Chondroitin Sulphate

Methacrylated chondroitin sulphate (MCS) was synthesized by reacting glycidyl methacrylate with chondroitin sulphate in aqueous solution (Li et al. 2003). Chondroitin sulphate was dissolved in Type I water to a final concentration of 1% w/v (22.5 mM of disaccharide repeating units) and the pH was adjusted to 10.5 with 1 N NaOH. Three molar equivalents of glycidyl methacrylate (67.4 mM, 1:1 with free hydroxyls) were added to the reaction mixture and the vessel was sealed and covered in foil to protect it from light. The reaction mixture was stirred at room temperature for 48 h and then dialyzed (MWCO 3.5 kg/mol) against Type I water for at least 48 h with 4 water changes. After dialysis, the solution was snap frozen and lyophilized, and the product was stored at 4 °C under argon. The degree of substitution (DOS) was confirmed by ^{1}H NMR in D_2O at 60 °C with a Bruker AVANCE-500 MHz spectrometer. Integrals of the methacrylate vinyl protons (δ=6.05, 6.46 ppm, 1xH) were compared to the C2 proton of the amino sugar (δ=3.67 ppm, 1xH) and the N-acetyl protons (δ=2.32 ppm, 3xH) of the repeating chondroitin sulphate residues. The DOS in terms of conjugated methacrylate groups per repeating disaccharide was calculated according to equation 1.

$$DOS = \frac{I_{\delta 6.05} + I_{\delta 6.46}}{2 \cdot I_{\delta 3.67}} \times 100\% \quad (1)$$

3.3.2 Synthesis of Peptide Modified, Methacrylated Chondroitin Sulphate

Three different peptides (GGGGGRGDS, GLOGEN, and GVOGEA) were conjugated to chondroitin sulphate using EDC/NHS conjugation chemistry. Methacrylated chondroitin sulfate (400 mg, 0.898 mmol) was dissolved in 0.1M MES buffer to a concentration of 4% w/v. Equimolar amounts of EDC (34.5 mg, 0.180 mmol) and sulfo-NHS (39.0 mg, 0.180 mmol) were dissolved in ~5 mL of MES buffer and added to the reaction vessel to target 20% of the carboxyl groups of chondroitin sulphate. The reaction was stirred at 4 °C for 15 min to activate the carboxyl groups of MCS. The peptide (0.180 mmol) was dissolved in ~1 mL of Type I water and added to the reaction vessel and the volume was brought up to 20 mL (2% w/v solution of MCS) with 0.1 M MES buffer. The reaction solution was stirred for 24 h at room temperature followed by dialysis (MWCO 3.5 kg/mol) against Type I water. The dialysis water was changed 4 times over 48 h and then the sample was snap frozen and lyophilized to yield a white powder. The DOS was confirmed by ^{1}H NMR spectra obtained in D_2O at 60 °C with a Bruker AVANCE-500 MHz spectrometer. To calculate the degree of conjugation of the peptide to the polymer backbone, the integrals of the leucine (GLOGEN, δ=1.28 ppm 6xH), valine (GVOGEA, δ=1.22 ppm 6xH), and arginine protons (RGD, δ=1.96 ppm) were compared to the C2 proton of the amino sugar (δ=3.67 ppm 2xH) and the N-acetyl protons (δ=2.32 ppm, 3xH) of each chondroitin sulphate residue. The lyophilized product was stored under argon at -20 °C until ready for use.

3.3.3 Synthesis of PEG-PTMC Macromers

Methacrylate-poly(ethylene glycol)-*block*-poly(trimethylene carbonate) (MA-PEG-PTMC) di-block copolymers were synthesized by the ring-opening polymerization of trimethylene carbonate (Amsden et al. 2004), using MA-PEG as the initiator. The PEG

initiator was dried in a 50 °C vacuum oven for 48 h before beginning the polymerization. Two different molecular weight (MW) MA-PEG-PTMC copolymers were prepared by combining a 1:5 and 1:10 ratio of MA-PEG initiator to TMC monomer. The MA-PEG initiator (3.09 and 1.55 g, 5.9 and 2.9 mmol for 1:5 and 1:10 respectively), TMC (3.00 g, 29.4 mmol), and tin(II) 2-ethylhexanoate catalyst (0.03 mmol) were added to a dry glass ampoule and vacuum-sealed. The melt polymerization was carried out in a 110 °C oven for 4 h, vortexing every hour. After 4 h, the contents were transferred to a flame-dried round bottom flask and the flask was purged with argon. To convert the PTMC terminal hydroxyl group to an acrylate and form a methacrylate-PEG-PTMC-acrylate (MA-PEG-PTMC-A) functionalized di-block copolymer, the polymer was dissolved in approximately 150 mL of dry dichloromethane (DCM). Approximately 5 mg of 4-dimethylaminopyridine (DMAP) was added to the flask as catalyst and TEA was added in 1.3 molar excess to terminal hydroxyl groups. Acryloyl chloride (1.5 molar excess) was mixed in ~8 mL of dry DCM before slowly being added to the reaction mixture over the course of several hours. The round bottom flask was protected from light and stirred for 24 h at room temperature. Most of the DCM solvent was then removed by roto-evaporation and TEA·HCl was precipitated in ethyl acetate. After removing the TEA·HCl by filtration, the excess ethyl acetate was evaporated and the polymer product was precipitated in n-hexanes at -20 °C for at least 12 h. The n-hexanes were decanted and the polymer product was transferred to a glass vial and purged with argon for storage at 4 °C.

High molecular weight diacrylate ABA tri-block macromers (A-PTMC-*block*-PEG-*block*-PTMC-A) were made using 3.4 and 20 kg/mol PEG diol initiators. PEG diol initiators were dried by azeotropic distillation in toluene (10 g in 100 mL toluene) at 108 °C until the

volume was reduced to 50 mL. TMC monomer (10:1 molar ratio to initiator) and tin(II) 2-ethylhexanoate (0.01:1 molar ratio to initiator) were added to the reaction flask and the contents were stirred for 16 h at 108 °C. Toluene was removed by roto-evaporation and the product was dissolved in 100 mL of dry DCM for acrylation. The acrylation and purification protocol were as described above, and the final product was further purified by dialysis (MWCO 0.5 or 3.5 kg/mol) against Type I water for 48 h with 4 water changes. The product was snap frozen, lyophilized, and stored under argon at 4 °C until ready for use.

The degree of acrylation and Mn of the di-block and tri-block copolymers was confirmed by ^{1}H NMR in DMSO-d_6 with a Bruker AVANCE-500 MHz spectrometer. Integrals of the acrylate vinyl protons (δ = 6.33, 6.18, 5.94 ppm), PEG methylene protons (δ = 3.51 ppm), and TMC (δ = 4.13, 1.94 ppm) were compared to the shifted PEG methylene (δ = 3.61 ppm) and methacrylate vinyl (δ = 6.03, 5.67 ppm) protons. MA-PEG-PTMC acrylate di-block copolymer molecular weights and degrees of acrylation were calculated according to equations 2-5 after normalizing the methacrylate proton integrals to unity.

$$PEG\ block\ MW = \left(I_{\delta 3.51} + 4\right)\frac{44\ g/mol}{4} \quad (2)$$

$$TMC\ block\ MW = \left(\frac{I_{\delta 4.13} - 4}{2} + I_{\delta 1.94}\right)\frac{102\ g/mol}{4} \quad (3)$$

$$Mn = PEG\ MW + TMC\ MW + \frac{55.g}{mol} + \frac{69\ g}{mol} \quad (4)$$

$$\%\ Acrylation = \frac{\frac{I_{\delta 6.33} + I_{\delta 6.18} + I_{\delta 5.94}}{3}}{\frac{I_{\delta 6.33} + I_{\delta 6.18} + I_{\delta 5.94}}{3} + I_{\delta 4.57}} \times 100\% \quad (5)$$

A-PTMC-PEG-PTMC-A tri-block copolymer molecular weights and degrees of acrylation were calculated according to equations 2, 3, 6, and 7 after normalizing the shifted PEG methylene protons integral to 4.

$$Mn = PEG\ MW + TMC\ MW + 2 \cdot \frac{55\ g}{mol} \quad (6)$$

$$\%\ Acrylation = \frac{\frac{I_{\delta 6.33}+I_{\delta 6.18}+I_{\delta 5.94}}{6}}{\frac{I_{\delta 6.33}+I_{\delta 6.18}+I_{\delta 5.94}}{6}+\frac{I_{\delta 4.57}}{2}} \times 100\% \quad (7)$$

3.3.4 Cytotoxicity Assay

Cytotoxicity of the purified MA-PEG-PTMC-A 1:5 di-block copolymer was assessed by culturing bASCs in 1% w/v solutions of MCS and di-block copolymers prepared following the methods described below. Complete medium alone was used as a negative control for bASC viability. The 1:5 di-block copolymer described above (Synthesis of PEG-PTMC Macromers) was precipitated in isopropanol two extra times to remove residual TEA·HCl or washed with Type I water and lyophilized to yield the 1:5 di-block precipitated and rinsed copolymers. bASC viability following incubation in the polymer solutions was measured in monolayer cultures seeded on TCPS at $5x10^4$ cells/cm^2 using both the GUAVA viacount assay and WST-1 assay, as described in detail below.

Cultures analyzed with GUAVA viacount reagent were seeded in 6-well plates to provide sufficient cells for the count. bASCs were initially cultured in growth medium for 24 h to allow attachment before replacing the media with 1% w/v solutions of MCS or di-block copolymers in complete medium. Replicates of the GUAVA viacount assay (n=3) were analyzed at day 1 and 3. Cells were trypsin-released from the 6-well plates, centrifuged at 1200xg for 5 min, and re-suspended in 0.5 mL of PBS. 50 µL of cell suspension was added to 450 µL of GUAVA viacount reagent and added to duplicate wells of a 96-well plate. Viability was analyzed with a Guava easyCyte 8HT flow cytometer (Millipore, 0500-4008).

WST-1 cultures (n = 3) were seeded in 96-well plates and analyzed on days 1 and 3. For the metabolic assay, 10 µL of WST-1 reagent was added to each well and incubated for

4 h at 37 °C. The solution was pipetted up and down to ensure thorough mixing before measuring the absorbance at 450 nm and 690 nm with a Perkin Elmer EnSpire® multimode plate reader (2300-001M, Waltham, Massachusetts). The adjusted absorbance reading was calculated according to equation 8.

$$Adjusted\ Absorbance = \frac{(A_{450}-A_{690})_{sample}}{(A_{450}-A_{690})_{TCPS\ control}} \quad (8)$$

3.3.5 Hydrogel Formation

The hydrogels were made by blending MCS with (meth)acrylated PEG-PTMC copolymers to reduce swelling and increase toughness while maintaining the natural biological properties of chondroitin sulphate. Four different synthetic polymers were investigated during the course of viability and mechanical property measurements, and gels were made with mass percentages of the various components as summarized in Table 1.2.

Table 1.2: Mass percent of the various components used to make hydrogels for this study. The first three rows describe the composition of cell-laden hydrogels formed for viability measurements and the last two rows outline the compositions used for mechanical measurements.

Experiment	MCS Component	PEG-PTMC Component	PBS	bASC suspension (medium w/ 10% FBS)	APS/TEMED (200 mM)
LIVE/DEAD of diblock and triblock	20%	-	50%	20%	5%/5%
		A-PTMC-PEG-PTMC-A /MA-PEG-PTMC-A			
	20%	5%	45%	20%	5%/5%
		20%	30%		
LIVE/DEAD & MTT of 20 wt% with GLOGEN	20%	-	50%	20%	5%/5%
		A-PTMC-PEG-PTMC-A			
	10%	10%	50%	20%	5%/5%
LIVE/DEAD & MTT of 20 wt% with RGD & GVOGEA	20%	-	50%	20%	5%/5%
		A-PTMC-PEG-PTMC-A			
	10%	10%	50%	20%	5%/5%
Compressive modulus	20%	-	70%	-	5%/5%
	30%	-	60%	-	

		A-PTMC-PEG-PTMC-A			
	10%	10%	70%	-	5%/5%
	15%	15%	60%	-	
Toughness, ultimate strain, equilibrium water content, sol content	20%	-	70%	-	5%/5%
		A-PTMC-PEG-PTMC-A			
	10%	10%	70%	-	5%/5%

The MCS and PEG-PTMC macromers were added to a 2 mL eppendorf tube and dissolved in PBS to obtain the concentrations noted in Table 1.2. The contents were vortexed until a uniform mixture was achieved. Viability experiments included a cell suspension component, which consisted of bASCs re-suspended in complete (10% FBS) growth medium at a concentration of $25x10^6$ cells/mL. The cell fraction was added to the prepolymer solution to achieve a final cell concentration of $5x10^6$ cells/mL, and the solution was thoroughly mixed with a pipette tip. The 20x concentrated APS/TEMED solutions were added to achieve a final concentration of 10 mM and mixed with a pipette tip. The macromer solution was quickly transferred to syringe molds (Figure 1.5) and placed in a 37 °C incubator to increase the rate of radical production by the APS/TEMED system.

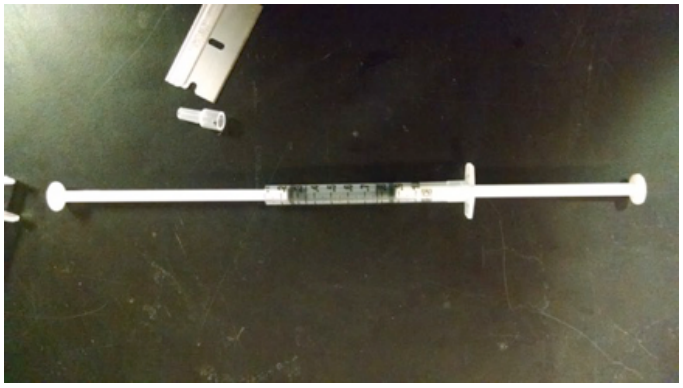

Figure 1.5: An image of the syringe molds used to form cylindrical hydrogels with consistent diameters. The tapered tip of a 1 mL syringe was cut off and the plunger from a second syringe was removed and pushed into the cut end to form the prepolymer between two flat surfaces.

The solutions were crosslinked for 15 min at 37 °C then transferred into 24-well plates with 1.5 mL of complete growth medium. The medium was changed after 30 minutes to remove residual APS/TEMED and hydrogel sol content. Hydrogels were cultured in complete growth medium at 37 °C and 5% CO_2 until ready for analysis and medium was exchanged every 2-3 days.

3.4 bASC Viability Following Encapsulation

3.4.1 Viability of Encapsulated Bovine ASCs

The viability of bASCs encapsulated in A-PTMC-PEG-PTMC-A/MCS hydrogels was measured directly with LIVE/DEAD stain or indirectly with the MTT metabolic assay. Hydrogels analyzed with LIVE/DEAD cell viability staining were first rinsed in PBS for 5 min.

Table 1.3: Summary of hydrogel compositions and LIVE/DEAD and MTT replicates investigated in viability experiments.

Experiment	MCS Component	(meth)acrylate-PEG-PTMC Component	LIVE/DEAD replicates	MTT replicates
MCS with 5% and 20% (meth)acrylate-PEG-PTMC	20%	- 5% 20%	3	-
3.4k w/ GLOGEN	20% 10%	- 10%	3	3
RGD & GVOGEA	20% 10%	- 10%	3	5

Gels were transferred into wells of a 24-well plate containing a PBS solution with 5 µM calcein AM and 4 µM ethidium homodimer. The gels were cut in half to facilitate staining and imaging of cells in the central regions. The well plates were placed in a 37 °C incubator for 30 minutes, after which the cut faces of the hydrogels were imaged using an FV1000 Fluoview confocal microscope with FITC and TRITC filters. The number of calcein

($N_{calcein}$) (green, live) and ethidium ($N_{ethidium}$) (red, dead) stained cells were counted with ImageJ analysis software and viability was calculated according to equation 9.

$$\%\, Viability = \frac{N_{calcein}}{N_{calcein}+N_{ethidium}} \times 100\% \quad (9)$$

The MTT assay was performed by incubating hydrogels in the MTT solution for 4 h at 37 °C. The MTT solution was prepared by dissolving 19 mg of solid MTT reagent in 50 mL of complete media and filtering to remove any precipitate. After 4 h, the gels were rinsed twice in PBS to remove media and the hydrogels were crushed with plastic conical indenters to expose more surface area. Approximately 750 μL of DMSO was added to each crushed gel to solubilize the formazan product. The vials were centrifuged at 1200xg for 5 min to separate the gel fragments from the DMSO supernatant and 200 μL of the supernatant was added to triplicate wells of a 96-well plate. Background absorbance was measured at 690 nm (A_{690}) and subtracted from sample measurements at 570 nm (A_{570}). Unseeded gel absorbance was then subtracted from the seeded samples to provide the final adjusted absorbance (equation 10).

$$Adjusted\ Absorbance = (A_{570} - A_{690})_{seeded} - (A_{570} - A_{690})_{unseeded} \quad (10)$$

3.5 Hydrogel Characterization

3.5.1 Mechanical Measurement of Hydrogels

Mechanical measurements were performed on swollen hydrogels by soaking in PBS for at least 24 h before performing unconfined compression measurements. The hydrogels were also surrounded by PBS during data collection to maintain the swollen state. A MACH 1 Micromechanical System (Biosyntech, Laval, Quebec) with a 10 kg load cell was used for all compression measurements (Figure 1.6). Hydrogels were compressed with an

impermeable indenter in five steps of 4% strain at 10 %/sec for a total of 20% strain (Korhonen et al. 2002; Cloyd et al. 2007). The criterion for reaching equilibrium was a force versus displacement slope less than 0.2 g/min at which the next step compression was performed. Force versus displacement data was collected during stress relaxation of the hydrogels and the last 10 data points of each relaxation phase were averaged to provide the equilibrium force at the given strain. Force and displacement values were converted to stress versus strain and a line of best fit was calculated for the equilibrium pressure values to obtain a compressive modulus.

Figure 1.6: Biosyntech MACH 1 Micromechanical System with A-PTMC-PEG-PTMC-A/MCS hydrogels for mechanical property measurements.

Ultimate strain and toughness were calculated for A-PTMC-PEG-PTMC-A tri-block copolymers and MCS blends. Gel properties were measured with the same setup as equilibrium modulus, but hydrogels were compressed at a constant strain rate of 1 %/sec until failure (Hayami et al. 2015). Force versus displacement data was converted to stress versus strain using the diameter and height of the gels respectively. The ultimate strain was equivalent to the strain at peak stress and the toughness was determined by calculating the area under the stress versus strain curve from a strain of zero until failure.

3.5.2 Physical Properties of Hydrogels

The physical properties of A-PTMC-PEG-PTMC-A/MCS (10/10 wt%) hydrogels (Table 1.2) were evaluated by scanning electron microscopy (SEM), equilibrium water content measurements, and sol content measurements. For SEM analysis, the MCS and A-PTMC-PEG-PTMC-A triblock copolymer (MCS, 3.4k/MCS, and 20k/MCS) hydrogels were incubated in complete growth medium at 37 °C for 24 h and then freeze-fractured to expose the interior region of the gel. The gel fragments were lyophilized for 24 h then mounted on SEM stubs and sputter-coated with gold. Images of the gel interior were taken with a Hitachi S-2300 scanning electron microscope (accelerating voltage = 20 kV and working distance = 15 mm).

Equilibrium water content and sol content were measured for the same hydrogel compositions as the SEM study (Table 1.2) following established methods (Hayami et al. 2011). In brief, hydrogels were cut in half and the wet mass of both halves was recorded (m_{1w} and m_{2w}). The first half was lyophilized and the dry mass was recorded (m_{1d}), while the second half was swollen in Type I water for 24 h with three water changes and the swollen mass was recorded (m_{2s}). The swollen half was lyophilized and the dry mass was recorded (m_{2d}). Equilibrium water content (EWC) and sol content were calculated according to equations 11 and 12 respectively.

$$EWC = \frac{m_{2s} - m_{2d}}{m_{2s}} \times 100\% \quad (11)$$

$$Sol\ Content = \left[1 - \frac{m_{2d}}{\frac{m_{2w} \cdot m_{1d}}{m_{1w}}}\right] \times 100\% \quad (12)$$

3.6 Statistical Analyses

All data is reported as mean ± standard deviation (SD) and the number of samples per group (n) is indicated for each experiment. Unless otherwise stated, the means of groups in migration and viability assays were compared with a two-way analysis of variance (two-way ANOVA). The means of the mechanical property groups were analyzed by one-way ANOVA. Multiple comparisons were performed with Tukey's post hoc analysis and $p < 0.05$ was considered statistically significant ("*"=$p<0.05$). All statistical analyses were performed using GraphPad Prism 6.

Chapter 4

Results

4.1 Chondrocyte Migration

The migration of P0 (primary isolates) and P2 (cultured) bovine articular chondrocytes under varying oxygen tensions was assessed using a modified Boyden chamber assay. P0 chondrocytes had significantly lower migration as compared to P2 chondrocytes for all conditions investigated (Figure 1.1). The percentage of P0 chondrocytes that had migrated across the membrane was less than 3% of seeded cells for all conditions, with no significant difference between groups. Culture-expanded P2 chondrocytes exhibited enhanced migration with all conditions resulting in greater than 50% migration. Comparing the groups at 21% O_2 and 5% O_2, oxygen tension was not observed to have a significant effect on chondrocyte migration. However, a significant increase in P2 chondrocyte migration was observed at 1% O_2 in the bASC monolayer and conditioned media wells as compared to the other oxygen tension levels. Contrary to the initial hypothesis, migration was enhanced in the control medium group as compared to both the bASC-seeded and conditioned media groups at 21% O_2. This trend was not observed at 5% and 1% oxygen tensions.

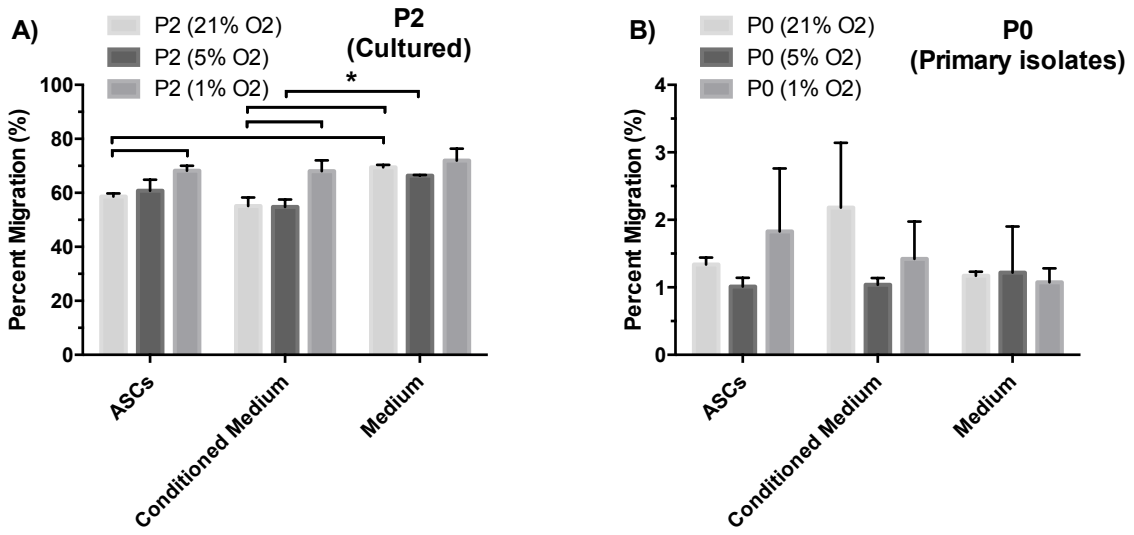

Figure 1.1: Migration of A) P2 and B) P0 bovine articular chondrocytes at 24 h measured by a modified Boyden chamber assay (n = 3). Well chemoattractants included DMEM:F12 medium supplemented with 2% FBS and monolayer bASCs or conditioned medium from bASC monolayer culture. "*" Indicates a statistically significant difference ($p < 0.05$).

Evidence that the presence of bASCs in the well may have been inhibiting chondrocyte migration led to the second migration assay with a 48 h incubation. The results (Figure 1.2) show a significant difference between bASC and medium conditions and clearly support the initial finding that the presence of bASCs in the well reduced chondrocyte migration as compared to the media controls. The P0 chondrocyte migration was also noticeably higher than the previous migration assay, which is attributed to the longer migration period.

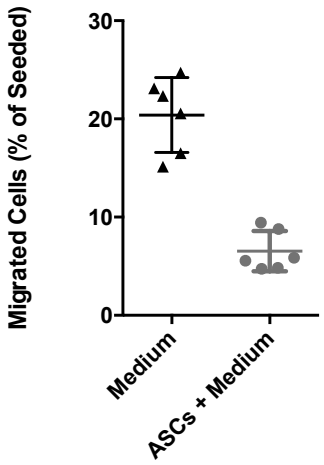

Figure 1.2: Migration of P0 bovine articular chondrocytes at 48 h in a modified Boyden chamber assay, measured using GUAVA viacount reagent (n = 6). An unpaired t-test was used to compare the means and the two groups were statistically significant ($p < 0.05$).

Increasing the density of bASCs in the wells of the Boyden chamber assay did not result in a significant difference in P0 chondrocyte migration (Figure 1.3). Encapsulating bASCs in MCS hydrogels to obtain $1x10^6$ cells/well still resulted in a low chondrocyte migration of less than 0.3%.

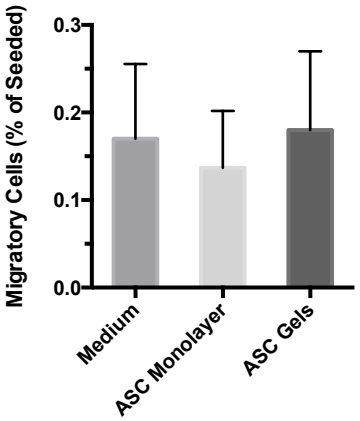

Figure 1.3: Migration of P0 bovine articular chondrocytes at 24 h, towards bASCs in monolayer or encapsulated in MCS hydrogels (n = 3).

The effect of bASCs on chondrocyte migration was investigated in varying concentrations of FBS for migration experiment 4. FBS concentration was examined to determine if increasing concentrations of FBS could significantly increase chondrocyte migration. A positive result would mean that a higher concentration of FBS might increase

chondrocyte outgrowth following ASC encapsulation and delivery to the cartilage defect site. Once again, the migration within the P0 chondrocyte groups was very low (< 2%), and there were no significant differences under varying hypoxic conditions or FBS concentration (Figure 1.4).

In terms of the cultured chondrocyte groups, P2 chondrocyte migration increased under hypoxic conditions in the presence of FBS as compared to BSA ($p<0.05$) (Figure 1.4). This same trend was not statistically significant under normoxic conditions. bASC groups generally migrated to a lesser extent than their medium only counterparts, which confirmed the results found in the previous migration assays in this study. The difference in migration between bASC groups and the medium only group with the same FBS concentration was more pronounced at higher FBS concentrations and only statistically significant under hypoxic conditions.

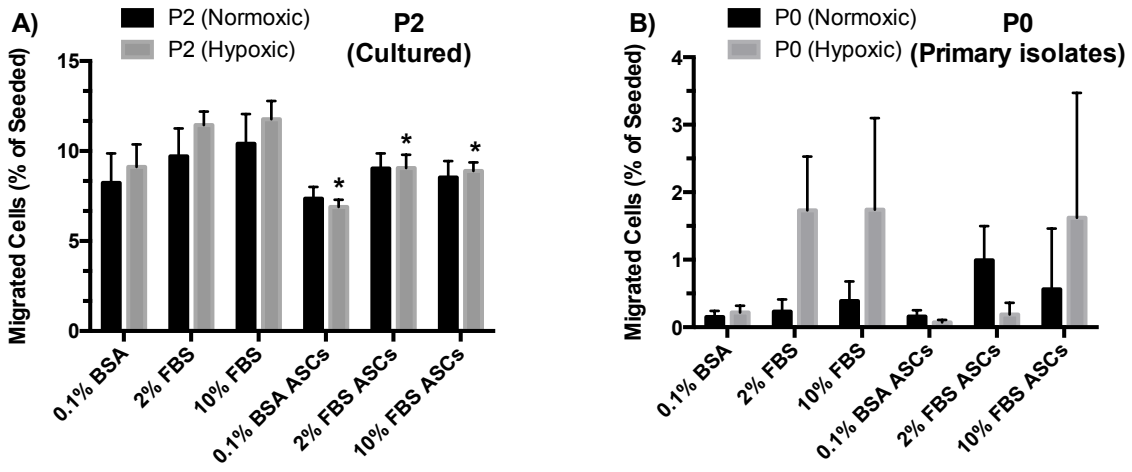

Figure 1.4: Migration of A) P0 and B) P2 bovine articular chondrocytes at 24 h in the presence of various concentrations of BSA and FBS, with or without bASCs seeded in the wells (n = 4). Inserts were incubated under normoxic (21% O_2) and hypoxic (5% O_2) conditions. "*" Indicates a statistically significant difference from the corresponding medium only group.

In a final study, PDGF-BB and IGF-I were added to the wells of the modified Boyden chambers in migration experiment 5 as a positive control for chondrocyte migration

(Figure 1.5) (McGregor et al. 2011). The addition of either growth factor failed to promote P0 chondrocyte migration across the insert membrane. This result reinforced the findings from the previous migration assays in this study involving primary isolated articular chondrocytes. However, the presence of the growth factor in the wells did promote cultured chondrocyte chemotaxis. Migration towards 10 ng/mL of IGF-I was significantly higher than 0, 2.5 and 100 ng/mL ($p<0.05$). P2 chondrocyte migration towards PDGF-BB was consistently higher than 0 ng/mL controls, and 25 and 50 ng/mL groups were also significantly higher than the 5 ng/mL group. Migration was increased by as much as 40% with addition of PDGF-BB and IGF-I to the wells.

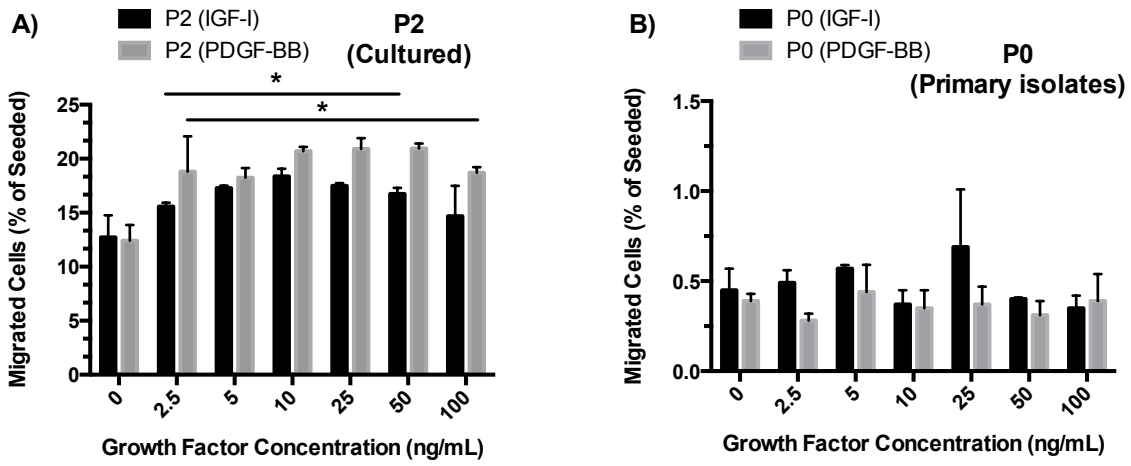

Figure 1.5: Migration of A) P2 and B) P0 bovine articular chondrocytes at 24 h towards concentrations from 0 - 100 ng/mL of PDGF-BB and IGF-I. "*" indicates a statistically significant difference from the 0 ng/mL group (n = 3, $p < 0.05$).

McGregor *et al.* reported an equivalent, approximately 40% increase in primary chondrocyte migration at 25, 50, and 100 ng/mL for both PDGF-BB and IGF-I as compared to controls (McGregor et al. 2011). In contrast, there were no significant differences between any P0 chondrocyte groups in this study. However, P2 chondrocyte migration seems to be in close agreement with results reported by McGregor. The discrepancy in results may be due to some ambiguity in the type of chondrocytes used by McGregor *et al.*

Primary chondrocytes may refer to freshly isolated chondrocytes or primary isolates that had been cultured on TCPS before use. The latter would put findings in this work in close agreement with results from McGregor *et al.* Overall, this final migration assay further supports that primary, freshly isolated chondrocytes have limited migratory capacity under 2-D *in vitro* culture conditions. Although Hidaka *et al.* reported significantly increased P0 chondrocyte migration towards FBS compared to controls, these results were obtained with chondrocytes from much younger 1-4 month old calves (Hidaka et al. 2006).

4.2 Polymer Synthesis and Characterization

Methacrylate-PEG-PTMC-acrylate (MA-PEG-PTMC-A) di-block copolymers were synthesized by the ring opening polymerization of TMC in the presence of tin catalyst and MA-PEG initiator. Successful polymerization of TMC and subsequent acrylation was confirmed from ^{1}H NMR spectra obtained in deuterated DMSO-d_6. Representative ^{1}H NMR spectra of the 1:5 and 1:10 diblock copolymers are shown in Figure 1.6. Vinyl protons corresponding to the acrylate peaks were clearly visible at δ = 6.33, 6.18, and 5.94 ppm, while peaks corresponding to the methylene protons of the ring-opened TMC were visible at δ=4.41 and 1.94 ppm. Significant amounts of residual TEA·HCl were also visible at 1.18 ppm. Precipitation in ethyl acetate and subsequent precipitations in n-hexanes did not sufficiently remove TEA·HCl and further purification was necessary before cell encapsulation experiments.

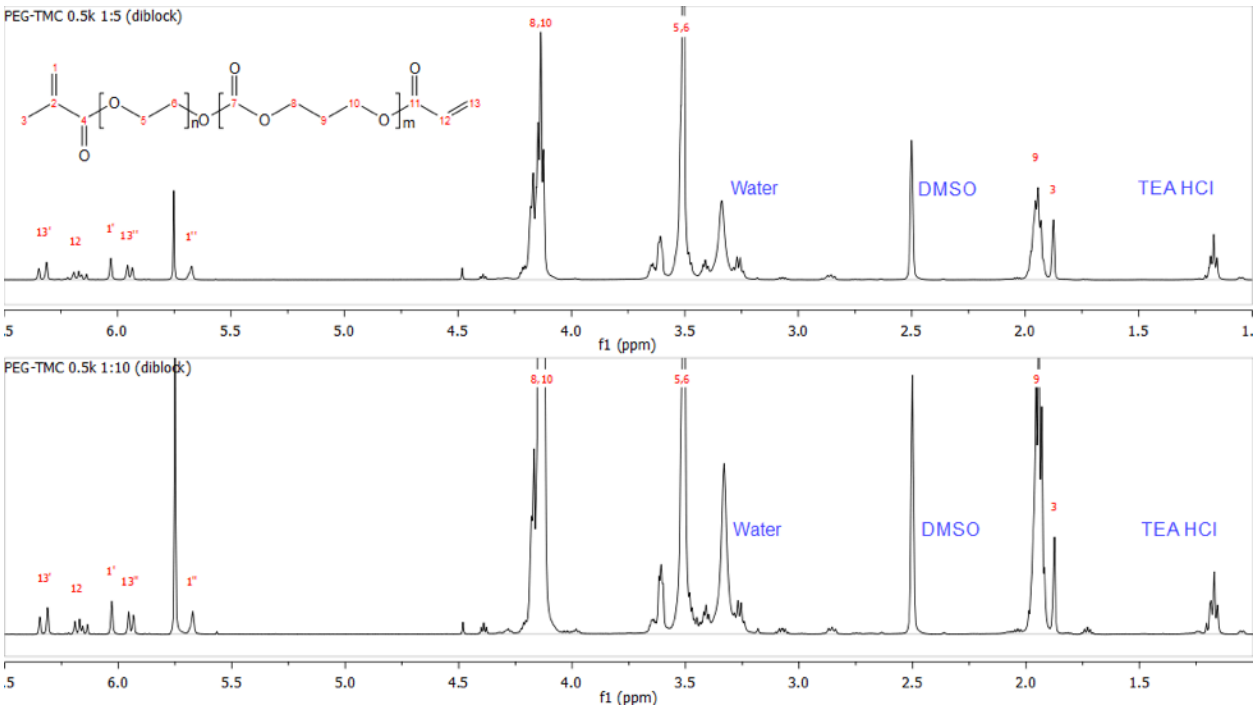

Figure 1.6: ^{1}H NMR spectra of 0.5k 1:5 and 1:10 MA-PEG-PTMC-A di-block copolymers after precipitation in n-hexanes, but before additional purification measures (i.e. dialysis or silica chromatography). The chemical structure and peak assignments are shown in the top spectrum.

The theoretical number average molecular weight (Mn) and the calculated molecular weights of the 1:5 and 1:10 di-block copolymers stocks shown in Figure 1.6 are summarized in Table 1.1. The target TMC molecular weights were chosen to be approximately equal to the PEG block in the 1:5 and 2x the PEG block in the 1:10. These ratios were relatively high but were chosen to control swelling of the hydrogels by incorporating relatively large hydrophobic blocks. The 1:5 di-block was also purified in preparation for the cytotoxicity assay by extra precipitations in isopropanol or washing with Type I water (Cytotoxicity Assay – Materials and Methods). The theoretical Mn of the 1:5 and 1:10 di-block copolymers were 1100 and 1640 g/mol respectively. The Mn calculated from the ^{1}H NMR spectra were 1470 and 2190 g/mol respectively, which is expected given that higher molecular weight chains are precipitated during purification

while the lower molecular weight chains are removed in the solvent. The calculated degree of acrylation for all di-block copolymers was ~100%.

Table 1.1: Summary of PEG-PTMC copolymer molecular weights and composition based on integration of the respective ^{1}H NMR spectra. The 1:5 copolymer was further purified by either washing with water or precipitation in isopropanol and the 1:10 copolymer was purified by silica chromatography. The 3.4k and 20k tri-block copolymers were purified by dialysis and lyophilization.

	Theoretical Mn (g/mol)	Calculated Mn (g/mol)	PEG block MW (g/mol)	TMC block MW (g/mol)	Acrylation (%)
Di-block copolymers					
1:5 stock	1100	1470	650	910	~100%
1:5 washed	1100	1340	420	1040	~100%
1:5 precipitated	1100	1550	640	1030	~100%
1:10 stock	1640	2190	540	1530	~100%
1:10 silica	1640	2160	440	1590	~100%
Tri-block copolymers					
3.4k	4950	5250	4180	950	~100%
20k	21540	21500	19980	1400	84%
Modified CS					
MCS	50,000	-	-	-	11%

Washed and precipitated samples of the 1:5 di-block had very similar TMC molecular weights and differed mostly by the molecular weight of the PEG block. This is likely a result of the copolymers with higher PEG molecular weight chains being solubilized and removed in the water-washing step. Another significant difference between the stock and purified di-blocks was the large reduction in the TEA·HCl peak at δ = 1.18 ppm following further purification. Washing with water was especially effective at removing residual TEA·HCl, and has the added benefit of removing excess solvent. After this finding, dialysis against Type I water was included as a final purification step for all PEG-PTMC copolymers used after the cytotoxicity assay.

The ^{1}H NMR spectra of the 3.4k and 20k tri-block copolymers after dialysis and lyophilization are shown in Figure 1.7. The calculated molecular weights and degree of acrylation are also summarized in Table 1.1. The targeted TMC molecular weights were chosen to incorporate approximately 5 TMC monomers onto each end of the PEG initiator,

taking into account inefficiencies due to solution polymerization. The goal was to incorporate enough TMC monomers to produce large hydrophobic domains for uncoiling under stress and allowing degradation, while maintaining the water solubility of the prepolymer.

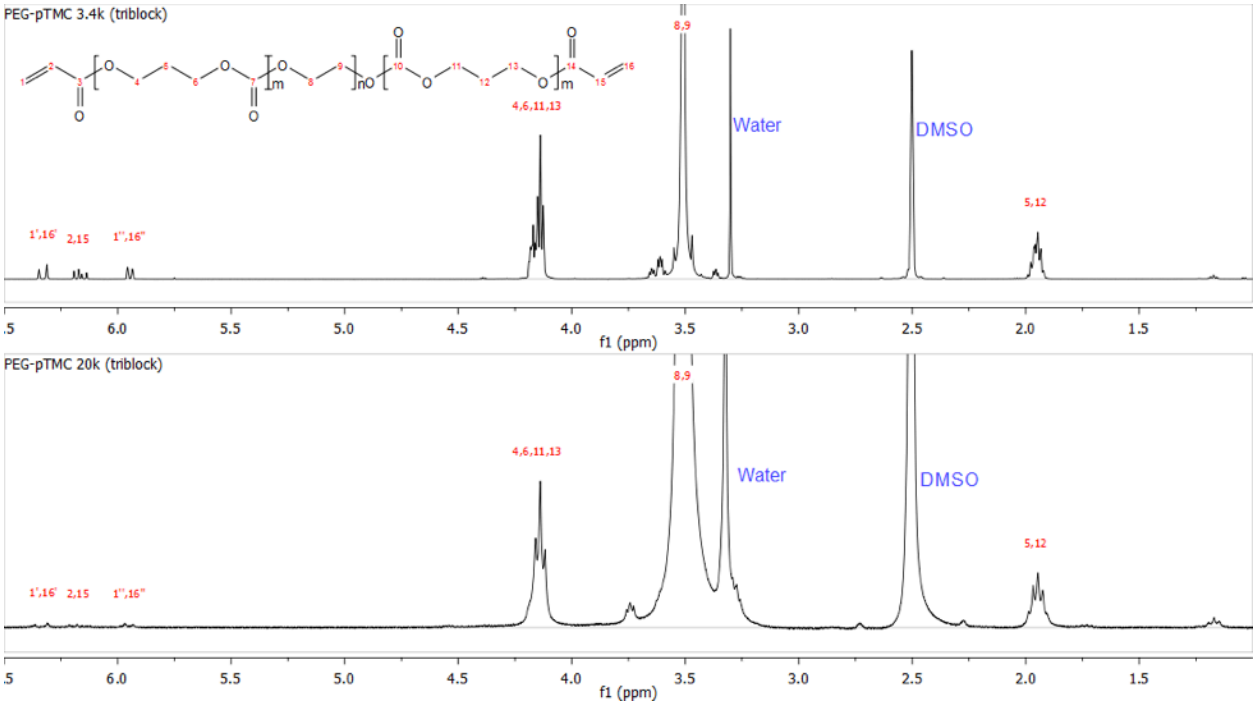

Figure 1.7: ^{1}H NMR spectra of A-PTMC-PEG-PTMC-A tri-block copolymers synthesized using 3.4 and 20 kg/mol PEG diols, after dialysis and lyophilization.

4.2.1 MA-PEG-PTMC-A Cytotoxicity

The cytotoxicity of MCS and the purified MA-PEG-PTMC-A 1:5 di-block copolymers in solution was tested on bASCs with the use of GUAVA Viacount reagent and WST-1 assay. Figure 1.8 shows that the 1% w/v solutions of the 1:5 di-block caused significant cell death after 1 day of culture, whether purified by isopropanol precipitation or washing. In contrast, bASC viability was maintained at high levels in the MCS and medium control groups.

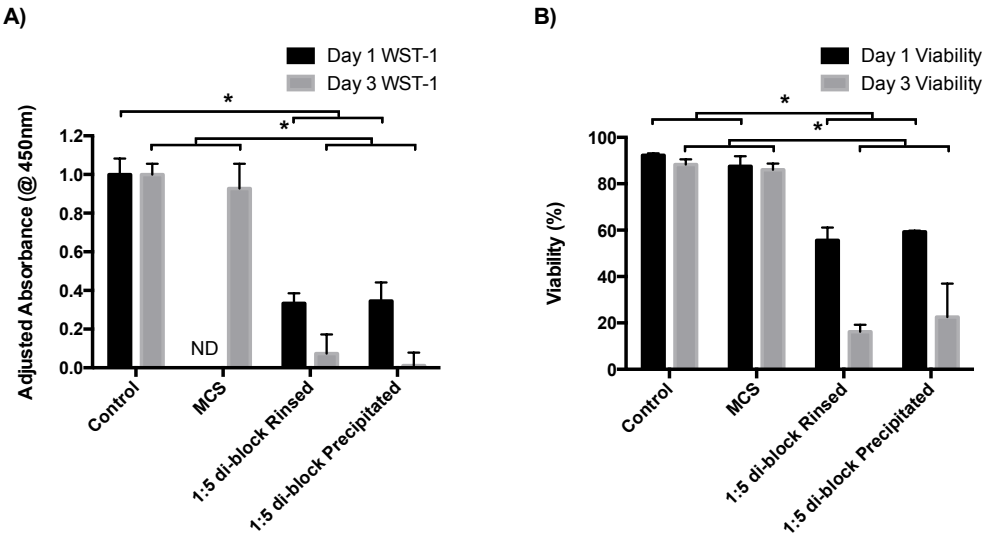

Figure 1.8: Cytotoxicity of MCS and MA-PEG-PTMC-A di-block copolymer measured with: A) WST-1 metabolic assay (n=3) and B) GUAVA viacount reagent (n=3). WST-1 of the MCS group on day 1 was not reported due to very low sample volumes when performing the assay. "*" Indicates a statistically significant difference ($p < 0.05$).

It was postulated that the molecular weight of the di-block was too low for encapsulation of bASCs with high viability. This was based on results reported by Shin *et al.* that compared MSC viability after exposure to PEG-diacrylates (PEG-DA) of low (575 g/mol) and high (3400 g/mol) molecular weight. Shin *et al*. found that MSC viability was significantly lower after exposure to the low molecular weight PEG-DA and that this effect was due to the molecular weight and not total acrylate concentration (Shin et al. 2003). To address this limitation, PEG diols with molecular weights of 3.4k and 20k were used in subsequent studies as initiators to polymerize higher molecular weight A-PTMC-PEG-PTMC-A tri-block copolymers. Tri-block copolymers were chosen due to the abundance of PEG-diol initiators with varying molecular weights, and azeotropic distillation of MA-PEG initiators might result in polymerization of the methacrylate groups.

4.3 bASC Viability Following Encapsulation

The viability of bASCs encapsulated in MCS and PEG-PTMC tri-block and di-block copolymer hydrogels was measured with LIVE/DEAD staining (Figure 1.9). MA-PEG-PTMC-

A di-block copolymers (1:5 and 1:10) were included to see if prolonged exposure to acrylate and methacrylate groups was the reason for high cytotoxicity in solution. However, hydrogel blends with lower molecular weight MA-PEG-PTMC-A typically had lower viability at days 1 and 5. Viability within all MA-PEG-PTMC-A di-block hydrogels at day 5 was less than 10%, regardless of the weight fraction of MA-PEG-PTMC-A. Hydrogels made with the higher molecular weight A-PTMC-PEG-PTMC-A tri-block copolymers had significantly higher viability than those made with di-block copolymers at the same wt%, except the 20 wt% 3.4k hydrogel which also had low viability.

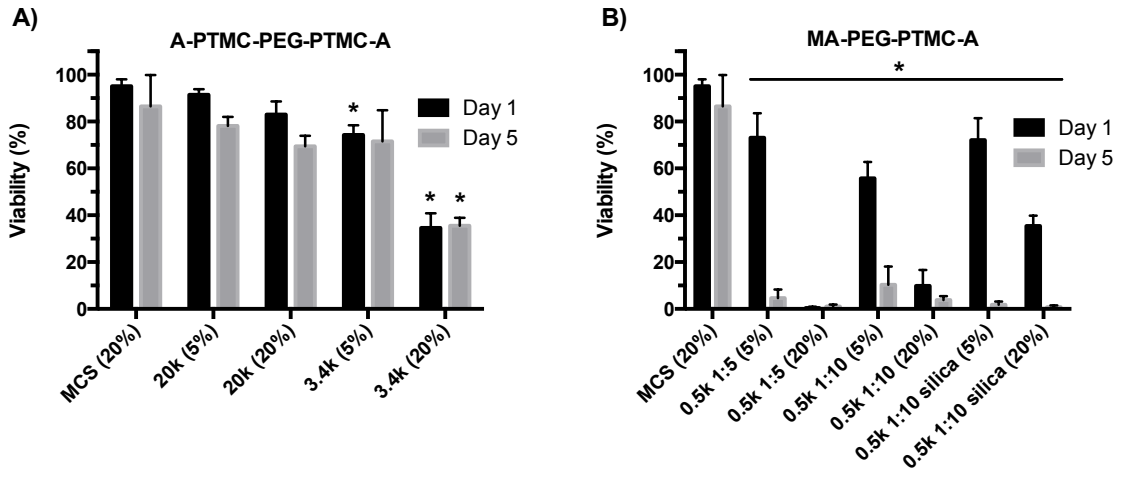

Figure 1.9: Viability of encapsulated bASCS in MCS/PEG-PTMC hydrogel blends measured by LIVE/DEAD stain. A) hydrogels made with A-PTMC-PEG-PTMC-A tri-block copolymers and B) with MA-PEG-PTMC-A di-block copolymers. All hydrogels include 20 wt% MCS and conditions plotted to the right of the MCS control include an additional 5 or 20 wt% PEG-PTMC. "*" indicates a statistically significant difference from the MCS (20%) group on the same day (n=3, p<0.05).

Results of the first hydrogel viability test confirmed that the MA-PEG-PTMC-A di-block compositions tested were unsuitable for encapsulation of bASCs. The higher molecular weight tri-block hydrogels had greater than 80% viability at day 1 when incorporated at 5% w/w. As a result, the tri-block copolymers were used for all proceeding viability experiments because of the higher viability maintained within hydrogels.

The viability of encapsulated bASCs was measured once again with 20 wt% total polymer hydrogels and the more promising A-PTMC-PEG-PTMC-A tri-block copolymers. Hydrogels were made with 20 wt% polymer because cell viability and imaging clarity were greater in the lower wt% hydrogels. MCS conjugated with the collagen III peptide, GLOGEN, was included to determine if a cell-adhesive peptide could enhance cell viability in the 3.4k hydrogels. Sukarto *et al.*, Nuttelman *et al.*, and Salinas *et al.* have all shown that integrin binding peptides improve cell viability following crosslinking and encapsulation (Sukarto et al. 2012; Nuttelman et al. 2005; Salinas & Anseth 2008b). MTT and LIVE/DEAD assays were performed as a means of measuring cellular viability within the hydrogels.

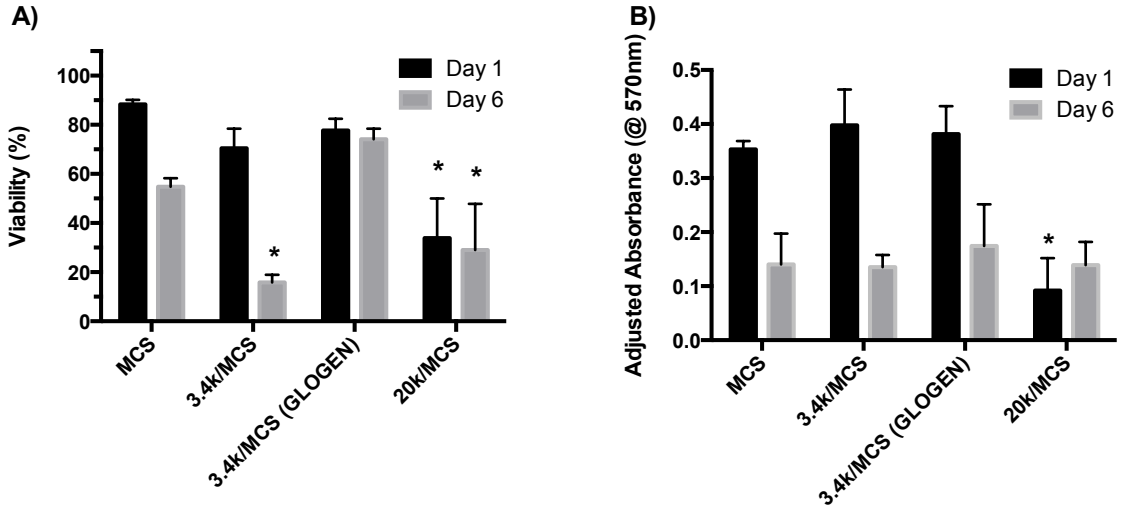

Figure 1.10: Viability of 20 wt% hydrogels made from blends of MCS, MCS GLOGEN, and A-PTMC-PEG-PTMC-A tri-block copolymers as measured by A) LIVE/DEAD stain (n=3) and B) MTT assay (n=3). "*" indicates a statistically significant difference from the MCS group on the same day ($p<0.05$).

Values from the MTT and LIVE/DEAD assay were in close agreement for most conditions except for the hydrogel group made with 3.4k A-PTMC-PEG-PTMC-A tri-block and MCS-GLOGEN. In this case the presence of GLOGEN improved cell viability while metabolic activity of the encapsulated cells decreased. The overall number of cells in each gel was roughly the same at days 1 and 6, so differences between LIVE/DEAD staining and

MTT reading were due to metabolic differences as opposed to cell number. LIVE/DEAD staining of the 3.4k/MCS hydrogels at day 6 still had greater than 75% viability, but the MTT absorbance was less than 50% of its value from day 1. The 20k A-PTMC-PEG-PTMC-A tri-block hydrogels had poor viability at days 1 and 6. One possible reason for these discrepancies could be the slightly higher TEA·HCl peak in the 20k tri-block copolymer as compared to the 3.4k tri-block copolymer.

The RGD integrin binding motif, GLOGEN peptide from collagen III, and GVOGEA peptide from collagen II were conjugated to MCS using EDC/NHS chemistry. These peptides were chosen to compare the effects of the different peptides on bASC viability following crosslinking, and because collagens II and III are present in articular cartilage. Peptide conjugation to MCS was confirmed via ^{1}H NMR analysis and the final DOS of RGD, GLOGEN, and GVOGEA on MCS was approximately 6.2%, 1.2%, and 4.8% of disaccharide units (Appendix). The final concentration of peptide in the hydrogels was controlled at 4 mM by mixing with unmodified MCS.

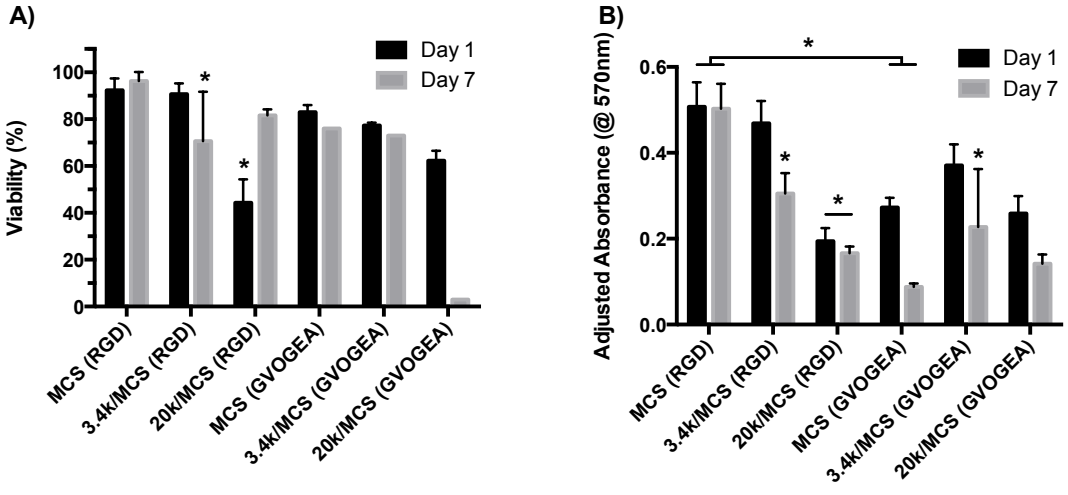

Figure 1.11: Viability of bASCS within 20 wt% hydrogels made from blends of MCS-RGD, MCS-GVOGEA, and A-PTMC-PEG-PTMC-A tri-block copolymers as measured by: A) LIVE/DEAD stain (n=3, n=1 for GVOGEA on day 7) and B) MTT assay (n=5). "*" indicates a statistically significant difference from the MCS group on the same day ($p<0.05$)

Total cell numbers actually decreased from day 1 to day 7 in this experiment, so reductions in metabolic activity may be caused by reduced cell number. However, clarity within the gels was also reduced, which may partially account for reduced cell numbers. Cell viability was higher in the presence of the RGD peptide compared to the GVOGEA peptide except for the 20k/MCS-GVOGEA hydrogels that had slightly higher viabilities than their RGD counterparts on day 1. LIVE/DEAD measurements were higher than 70% for all conditions on day 7 except the 20k/MCS GVOGEA. MCS control hydrogels had greater than 95% viability throughout the 7-day culture period and had the highest MTT absorbance readings.

The LIVE/DEAD measurements are compiled in Figure 1.12 to see the effect of the various integrin-binding peptides. All peptides improve bASC viability in the A-PTMC-PEG-PTMC-A/MCS hydrogels.

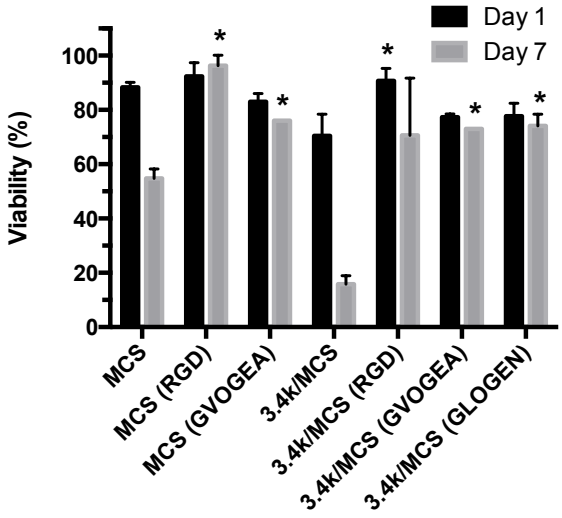

Figure 1.12: LIVE/DEAD viability of MCS, 3.4k/MCS, and peptide-modified hydrogels on days 1 and 7. "*" indicates a statistically significant difference from the MCS group on the same day (n=3, $p<0.05$).

4.4 Hydrogel Characterization

4.4.1 Mechanical Properties

The equilibrium modulus, water content, sol content, maximum strain and toughness were determined for MCS and PEG-PTMC tri-block copolymer gels. Hydrogels containing the 3.4k or 20k A-PTMC-PEG-PTMC-A tri-blocks were a 1:1 (w/w) blend of tri-block and MCS for a total polymer content of either 20 or 30 wt%. Gels were compressed in five steps of 4% strain with each step followed by a relaxation at constant strain.

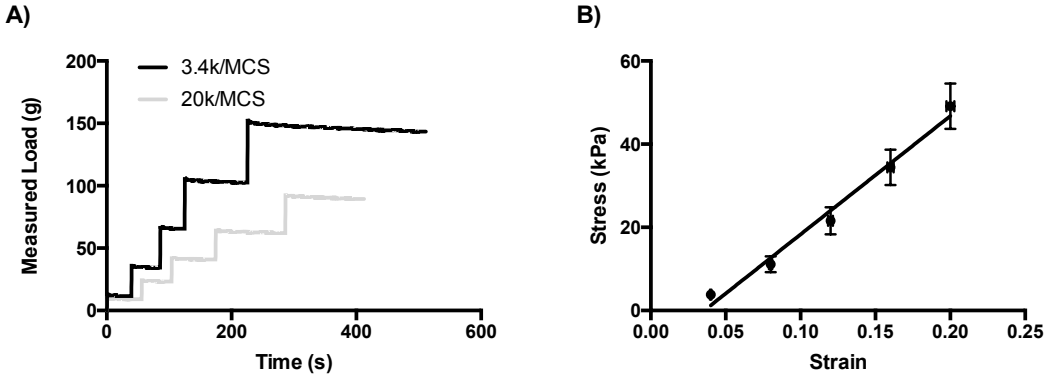

Figure 1.13: A) Representative load *vs.* time data collected for measurements of the equilibrium modulus and B) the stress *vs.* strain data calculated from raw data of hydrogels at equilibrium for the 3.4k/MCS hydrogels. The slope obtained from linear regression in B) provides the equilibrium compressive modulus of the gels.

Equilibrium stress values were plotted as a function of strain and the slope from linear regression of these data was taken as the equilibrium compressive modulus. Figure 1.13 A shows three separate runs on three separate gel compositions and B shows the result of linear regression on 6 replicates of the 3.4k/MCS (20%) hydrogels. Figure 1.14 summarizes the final equilibrium modulus results from unconfined compression.

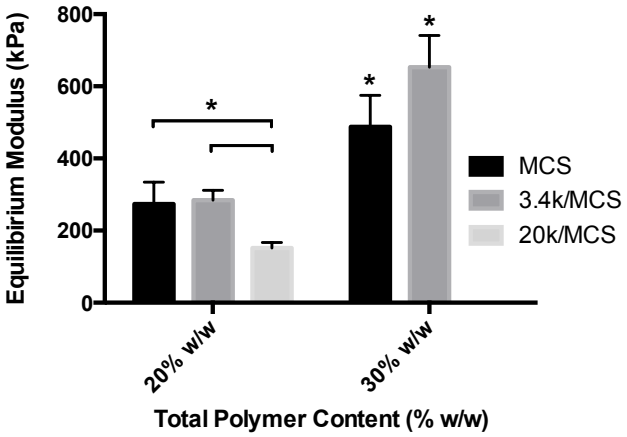

Figure 1.14: Equilibrium moduli of 20 and 30 wt% hydrogels of MCS alone and A-PTMC-PEG-PTMC-A/MCS blends. Polymer mass fractions are split equally between MCS and tri-block copolymers for mixed hydrogels. "*" without a bar indicates a statistically significant difference from all other groups (n=6, $p<0.05$).

Equilibrium compressive moduli of 20% w/w gels were above 150 kPa for all compositions, although the 20k/MCS gels had a significantly lower modulus than the 3.4k/MCS and MCS alone gels. An increase in total polymer content to 30% w/w had a more pronounced effect on equilibrium modulus and led to equilibrium moduli of 650 ± 40 and 490 ± 40 kPa for the 3.4k/MCS and MCS alone gels respectively. The moduli of the corresponding hydrogels at 20 wt% were 280 ± 10 and 270 ± 20 kPa for the 3.4k/MCS and MCS gels respectively. The 3.4k and 20k tri-block copolymers were further investigated as a high and low molecular weight group and the total polymer content was kept at 20 wt% due to diffusion limitations of nutrients and reagents above this point.

Toughness of MCS, 3.4k/MCS, and 20k/MCS hydrogels at 20% polymer content (w/w) were measured by unconfined compression at 1 %/sec until failure. Figure 1.15 demonstrates a representative stress vs. strain curve for each of the hydrogel compositions. MCS and 3.4k/MCS hydrogels follow a similar stress *versus* strain curve until 18% strain at which point the MCS alone gels fracture and fail. The 3.4k/MCS and 20k/MCS hydrogels fail at much higher strains than the MCS gels, but the lower modulus of the 20k/MCS gels results in a shallower toe region.

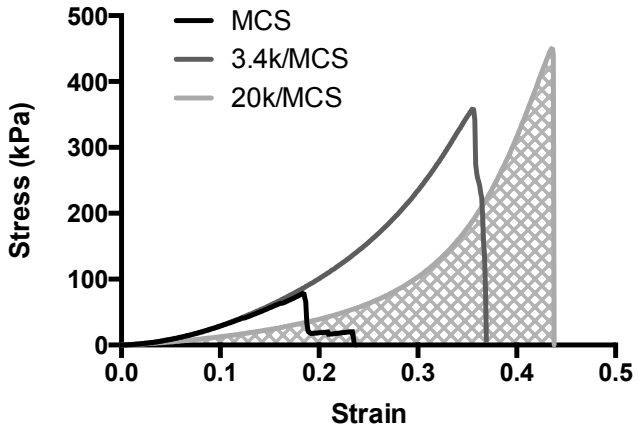

Figure 1.15: Representative stress *versus* strain curves for each of the hydrogel compositions analyzed by unconfined compression tests. The area under the curve, as demonstrated by the 20k/MCS gel, is equivalent to the gel toughness.

Measurements of toughness and ultimate strain are summarized in Figure 1.16. Ultimate strain and toughness increased with the fraction of tri-block in the hydrogels and with increasing molecular weight of the tri-block. The 20k/MCS gels were very elastic and could be strained to high degrees as evidenced by the stress *vs.* strain curves in Figure 1.15. On the other hand, MCS gels were quite brittle and would fail at approximately 19% strain.

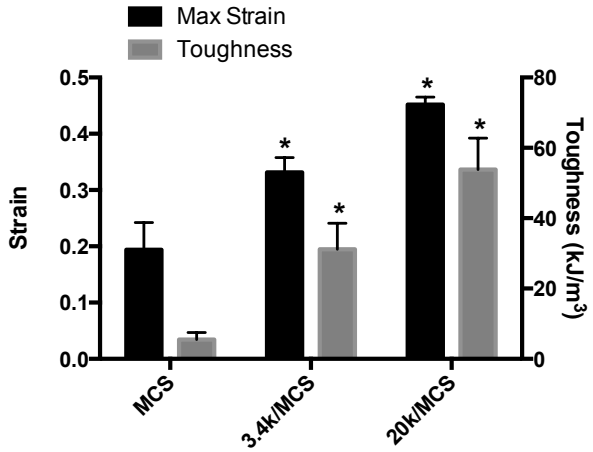

Figure 1.16: Toughness and ultimate strain of MCS and A-PTMC-PEG-PTMC-A tri-block hydrogels were determined by constant strain rate compression until failure (n=6). "*" indicates a statistically significant difference from MCS alone groups ($p<0.05$).

4.4.2 Physical Properties

The equilibrium water content and sol content of MCS, 3.4k/MCS, and 20k/MCS hydrogels were calculated according to equations 11 and 12 (Figure 1.17). The equilibrium

water content of all hydrogels was greater than 90 wt%, and the 20k/MCS gels had the highest water content at 94.8 ± 0.1 wt% while the 3.4k gels had the lowest at 91.3 ± 0.1%. The sol content of the MCS and 20k/MCS gels was significantly higher than the 3.4k/MCS gels, which may be a result of the lower acrylate and methacrylate concentration in pre-polymer solution.

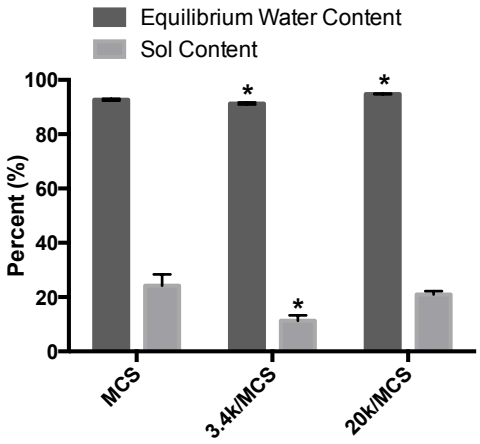

Figure 1.17: Equilibrium water content and sol content of the various A-PTMC-PEG-PTMC-A tri-block copolymers and MCS hydrogels (n=6). "*" indicates a statistically significant difference from MCS alone groups ($p<0.05$).

During equilibrium swelling, distinct regions were observed within the 3.4k hydrogels and to a lesser degree within the 20k/MCS hydrogels. These regions could be caused by phase separation of the relatively large hydrophobic blocks in 3.4k tri-block copolymer or by nonhomogeneous polymer concentrations within the gels. Stereomicroscope images of the various hydrogels were taken to characterize these distinct regions and scanning electron microscope (SEM) images were used to assess the overall morphology and structure of the hydrogels (Figure 1.18). Phase separation was visible in stereomicroscope images of the 3.4k/MCS gels, and the 20k/MCS gels were also more opaque than the MCS alone. Under SEM, the MCS and 20k/MCS gels had a more homogeneous pore structure and distribution, whereas the 3.4k/MCS gels were more

heterogeneous at both 50x and 400x magnification. However, the 20k/MCS gels had a more rounded pore morphology than the MCS gels, in which the pores appeared to be flattened.

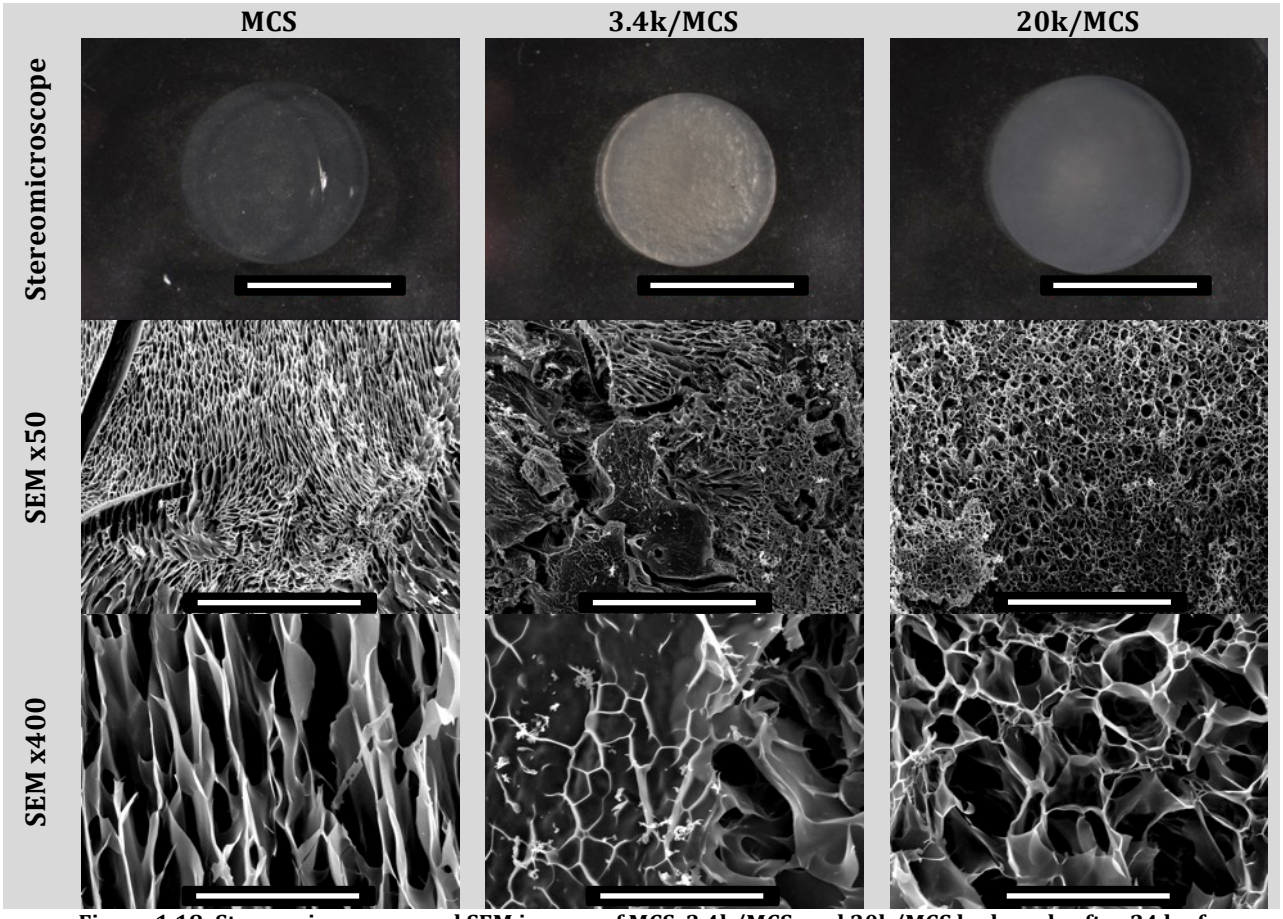

Figure 1.18: Stereomicroscope and SEM images of MCS, 3.4k/MCS, and 20k/MCS hydrogels after 24 h of incubation in complete media. Scale bars are 5 mm, 1 mm, and 100 µm for the top, middle, and bottom rows respectively.

Chapter 5

Discussion

5.1 Chondrocyte Migration

Chondrocyte adhesion and migration within 2-D and 3-D environments remains a topic of significant interest for understanding the mechanism of cartilage repair. Modified Boyden Chamber assays provide a convenient means for studying chondrocyte chemotaxis, chemokinesis, and haptotaxis *in vitro*. Migration of chondrocytes on and towards various substrates and chemoattractants has been studied extensively. Specifically, the factors bFGF (McGregor et al. 2011; Hidaka et al. 2006; Maniwa et al. 2001), PDGF-BB (McGregor et al. 2011; Mishima & Lotz 2008; Fujita et al. 2004), IGF-I (McGregor et al. 2011; Chang et al. 2003), and BMP-2 (Frenkel et al. 1996) have been shown to be chemotactic for primary chondrocytes. ECM proteins including fibronectin (Chang et al. 2003), hyaluronic acid (Maniwa et al. 2001), collagen I, and collagen II have also demonstrated a chemotactic effect on chondrocytes, while fibronectin, collagen I, and collagen II have exhibited a haptotactic effect as well (Shimizu et al. 1997).

However, Mishima *et al.*, Fujita *et al.*, and Frenkel *et al.* performed migration experiments with chondrocytes expanded on tissue-culture polystyrene (TCPS) (Mishima & Lotz 2008; Fujita et al. 2004; Frenkel et al. 1996). Chang *et al.* cultured chondrocytes in a roller bottle before use and Hidaka *et al.* used chondrocytes cultured for 0 and 4 days but the results do not differentiate between the two (Chang et al. 2003; Hidaka et al. 2006). The use of cultured chondrocytes raises a few concerns with regards to the phenotype since the de-differentiation of chondrocytes with 2-D culture has been well documented (Benya & Shaffer 1982; Schulze-Tanzil et al. 2002; Schiltz et al. 1973; Mayne et al. 1976). While some

investigators have hypothesized that chondrocytes may dedifferentiate while migrating and then recover the differentiated phenotype, this has yet to be confirmed (Frenkel et al. 1996). However, Morales *et al.* have shown this may not be the case, and that chondrocytes can maintain their differentiated phenotype during migration (Morales 2007). The migration assays performed in these studies were designed to compare the migratory capacity of bovine articular chondrocytes at P0 and P2. The results showed that P0 chondrocytes exhibited much lower migration than P2 chondrocytes, with less than 3% of seeded chondrocytes migrating across the membrane. On the other hand, P2 chondrocytes often exhibited upwards of 10% migration, with some conditions yielding approximately 70% migration.

These results confirm the findings Mishima *et al.*, Fujita *et al.*, and Chang *et al.* with respect to cultured chondrocyte chemotaxis towards FBS, IGF-I, and PDGF-AB and –BB. However, the lack of significant P0 chondrocyte migration towards any of these factors may signify that chemotaxis cannot be induced in this cell population within the 24 h migration period under the conditions of these studies. McGregor *et al.* did show increased chondrocyte migration towards PDGF-BB and IGF-I, but it is unclear if these cells were freshly isolated or primary chondrocytes that had been cultured. This finding does not indicate that P0 chondrocytes are not migratory, as longer migration times, different substrates, or an alternative migration assay may yield differing effects. In fact, several groups have observed the population of acellular scaffolds by chondrocytes both in an explant model *in vitro* (Secretan et al. 2010; Seol et al. 2014) and *in vivo* (Schüettler et al. 2013). The source and phenotype of the migratory cells *in vivo* have yet to be confirmed, but some have hypothesized that the cells found in the scaffolds are actually chondrogenic

progenitor cells (Seol et al. 2012; Dowthwaite et al. 2004; Alsalameh et al. 2004). The source of chondrocytes found within repair tissue *in vivo* has yet to be confirmed, although the successful invasion of acellular scaffolds *in vitro* suggests that the cell source may be contained within cartilage. Despite the limited migration of P0 chondrocytes on gelatin over 24 h, the findings from other groups show that longer culture times in a cartilage defect model may be necessary for significant chondrocyte migration. The phenotype and gene expression patterns of any such cells should be monitored to determine whether they are in fact chondroprogenitors, differentiated chondrocytes, or dedifferentiated chondrocytes.

A second aim of the migration assays was to study the effect of bASCs and their soluble factors on chondrocyte migration. The production of a wide array of soluble factors by ASCs has been extensively researched and reviewed (Skalnikova et al. 2011; da Silva Meirelles et al. 2009; Maxson et al. 2012; Hsiao et al. 2012). These factors can be divided into subcategories including immunomodulatory, angiogenic, anti-fibrotic, and chemoattractant factors, and vascular endothelial growth factor (VEGF), TGF-β, bFGF, stromal cell-derived factor-1 (SDF-1), and some MMPs are among the factors produced (Ruetze & Richter 2014). Secretion of these factors and others make ASCs a potential source of chondrocyte chemoattractants. Continuous production of chemotactic factors would establish a gradient for chondrocyte chemotaxis towards ASCs encapsulated within a tissue-engineered construct. However, in the four experiments that included bASCs seeded in the wells of the Boyden chamber, there was either no significant difference compared to controls or a decrease in migration was observed. This effect was particularly pronounced in the second migration assay in which migration was measured by counting

trypsin-released migrated chondrocytes from the membrane using the GUAVA viacount reagent. Automatic counting is likely to give a more reliable and consistent measure of cell migration compared to counting of select fields of a membrane. It should also be noted that P0 chondrocytes were used for this experiment, albeit with a longer 48 h migration time.

Considering all experiments together, there does appear to be evidence of decreased chondrocyte chemotaxis in the presence of ASCs as compared to media only controls. The decreased migration could be a result of inhibitory factors produced by the bASCs under the low oxygen tension and low serum conditions of some experiments. Stadler *et al.* and Palmer *et al.* have reported the production of nitric oxide in chondrocytes after exposure to catabolic factors such as TNF-α, IL-1, and IL-18, which can be produced by bASCs under hypoxia (Olee et al. 1999; Palmer et al. 1993; Stadler et al. 1991). In turn, the presence of nitric oxide inhibits chondrocyte migration (Frenkel et al. 1996). Decreased chondrocyte migration towards bASCs might also be explained by the production of trophic factors that maintain the differentiated phenotype of chondrocytes. The findings of this study with regards to differentiated chondrocytes (P0 chondrocytes) indicate that a more differentiated phenotype might exhibit lower migration. Overall, the decreased chondrocyte migration towards bASCs in a Boyden Chamber assay may not be representative of events in 3-D culture or *in vivo*. Further co-culture experiments between ASCs and chondrocytes would be useful for elucidating the cellular response and protein expression of the two cells types. Moving to a 3-D co-culture model within hydrogels or a cartilage defect model with encapsulated ASCs would be more representative of the conditions found *in vivo*.

5.2 bASC Viability Following Encapsulation

A further and separate aim of the present study was to develop and analyze a hydrogel system for encapsulation and delivery of ASCs to a cartilage defect. The initial gel composition selected for cell encapsulation was a blend of MCS and the MA-PEG-PTMC-A di-block copolymers described in this study. Gels formed with MCS alone have exhibited relatively high swelling ratios (Varghese et al. 2008; Li et al. 2004; Wang et al. 2003), which poses a problem for hydrogel persistence in a cartilage defect. The MA-PEG-PTMC-A di-block was incorporated into MCS hydrogels to reduce the swelling and to increase the compressive modulus. The presence of the hydrophobic TMC block was hypothesized to reduce swelling and provide a means for degradation through hydrolysis or enzymatic degradation of the synthetic polymer (Zhu et al. 1991; Zhang et al. 2006). However, the cytotoxicity assay showed that even low concentrations (1% w/v) of the di-block in growth medium caused significant cell death after 1 day, even following purification.

The MA-PEG-PTMC-A 1:10 di-block copolymer was purified by silica column chromatography and dialyzed against water to remove impurities. The cytocompatibility of the silica-purified 1:10 and dialyzed 1:5 and 1:10 copolymers was measured by encapsulating bASCs in hydrogels of MCS and the synthetic polymers. The results showed that the presence of the di-blocks, regardless of molecular weight or purification technique, resulted in almost complete cell death after 5 days of culture. Despite the extensive cell death by day 5, the silica column purified 1:10 copolymer had significantly higher viability in the 5 and 20 wt% hydrogels after 1 day compared to the dialyzed 1:5 and 1:10 copolymers. The increase in viability is likely due to the removal of impurities such as TEA·HCl and not the removal of a low molecular weight fraction since all polymers were

dialyzed against the 500 MWCO membrane. The dominant contributor to cytotoxicity is still clearly the polymer itself. Some groups have examined the effect of pre-polymer molecular weight on cell viability in hydrogels and found that PEG-based polymers with molecular weights below 1,000 g/mol cause greater cell death than those above 3,400 g/mol (Suggs et al. 1998; Shin et al. 2003; Mao et al. 2005). Specifically, PEG molecular weights above 3,400 g/mol and hydrophobic domains with molecular weights below 2,500 g/mol have reduced cytotoxicity during and after hydrogel formation (Shin et al. 2003; Mao et al. 2005). The use of APS and TEMED in the present study is likely a small contributor to cytotoxicity due to the short crosslinking times (10 min) and relatively low concentration of APS/TEMED (10 mM each) (Duan 2005). The poor viability of bASCs within MA-PEG-PTMC-A 1:5 and 1:10 di-block copolymer hydrogels led to the investigation of A-PTMC-PEG-PTMC-A tri-block copolymer formulations made with higher PEG molecular weight and relatively low PTMC molecular weights than used to prepare the di-block copolymers.

The A-PTMC-PEG-PTMC-A tri-block copolymers were synthesized from PEG diols with molecular weights that led to the naming scheme of the final product. The A-PTMC-PEG-PTMC-A 3.4k and 20k tri-block copolymers were created from PEG diols (3.4 and 20 kg/mol) and approximately 7 TMC monomers polymerized on each end of the PEG chain. These molecular weights were chosen to increase bASC viability within MCS and A-PTMC-PEG-PTMC-A hydrogels. Initial results from LIVE/DEAD staining of bASC-seeded hydrogels with 20 wt% MCS and 5 or 20 wt% PEG-PTMC copolymers showed that increasing PEG molecular weight resulted in increased viability. Promising results led to further viability measurements with the 3.4k and 20k copolymers to confirm initial findings and investigate the effect of RGD, GLOGEN, and GVOGEA peptides. In subsequent experiments, the viability

of bASCs within 3.4k/MCS and MCS hydrogels was actual higher than in the 20k/MCS gels. These findings are in contrast to results from Shin *et al.* and Suggs *et al.* who found that macromers with a molecular weight above 3,400 g/mol formed hydrogels with greater cell viability. The discrepancy could be the result of higher quantities of residual TEA·HCl or the higher sol content in 20k/MCS gels than 3.4k/MCS gels.

The viability experiment with GLOGEN-modified MCS saw a significant decrease in viability within MCS hydrogels after 6 days. This result was surprising given the relatively high cellular viability after encapsulation in MCS hydrogels reported previously (Li et al. 2004; Hayami et al. 2015). However, these studies used articular chondrocytes with relatively low metabolic activity and Williams et al. have demonstrated that cells with lower metabolism exhibit reduced cell death upon crosslinking (Williams et al. 2005). The same trend was seen across several studies using PEG-based hydrogels with photoencapsulation. Osteoblasts (Burdick & Anseth 2002) and chondrocytes (Bryant & Anseth 2001) exhibited high viability (>90%) after 1 week of culture while hMSCs were only 60% viable after the same culture time (Nuttelman et al. 2004). The differences in bASC viability between the 3.4k and 20k hydrogels in the present study could be the result of slightly different purification steps. The 3.4k A-PTMC-PEG-PTMC-A was precipitated twice in isopropanol in addition to the three precipitations in hexanes to remove residual TEA·HCl. TEA·HCl precipitation in ethyl acetate followed by filtering was not enough to remove all salts, and dialysis still left traces detectable by ^{1}H NMR. Further purification may be necessary for long-term culture of bASCs in the A-PTMC-PEG-PTMC-A copolymer hydrogels. Several groups have used sephadex for gel filtration of the synthetic product followed by dialysis and lyophilization (Zhang et al. 2011; Nguyen et al. 2012).

The effect of three different peptides on bASC viability was also investigated in the present study. RGD is a commonly used integrin-binding motif found in collagen, fibronectin, and other ECM proteins (Ruoslahti & Pierschbacher 1987). GLOGEN and GVOGEA are collagen III and collagen II peptide sequences, respectively (Fertala et al. 2001). Conjugation of the GGGGGRGDS peptide onto the MCS prepolymer maintained greater than 95% viability in MCS hydrogels over 7 days. In contrast, bASC viability in MCS hydrogels without the RGD motif dropped to ~55% after 6 days of culture. The presence of GLOGEN in hydrogels containing both MCS and 3.4k tri-block copolymer increased viability as measured by LIVE/DEAD staining, as compared to 3.4k/MCS gels without peptide. Interestingly, the MTT measurement still showed a drop similar to that found in the 3.4k hydrogels without GLOGEN. This finding suggests that cell survival increases in the presence of GLOGEN, but cell metabolism decreases during culture. Drawing absolute conclusions from these results is premature, due to the difficulty of measuring cell viability, proliferation, and metabolism in 3-D scaffolds (Ng et al. 2005). Many of the assays used to measure these variables, including the MTT assay, are designed for low cell densities in 2-D culture and do not correlate linearly with increasing cell density in 3-D. Further experiments would need to be conducted to determine the protein expression patterns and phenotype of cells seeded in GLOGEN-containing hydrogels. GVOGEA had a similar effect to the GLOGEN peptide in terms of cell metabolic activity. Despite a similar viability to MCS-RGD gels by LIVE/DEAD staining, the MTT measurement after 1 day of culture was approximately half of the MCS-RGD measurement.

Viability and metabolic activity of bASCs was highest in the RGD-containing hydrogels, but this does not mean that the peptide is the best choice for an engineered cartilage tissue.

Some groups have even found that RGD peptide actually encourages a fibrotic phenotype *in vitro* and results in collagen I production (Smith Callahan et al. 2013; Connelly et al. 2008). This effect was usually observed in biologically inert scaffolds such as agarose or PEG hydrogels. Kim *et al.* have found that chondrogenesis and cartilage-like ECM production can be promoted in RGD-modified scaffolds containing chondroitin sulphate and hyaluronic acid (Kim et al. 2015). Chondrogenesis of ASCs in the presence of the three peptides would have to be assessed to determine the sequence best suited for cartilage regeneration. There is promise for the GLOGEN and GVOGEA peptides specifically for this application. Both peptides are high affinity ligands for the $\alpha_1\beta_1$ integrin and GLOGEN is also a ligand for the $\alpha_2\beta_1$ integrin receptor (Hamaia et al. 2012). The $\alpha_1\beta_1$ and $\alpha_2\beta_1$ integrins are expressed in human chondrocytes and preferentially bind collagen VI and collagen II, respectively (Loeser et al. 2000; Dürr et al. 1993). The rationale of incorporating GLOGEN and GVOGEA peptides in scaffolds was to mimic some of the interactions chondrocytes would have within the native extracellular environment.

5.3 Hydrogel Characterization

Another goal of the modified A-PTMC-PEG-PTMC-A/MCS hydrogels was to attempt to match the mechanical properties of articular cartilage. As a minimum design requirement, the gels should be able to withstand relatively high loads and strains without excessive swelling. These attributes should allow the gels to persist in the defect site with repetitive loading of the joint and hydrogels. The equilibrium compressive moduli of MCS, 3.4k/MCS, and 20k/MCS hydrogels were measured in unconfined compression. At 20% total polymer content, the MCS and 3.4k/MCS hydrogels had the highest moduli although only the 3.4k/MCS gels were significantly stiffer than the 20k/MCS. This was expected given the

larger molecular weight between functional groups in the A-PTMC-PEG-PTMC-A chains of the 20k versus 3.4k. The increased molecular weight results in a larger molecular weight between crosslinks and a lower modulus in crosslinked gels. Comparisons to articular cartilage can be difficult due to the wide array of equipment setups and protocols (Anseth et al. 1996; Oyen 2014). Mechanical properties also vary with species, depth within cartilage, and location within the joint (Athanasiou et al. 1991; Mow et al. 1980). However, the compressive modulus of articular cartilage is approximately 0.5-1 MPa, which is at least 2 times higher than the compressive moduli of the 20% w/w hydrogels formed in the present study (Buckwalter et al. 2005; Athanasiou et al. 1991). Considering the moduli are within the same order of magnitude and A-PTMC-PEG-PTMC-A increases the hydrogel toughness, the gels may persist in the defect site long enough for cartilage remodeling to occur. Part of the discrepancy between moduli can be attributed to the much higher equilibrium water content of the hydrogels compared to cartilage. Cartilage is cited as containing 70% – 80% water (Mow et al. 1980), whereas the MCS, 3.4k/MCS, and 20k/MCS hydrogels all had water contents above 90%. Hydrogel toughness and strain at failure were also measured to determine how much energy the gels can absorb before failure. The 20k/MCS gels were able to absorb 8 times as much energy as MCS only gels, and they failed at twice the strain. Comparison to the toughness of articular cartilage is difficult since the fracture toughness of articular cartilage is historically performed with notch tests in tension (Xiao et al. 2013; Simha et al. 2004). The fracture toughness of bovine articular cartilage calculated by Simha *et al.* was 1.10 ± 14 kN/m. These results show that incorporating the A-PTMC-PEG-PTMC-A copolymers into MCS gels allows them to absorb more energy without significant losses in stiffness.

Chapter 6

Conclusions and Future Recommendations

6.1 Summary and Conclusions

An affordable cartilage tissue engineering strategy is of growing importance due to the increasing prevalence of OA (Bitton 2009; Murphy & Helmick 2012). ASCs have been extensively investigated for such a purpose because of their capacity for chondrogenic differentiation and trophic effects on neighboring cells (Ruetze & Richter 2014; Perdisa et al. 2015). In the present work, the soluble factors secreted by ASCs were hypothesized to encourage chondrocyte chemotaxis and the first aim of this study was to measure chondrocyte migration towards ASCs. Contrary to the initial hypothesis, Boyden chamber migration assays showed that bASCs might not be capable of promoting chondrocyte migration. Long-term migration in a 3-D environment has yet to be tested, but migration of P0 chondrocytes was less than 3% on 2-D membranes after 24 h for all conditions analyzed. This finding indicates that ASCs alone may not be capable of encouraging chondrocyte migration from the defect periphery into an ASC-seeded scaffold filling the defect site. The incorporation of specific chondrocyte chemoattractants in the tissue engineering approach may be necessary to promote chondrocyte migration.

The second aim of the study was to develop and refine an injectable and *in situ* gelling PEG-PTMC and MCS hydrogel for ASC encapsulation. End functionalized, low molecular weight di-block copolymers (1000 – 1500 g/mol) were synthesized first to reduce the swelling and increase the compressive modulus of MCS hydrogels. However, cytotoxicity and encapsulation experiments showed that the di-block copolymers caused significant ASC death. To improve the viability of encapsulated ASCs, higher molecular weight tri-

block copolymers were synthesized from 3.4k and 20k g/mol PEG initiators. The hydrogels formed with the A-PTMC-PEG-PTMC-A tri-block copolymers and MCS had greater toughness and higher ultimate strain as compared to MCS hydrogels. Specifically, hydrogels with 10 wt% A-PTMC-PEG-PTMC-A had an ultimate strain and toughness at least 50% and 600% higher than MCS hydrogels, respectively. ASC viability in A-PTMC-PEG-PTMC-A/MCS hydrogels was lower than MCS alone counterparts, but incorporation of RGD, GLOGEN, and GVOGEA peptides increased viability as measured by LIVE/DEAD stain. When viability was measured with MTT reagent the effect of peptide conjugation was no longer apparent, indicating that cell metabolism was decreased while maintaining cell viability. There is room for improvement in terms of bASC viability within the hydrogels, but further experiments with peptide modification and gel filtration of the A-PTMC-PEG-PTMC-A macromer might yield improvements. These preliminary results show promise for the A-PTMC-PEG-PTMC-A and MCS hydrogels as scaffolds for bASC encapsulation and cartilage tissue engineering.

6.2 Contributions

Specific contributions of this thesis to the field are listed as follows:

- Compared the migration of P0 and P2 chondrocytes
    - Demonstrated the significant difference in migration between P2 and freshly isolated articular chondrocytes
- Measured the migration of chondrocytes towards bASCs, PDGF-BB, and IGF-I
    - The presence of bASCs in the well actually reduced chondrocyte migration compared to medium only controls

    - Confirmed that PDGF-BB and IGF-I are P2 chondrocyte chemoattractants from 2.5 ng/mL up to 100 ng/mL
- Synthesized and measured mechanical properties of di-block and tri-block PEG-PTMC copolymers and measured ASC viability within A-PTMC-PEG-PTMC-A/MCS hydrogels
    - Showed that low molecular weight MA-PEG-PTMC-A di-block colpolymers cause significant ASC death when dissolved in medium or combined in MCS hydrogels
    - Showed that incorporation of mimetic peptides including RGD, GLOGEN, and GVOGEA increase bASC viability as measured by LIVE/DEAD stain

6.3 Future Work and Recommendations

The specific aims of this study can be further investigated before analyzing the differentiation and tissue remodeling aspect of the hypothesis. Specifically, the migration of chondrocytes in a long-term, 3-D scaffold would be more representative of the *in situ* environment. Further refinements to the A-PTMC-PEG-PTMC-A/MCS hydrogel system may increase the viability of encapsulated ASCs while maintaining the toughness and modulus measured in this study.

- **Chondrocyte migration towards ASCs**
    - Determine the migration of P0 chondrocytes towards ASCs, PDGF-BB, and IGF-I in the A-PTMC-PEG-PTMC-A /MCS hydrogel system by encapsulating chondrocytes in peptide-modified hydrogels and exposing them to a gradient

of the chemoattractant (*i.e.* ASCs encapsulated in the second half of the gel or growth factors in wells and chondrocyte gels in inserts)

- Incorporate RGD, GLOGEN, and GVOGEA peptides in the hydrogels to measure any differences in chondrocyte migration on the various integrin-binding peptides
- Measure the migration of chondrocytes in a cartilage explant model using cartilage biopsies surrounded by ASCs encapsulated in the A-PTMC-PEG-PTMC-A /MCS hydrogel system (this approach is more representative of the *in situ* environment, but may be more challenging)

- **Refined PEG-PTMC/MCS hydrogels**
  - Perform gel filtration of the A-PTMC-PEG-PTMC-A macromers as a final purification step before encapsulation studies (possible removal of any residual TEA·HCl)
  - Compare a number of viability and cell counting assays for measuring ASC viability (*e.g.* LIVE/DEAD, MTT, PicoGreen, CellTiter-Glo, *etc.*) to determine which assays provide the most robust measure of cell viability
  - Synthesize copolymers with lower TMC molecular weights to see if there is a noticeable correlation between cell survival and TMC block length, and compare results to PEG-DA as an unmodified condition. Use the final results to choose a A-PTMC-PEG-PTMC-A composition for future studies
  - Measure the mechanical properties, injection dynamics, and gelling dynamics of the proposed hydrogel system
- **Measuring Tissue Remodeling**

- Compare the viability of ASCs and chondrocytes in the peptide-modified hydrogel system and measure chondrogenic genes during the culture period to monitor the differentiation of ASCs and determine which peptide is best suited for cartilage regeneration. Section and stain the hydrogels for cartilage matrix molecules such as collagen II, sulphated GAGs, and aggrecan
- Perform a similar experiment with a cartilage explant model before moving on to filling cartilage defects in an animal mode

References

Ahmed, T.A.E. & Hincke, M.T., 2010. Strategies for articular cartilage lesion repair and functional restoration. Tissue Engineering Part B, Reviews, 16(3), pp.305–329.

Akizuki, S., Yasukawa, Y. & Takizawa, T., 1997. Does arthroscopic abrasion arthroplasty promote cartilage regeneration in osteoarthritic knees with eburnation? A prospective study of high tibial osteotomy with abrasion arthroplasty versus high tibial osteotomy alone. Arthroscopy, 13(1), pp.9–17.

Albertsson, A. & Eklund, M., 1995. Influence of molecular structure on the degradation mechanism of degradable polymers: in vitro degradation of poly(trimethylene carbonate), poly(trimethylene carbonate-co-caprolactone), and poly(adipic anhydride). Journal of Applied Polymer Science, 57(1), pp.87–103. Available at: http://doi.wiley.com/10.1002/app.1995.070570109.

Alsalameh, S. et al., 2004. Identification of Mesenchymal Progenitor Cells in Normal and Osteoarthritic Human Articular Cartilage. Arthritis and Rheumatism, 50(5), pp.1522–1532.

Amsden, B. et al., 2004. Development of biodegradable injectable thermoplastic oligomers. Biomacromolecules, 5(2), pp.637–642.

Anderson, C.E., 1962. The structure and function of cartilage. The Journal of Bone and Joint Surgery. American Volume, 44-A, pp.777–786.

Anseth, K.S., Bowman, C.N. & Brannon-Peppas, L., 1996. Mechanical properties of hydrogels and their experimental determination. Biomaterials, 17(17), pp.1647–1657.

Athanasiou, K.A. et al., 1991. Interspecies comparisons of in situ intrinsic mechanical properties of distal femoral cartilage. Journal of Orthopaedic Research, 9(3), pp.330–340.

Bahney, C.S. et al., 2011. A bioresponsive hydrogel tuned to chondrogenesis of human mesenchymal stem cells. The FASEB Journal, 25(5), pp.1486–1496.

Balakrishnan, B. & Banerjee, R., 2011. Biopolymer-based hydrogels for cartilage tissue engineering. Chemical Reviews, 111(8), pp.4453–4474.

Becerra, J. et al., 2010. Articular cartilage- Structure and regeneration. Tissue Engineering Part B, 16(6), pp.617–627.

Benya, P.D. & Shaffer, J.D., 1982. Dedifferentiated chondrocytes reexpress the differentiated collagen phenotype when cultured in agarose gels. Cell, 30(1), pp.215–224.

Bettini, R., Colombo, P. & Peppas, N. a., 1995. Solubility effects on drug transport through pH-sensitive, swelling-controlled release systems: Transport of theophylline and metoclopramide monohydrochloride. Journal of Controlled Release, 37(1-2), pp.105–111.

Bitton, R., 2009. The economic burden of osteoarthritis. The American journal of managed care, 15(8 Suppl), pp.S230–S235.

Block, G.J. et al., 2009. Multipotent stromal cells are activated to reduce apoptosis in part by upregulation and secretion of stanniocalcin-1. Stem cells, 27(3), pp.670–681.

Bosnakovski, D. et al., 2006. Chondrogenic Differentiation of Bovine Bone Marrow Mesenchymal Stem Cells (MSCs) in Different Hydrogels : Influence of Collagen Type II Extracellular Matrix on MSC Chondrogenesis. Biotechnology and Bioengineering.

Böstman, O.M. & Pihlajamäki, H.K., 2000. Adverse tissue reactions to bioabsorbable fixation devices. Clinical orthopaedics and related research, (371), pp.216–227.

Boyle, J. et al., 1995. Characterization of proteoglycan accumulation during formation of cartilagenous tissue in vitro. Osteoarthritis and Cartilage, 3, pp.117–125.

Brittberg, M. et al., 1994. Treatment of Deep Cartilage Defects in the Knee with Autologous Chondrocyte Transplantation. The New England Journal of MedicineNew England Journal of Medicine, 331(14).

Bryant, S.J., Chowdhury, T.T., et al., 2004. Crosslinking density influences chondrocyte metabolism in dynamically loaded photocrosslinked poly(ethylene glycol) hydrogels. Annals of Biomedical Engineering, 32(3), pp.407–417.

Bryant, S.J., Anseth, K.S., et al., 2004. Crosslinking density influences the morphology of chondrocytes photoencapsulated in PEG hydrogels during the application of compressive strain. Journal of Orthopaedic Research, 22(5), pp.1143–1149.

Bryant, S.J., Bender, R.J., et al., 2004. Encapsulating chondrocytes in degrading PEG hydrogels with high modulus: engineering gel structural changes to facilitate cartilaginous tissue production. Biotechnology and Bioengineering, 86(7), pp.747–55. Available at: http://www.ncbi.nlm.nih.gov/pubmed/15162450 [Accessed March 26, 2013].

Bryant, S.J. & Anseth, K.S., 2003. Controlling the spatial distribution of ECM components in degradable PEG hydrogels for tissue engineering cartilage. Journal of Biomedical Materials Research - Part A, 64(1), pp.70–9. Available at: http://www.ncbi.nlm.nih.gov/pubmed/12483698.

Bryant, S.J. & Anseth, K.S., 2002. Hydrogel properties influence ECM production by chondrocytes photoencapsulated in poly(ethylene glycol) hydrogels. Journal of Biomedical Materials Research, 59(1), pp.63–72.

Bryant, S.J. & Anseth, K.S., 2001. The effects of scaffold thickness on tissue engineered cartilage in photocrosslinked poly(ethylene oxide) hydrogels. Biomaterials, 22(6), pp.619–626.

Bryant, S.J., Durand, K.L. & Anseth, K.S., 2003. Manipulations in hydrogel chemistry control photoencapsulated chondrocyte behavior and their extracellular matrix production. Journal of Biomedical Materials Research - Part A, 67(4), pp.1430–1436.

Buckwalter, J.A. & Mankin, H.J., 1997. Articular Cartilage Part I: Tissue Design and Chondrocyte-Matrix Interactions. The Journal of Bone and Joint Surgery. American Volume, 79-A(4), pp.600–611.

Buckwalter, J.A., Mankin, H.J. & Grodzinsky, A.J., 2005. Articular Cartilage and Osteoarthristis. AAOS Instructional Course Lectures, 54, pp.465–480.

Buckwalter, J.A. & Rosenberg, L., 1983. Structural Changes during Development in Bovine Fetal Epiphyseal Cartilage. Collagen and Related Research, 3(6), pp.489–504. Available at: http://dx.doi.org/10.1016/S0174-173X(83)80028-4.

Burdick, J.A. & Anseth, K.S., 2002. Photoencapsulation of osteoblasts in injectable RGD-modified PEG hydrogels for bone tissue engineering. Biomaterials, 23(22), pp.4315–4323.

Chang, C., Lauffenburger, D.A. & Morales, T.I., 2003. Motile chondrocytes from newborn calf: Migration properties and synthesis of collagen II. Osteoarthritis and Cartilage, 11(8), pp.603–612.

Chang, J., Nakajima, H. & Poole, C.A., 1997. Structural colocalisation of type VI collagen and fibronectin in agarose cultured chondrocytes and isolated chondrons extracted from adult canine tibial cartilage. Journal of Anatomy, 190 (Pt 4, pp.523–532.

Chen, W.C. et al., 2011. Compare the effects of chondrogenesis by culture of human mesenchymal stem cells with various type of the chondroitin sulfate C. Journal of Bioscience and Bioengineering, 111(2), pp.226–231. Available at: http://dx.doi.org/10.1016/j.jbiosc.2010.10.002.

Chen, X. et al., 2005. Quantitative proteomic analysis of the secretory proteins from rat adipose cells using a 2D liquid chromatography-MS/MS approach. Journal of Proteome Research, 4(2), pp.570–577.

Chiellini, C. et al., 2008. Characterization of human mesenchymal stem cell secretome at early steps of adipocyte and osteoblast differentiation. BMC Molecular Biology, 9, p.26.

Chung, C. & Burdick, J.A., 2009. Influence of three-dimensional hyaluronic acid microenvironments on mesenchymal stem cell chondrogenesis. Tissue Engineering Part A, 15(2), pp.243–254.

Clark, J.M., 1985. The organisation of collagen in cryofractured rabbit articular cartilage: a scanning electron microscopic study. Journal of Orthopaedic Research, 3(1), pp.17–29. Available at: http://www.ncbi.nlm.nih.gov/pubmed/3981292.

Cloyd, J.M. et al., 2007. Material properties in unconfined compression of human nucleus pulposus, injectable hyaluronic acid-based hydrogels and tissue engineering scaffolds. European Spine Journal, 16(11), pp.1892–1898.

Cohen, N.P., Mow, V.C. & Foster, R.J., 1998. Composition and Dynamics of Articular Cartilage : Structure , Function , and Maintaining Healthy State. Orthopaedic & Sports Physical Therapy, 28(4), pp.203–215.

Connelly, J.T., García, A.J. & Levenston, M.E., 2008. Interactions between integrin ligand density and cytoskeletal integrity regulate BMSC chondrogenesis. Journal of Cellular Physiology, 217(1), pp.145–154.

Cross, M. et al., 2014. The global burden of hip and knee osteoarthritis: estimates from the Global Burden of Disease 2010 study. Annals of the rheumatic diseases, 73(7), pp.1323– 30. Available at: http://www.ncbi.nlm.nih.gov/pubmed/24553908.

Dai, W.S. & Barbari, T.A., 1999. Hydrogel membranes with mesh size asymmetry based on the gradient crosslinking of poly(vinyl alcohol). Journal of Membrane Science, 156(1), pp.67–79.

Darling, E.M. & Athanasiou, K.A., 2005. Rapid phenotypic changes in passaged articular chondrocyte subpopulations. Journal of Orthopaedic Research, 23(2), pp.425–432.

De Ugarte, D. A., Morizono, K., Elbarbary, A., Alfonso, Z., Zuk, P. A., Zhu, M., & Hedrick, M. H. 2003. Comparison of multi-lineage cells from human adipose tissue and bone marrow. Cells tissues organs, 174(3), pp.101-109.

Dehne, T. et al., 2009. Chondrogenic differentiation potential of osteoarthritic chondrocytes and their possible use in matrix-associated autologous chondrocyte transplantation. Arthritis research & therapy, 11(5), p.R133.

Diaz-Romero, J. et al., 2005. Immunophenotypic analysis of human articular chondrocytes: Changes in surface markers associated with cell expansion in monolayer culture. Journal of Cellular Physiology, 202(3), pp.731–742.

Dowthwaite, G.P. et al., 2004. The surface of articular cartilage contains a progenitor cell population. Journal of Cell Science, 117(Pt 6), pp.889–897.

Dragoo, J.L. et al., 2003. Tissue-engineered cartilage and bone using stem cells from human infrapatellar fat pads. The Journal of Bone and Joint Surgery. British Volume, 85(5), pp.740–747.

Duan, S., 2005. Negative cooperative effect of cytotoxicity of a di-component initiating system for a novel injectable tissue engineering hydrogel. Chinese Science Bulletin, 50(11), p.1093. Available at: http://219.238.6.200/article?code=982004-459&jccode=98.

Dürr, J. et al., 1993. Localization of beta 1-integrins in human cartilage and their role in chondrocyte adhesion to collagen and fibronectin. Experimental cell research, 207(2), pp.235–244.

Ebert, J.R. et al., 2011. Clinical and magnetic resonance imaging-based outcomes to 5 years after matrix-induced autologous chondrocyte implantation to address articular cartilage defects in the knee. The American journal of sports medicine, 39(4), pp.753–763.

Elisseeff, J. et al., 1999. Transdermal photopolymerization of poly(ethylene oxide)-based injectable hydrogels for tissue-engineered cartilage. Plastic and Reconstructive Surgery, 104(4), pp.1014–22. Available at: http://www.ncbi.nlm.nih.gov/pubmed/10654741.

Erickson, I.E. et al., 2009. Differential maturation and structure-function relationships in mesenchymal stem cell- and chondrocyte-seeded hydrogels. Tissue Engineering Part A, 15(5), pp.1041–1052.

Eyre, D.R., Weis, M.A. & Wu, J.J., 2006. Articular cartilage collagen: An irreplaceable framework? European Cells and Materials, 12, pp.57–63.

Fertala, A., Han, W.B. & Ko, F.K., 2001. Mapping critical sites in collagen II for rational design of gene-engineered proteins for cell-supporting materials. Journal of Biomedical Materials Research, 57(1), pp.48–58.

Flynn, L. et al., 2007. Adipose tissue engineering with naturally derived scaffolds and adipose-derived stem cells. Biomaterials, 28, pp.3834–3842.

Frenkel, S.R. et al., 1996. Effects of nitric oxide on chondrocyte migration, adhesion, and cytoskeletal assembly. Arthritis and Rheumatism, 39(11), pp.1905–1912.

Fujita, T. et al., 2004. Runx2 induces osteoblast and chondrocyte differentiation and enhances their migration by coupling with PI3K-Akt signaling. Journal of Cell Biology, 166(1), pp.85–95.

Furukawa, T. et al., 1980. Biochemical studies on repair cartilage resurfacing experimental defects in the rabbit knee. The Journal of Bone and Joint Surgery. American Volume, 62(1), pp.79–89.

Gill, T.J. et al., 2005. Chondral defect repair after the microfracture procedure: a nonhuman primate model. The American journal of sports medicine, 33(5), pp.680–685.

Gooding, C.R. et al., 2006. A prospective, ranomised study comparing two techniques of autologous chondrocyte implantation for osteochondral defects in the knee: Periosteum covered versus type I/III collagen covered. The Knee, 13(3), pp.203–210.

Gosiewska, A. et al., 2001. Development of a three-dimensional transmigration assay for testing cell--polymer interactions for tissue engineering applications. Tissue Engineering, 7(3), pp.267–277.

Gotoh, T., Nakatani, Y. & Sakohara, S., 1998. Novel synthesis of thermosensitive porous hydrogels. Journal of Applied Polymer Science, 69(5), pp.895–906. Available at: http://doi.wiley.com/10.1002/(SICI)1097-4628(19980801)69:5<895::AID-APP8>3.0.CO;2-H.

Griffon, D.J. et al., 2006. Chitosan scaffolds: Interconnective pore size and cartilage engineering. Acta Biomaterialia, 2(3), pp.313–320.

Gu, W.Y., Lai, W.M. & Mow, V.C., 1993. Transport of fluid and ions through a porous-permeable charged-hydrated tissue, and streaming potential data on normal bovine articular cartilage. Journal of Biomechanics, 26(6), pp.709–723.

Guilak, F. & Mow, V.C., 2000. The mechanical environment of the chondrocyte: A biphasic finite element model of cell-matrix interactions in articular cartilage. *Journal of Biomechanics*, 33(12), pp.1663–1673.

Guilak, F., Ratcliffe, a. & Mow, V.C., 1995. Chondrocyte deformation and local tissue strain in articular cartilage: A confocal microscopy study. *Journal of Orthopaedic Research*, 13(3), pp.410–421.

Hamaia, S.W. et al., 2012. Mapping of potent and specific binding motifs, GLOGEN and GVOGEA, for integrin 1αβ1 using collagen toolkits II and III. Journal of Biological Chemistry, 287(31), pp.26019–26028.

Hangody, L. et al., 2008. Autologous osteochondral grafting-Technique and long-term results. Injury, 39(1 SUPPL), pp.32–39.

Harty M., 1978. In: Simon WH, editor. The human joint in health and disease. Anatomy and development of joints, Philadelphia: U. Pennsylvania, p. 3-8

Hattori, S., Oxford, C. & Reddi, A.H., 2007. Identification of superficial zone articular chondrocyte stem/progenitor cells. Biochemical and Biophysical Research Communications, 358(1), pp.99–103.

Hayami, J.W.S., Waldman, S.D. & Amsden, B.G., 2011. A Photocurable Hydrogel / Elastomer Composite Scaffold with Bi-Continuous Morphology for Cell Encapsulation a. Macromolecular Bioscience, 11, pp.1672–1683.

Hayami, J.W.S., Waldman, S.D. & Amsden, B.G., 2015. Photo-cross-linked methacrylated polysaccharide solution blends with high chondrocyte viability, minimal swelling, and moduli similar to load bearing soft tissues. European Polymer Journal, pp.1–11. Available at: http://linkinghub.elsevier.com/retrieve/pii/S0014305715000518.

Heino, J., 2007. The collagen family members as cell adhesion proteins. BioEssays, 29(10), pp.1001–1010.

Hennink, W.E. & van Nostrum, C.F., 2012. Novel crosslinking methods to design hydrogels. Advanced Drug Delivery Reviews, 64(SUPPL.), pp.223–236. Available at: http://dx.doi.org/10.1016/j.addr.2012.09.009.

Hidaka, C. et al., 2006. Maturational differences in superficial and deep zone articular chondrocytes. Cell and Tissue Research, 323(1), pp.127–135.

Hidaka, C. & Goldring, M.B., 2008. Regulatory Mechanisms of Chondrogenesis and Implications for Understanding Articular Cartilage Homeostasis. Current Rheumatology Reviews, 4(3), pp.136–147.

Hoffman, A.S., 2012. Hydrogels for biomedical applications. Advanced Drug Delivery Reviews, 64(SUPPL.), pp.18–23. Available at: http://dx.doi.org/10.1016/j.addr.2012.09.010.

Hsiao, S.T.-F. et al., 2012. Comparative Analysis of Paracrine Factor Expression in Human Adult Mesenchymal Stem Cells Derived from Bone Marrow, Adipose, and Dermal Tissue. Stem Cells and Development, 21(12), pp.2189–2203.

Hsu, S.H. et al., 2006. Evaluation of biodegradable polyesters modified by type II collagen and Arg-Gly-Asp as tissue engineering scaffolding materials for cartilage regeneration. Artificial Organs, 30(1), pp.42–55.

Huang, L.K., Mehta, R.C. & DeLuca, P.P., 1997. Evaluation of a Statistical Model for the Formation of Poly[Acryloyl Hydroxyethyl Starch] Microspheres. Pharmaceutical Research, 14(4), pp.475–482.

Hunziker, E.B., 2002. Articular cartilage repair: basic science and clinical progress. A review of the current status and prospects. Osteoarthritis and Cartilage, 10(6), pp.432–63.

Available at: http://www.ncbi.nlm.nih.gov/pubmed/12056848 [Accessed March 5, 2013].

Hunziker, E.B. & Quinn, T.M., 2003. Surgical removal of articular cartilage leads to loss of chondrocytes from cartilage bordering the wound edge. The Journal of Bone and Joint Surgery. American Volume, 85-A Suppl, pp.85–92.

Hwang, N.S. et al., 2006. Chondrogenic Differentiation of Human Embryonic Stem Cell-Derived Cells in Arginine-Glycine-Aspartate-Modified Hydrogels. Tissue Engineering, 12(9), pp.2695–2706.

Im, G. Il, Shin, Y.W. & Lee, K.B., 2005. Do adipose tissue-derived mesenchymal stem cells have the same osteogenic and chondrogenic potential as bone marrow-derived cells? Osteoarthritis and Cartilage, 13(10), pp.845–853.

Insall, J.N., 1967. Intra-articular surgery for degenerative arthritis of the knee. A report of the work of the late K. H. Pridie. The Journal of Bone and Joint Surgery. British Volume, 49(2), pp.211–228.

Jiang, Y. & Tuan, R.S., 2014. Origin and function of cartilage stem/progenitor cells in osteoarthritis. Nature Reviews Rheumatology, 11(4), pp.206–212. Available at: http://www.nature.com/doifinder/10.1038/nrrheum.2014.200.

Khan, W.S., Johnson, D.S. & Hardingham, T.E., 2010. The potential of stem cells in the treatment of knee cartilage defects. The Knee, 17(6), pp.369–374. Available at: http://dx.doi.org/10.1016/j.knee.2009.12.003.

Kilroy, G.E. et al., 2007. Cytokine Profile of HumanAdipose-Derived Stem Cells:Expression of Angiogenic,Hematopoietic, and Pro-Inflammatory Factors. Journal of Cellular Physiology, pp.702–709.

Kim, H.D. et al., 2015. Extracellular-Matrix-Based and Arg-Gly-Asp–Modified Photopolymerizing Hydrogels for Cartilage Tissue Engineering. Tissue Engineering Part A, 21(3-4), pp.757–766. Available at: http://online.liebertpub.com/doi/abs/10.1089/ten.tea.2014.0233.

Kim, S.H. & Chu, C.C., 2000. Synthesis and characterization of dextran-methacrylate hydrogels and structural study by SEM. Journal of Biomedical Materials Research, 49(4), pp.517–527.

Kisiday, J.D. et al., 2008. Evaluation of adult equine bone marrow- and adipose-derived progenitor cell chondrogenesis in hydrogel cultures. Journal of Orthopaedic Research, 26(3), pp.322–331.

Kock, L., Van Donkelaar, C.C. & Ito, K., 2012. Tissue engineering of functional articular cartilage: The current status. Cell and Tissue Research, 347(3), pp.613–627.

Koga, H. et al., 2008. Comparison of mesenchymal tissues-derived stem cells for in vivo chondrogenesis: Suitable conditions for cell therapy of cartilage defects in rabbit. Cell and Tissue Research, 333(2), pp.207–215.

Kopesky, P.W. et al., 2010. Adult equine bone marrow stromal cells produce a cartilage-like ECM mechanically superior to animal-matched adult chondrocytes. Matrix Biology, 29(5), pp.427–438. Available at: http://dx.doi.org/10.1016/j.matbio.2010.02.003.

Korhonen, R.K. et al., 2002. Comparison of the equilibrium response of articular cartilage in unconfined compression, confined compression and indentation. Journal of Biomechanics, 35(7), pp.903–909.

Kotlarz, H. et al., 2009. Insurer and out-of-pocket costs of osteoarthritis in the US: Evidence from national survey data. Arthritis and Rheumatism, 60(12), pp.3546–3553.

Kouri, J.B. et al., 1996. Ultrastructural study of chondrocytes from fibrillated and non-fibrilliated human osteoarthritis cartilage. Osteoarthritis and Cartilage, 4, pp.111–125.

Kuettner, K.E. et al., 1982. Synthesis of cartilage matrix by mammalian chondrocytes in vitro. I. Isolation, culture characteristics, and morphology. Journal of Cell Biology, 93(3), pp.743–750.

Lee, M.J. et al., 2010. Proteomic analysis of tumor necrosis factor-alpha-induced secretome of human adipose tissue-derived mesenchymal stem cells. Journal of Proteome Research, 9(4), pp.1754–1762.

Li, Q. et al., 2011. Comparing the chondrogenic potential in vivo of autogeneic mesenchymal stem cells derived from different tissues. Artificial cells, blood substitutes, and immobilization biotechnology, 39(1), pp.31–38.

Li, Q. et al., 2004. Photocrosslinkable polysaccharides based on chondroitin sulfate. Journal of Biomedical Materials Research - Part A, 68(1), pp.28–33.

Li, Q., Wang, D. & Elisseeff, J.H., 2003. Heterogeneous-phase reaction of glycidyl methacrylate and chondroitin sulfate: Mechanism of ring-opening-transesterification competition. Macromolecules, 36(7), pp.2556–2562.

Lien, S.M., Ko, L.Y. & Huang, T.J., 2009. Effect of pore size on ECM secretion and cell growth in gelatin scaffold for articular cartilage tissue engineering. Acta Biomaterialia, 5(2), pp.670–679. Available at: http://dx.doi.org/10.1016/j.actbio.2008.09.020.

Liu, S.Q. et al., 2010. Biomimetic hydrogels for chondrogenic differentiation of human mesenchymal stem cells to neocartilage. Biomaterials, 31(28), pp.7298–7307. Available at: http://dx.doi.org/10.1016/j.biomaterials.2010.06.001.

Livesley, P.J. et al., 1991. Arthroscopic lavage of osteoarthritic knees. The Journal of Bone and Joint Surgery. British Volume, 73(6), pp.922–926.

Loeser, R.F. et al., 2000. Integrin expression by primary and immortalized human chondrocytes: Evidence of a differential role for a1B1 and a2B1 integrins in mediating chondrocyte adhesion to types II and VI collagen. Osteoarthritis and Cartilage, 8(2), pp.96–105.

Lu, L. et al., 2005. Effects of dynamic fluid pressure on chondrocytes cultured in biodegradable poly(glycolic acid) fibrous scaffolds. Tissue Engineering, 11(11-12), pp.1852–1859.

Lu, Z. et al., 2010. Collagen type II enhances chondrogenesis in adipose tissue-derived stem cells by affecting cell shape. Tissue Engineering Part A, 16(1), pp.81–90.

Luzak, B. et al., 2003. Inhibition of collagen-induced platelet reactivity by DGEA peptide Circled white star. Acta Biochimica Polonica, 50(4), pp.1119–1128.

Lyman, J.R., Kelley, S.S. & Lee, G., 2000. Chondrocyte process extension and migration in response to partial thickness cartilage injuries in human explants, Orlando, Florida.

Maniwa, S. et al., 2001. Effects of hyaluronic acid and basic fibroblast growth factor on motility of chondrocytes and synovial cells in culture. Acta orthopaedica Scandinavica, 72(3), pp.299–303.

Mankin, H. J., Mow, V. C., Buckwalter, J. A., Iannotti, J. P., & Ratcliffe, A. 1994. Form and function of articular cartilage. Orthopaedic Basic Science. Rosemont, Ill: American Academy of Orthopaedic Surgeons, pp.1-44.

Mao, S. et al., 2005. Synthesis, characterization and cytotoxicity of poly(ethylene glycol)-graft-trimethyl chitosan block copolymers. Biomaterials, 26(32), pp.6343–6356.

Marsano, E. et al., 2000. Hydroxypropyl-cellulose derivatives: Phase behaviour of hydroxypropylcellulose methacrylate. Polymer, 41(2), pp.533–538.

Massia, S.P. & Hubbell, J.A., 1992. Tissue engineering in the vascular graft. Cytotechnology, 10, pp.189–204.

Maxson, S. et al., 2012. Concise Review: Role of Mesenchymal Stem Cells in Wound Repair. Stem Cells Translational Medicine, 1(2), pp.142–149.

Mayne, R. et al., 1976. Changes in type of collagen synthesized as clones of chick chondrocytes grow and eventually lose division capacity. Proceedings of the National Academy of Sciences of the United States of America, 73(5), pp.1674–1678.

Mazor, M. et al., 2014. Mesenchymal stem-cell potential in cartilage repair: an update. Journal of Cellular and Molecular Medicine, 18(12), pp.2340–2350. Available at: http://doi.wiley.com/10.1111/jcmm.12378.

McGregor, A.J., Amsden, B.G. & Waldman, S.D., 2011. Chondrocyte repopulation of the zone of death induced by osteochondral harvest. Osteoarthritis and Cartilage, 19, pp.242–248.

Mironi-Harpaz, I. et al., 2012. Photopolymerization of cell-encapsulating hydrogels: Crosslinking efficiency versus cytotoxicity. Acta Biomaterialia, 8(5), pp.1838–1848. Available at: http://dx.doi.org/10.1016/j.actbio.2011.12.034.

Mishima, Y. & Lotz, M., 2008. Chemotaxis of Human Articular Chondrocytes and Mesenchymal Stem Cells. Journal of Orthopaedic Research, 26(10), pp.1407–1412.

Morales, T.I., 2007. Review Chondrocyte moves: clever strategies? Osteoarthritis and Cartilage, 15, pp.861–871.

Mow, V.C. et al., 1980. Biphasic creep and stress relaxation of articular cartilage in compression? Theory and experiments. Journal of Biomechanical Engineering, 102(1), pp.73–84.

Mow, V.C., Holmes, M.H. & Lai, W.M., 1984. Fluid transport and mechanical properties of articular cartilage: a review. Journal of Biomechanics, 17(5), pp.377–394.

Mow, V.C., Ratcliffe, A. & Poole, A.R., 1992. Cartilage and diarthrodial joints as paradigms for hierarchical materials and structures. Biomaterials, 13(2), pp.67–97.

Murphy, L. & Helmick, C.G., 2012. The Impact of Osteoarthritis in the United States. Orthopaedic Nursing, 31(2), pp.85–91.

Muzzarelli, R.A.A. et al., 2012. Chitosan, hyaluronan and chondroitin sulfate in tissue engineering for cartilage regeneration: A review. Carbohydrate Polymers, 89(3), pp.723–739. Available at: http://dx.doi.org/10.1016/j.carbpol.2012.04.057.

Nakahara, H., Goldberg, V.M. & Caplan, A.I., 1991. Culture-expanded human periosteal-derived cells exhibit osteochondral potential in vivo. Journal of Orthopaedic Research, 9(4), pp.465–476.

Nettles, D.L. et al., 2004. Photocrosslinkable hyaluronan as a scaffold for articular cartilage repair. Annals of Biomedical Engineering, 32(3), pp.391–397.

Nevo, Z., et al. 1990. Culturing chondrocytes for implantation. Methods in Cartilage Research, Academic Press, London, pp.98-104.

Newman, A.P., 1998. Articular Cartilage Repair. Am. J. Sports Med., 26(2), pp.309–324. Available at: http://ajs.sagepub.com.proxy1.lib.umanitoba.ca/content/26/2/309.full.pdf html.

Ng, K.W., Leong, D.T.W. & Hutmacher, D.W., 2005. The Challenge to Measure Cell Proliferation in Two and Three Dimensions. Tissue Engineering, 11(1/2), pp.182–191.

Nguyen, Q.T. et al., 2012. Cartilage-like mechanical properties of poly(ethylene glycol)-diacrylate hydrogels. Biomaterials, 28, pp.997–1003.

Nomizu, M. et al., 1995. Structure-activity study of a laminin alpha 1 chain active peptide segment Ile-Lys-Val-Ala-Val (IKVAV). FEBS letters, 365(2-3), pp.227–231.

Nuttelman, C.R., Tripodi, M.C. & Anseth, K.S., 2004. In vitro osteogenic differentiation of human mesenchymal stem cells photoencapsulated in PEG hydrogels. Journal of Biomedical Materials Research, 68A, pp.773–782.

Nuttelman, C.R., Tripodi, M.C. & Anseth, K.S., 2005. Synthetic hydrogel niches that promote hMSC viability. Matrix Biology, 24, pp.208–218.

Ogilvie-Harris, D.J. & Jackson, R.W., 1984. The Arthroscopic Treatment of Chondromalacia Patellae. Journal of Bone and Joint Surgery, pp.660–665.

Olee, T. et al., 1999. IL-18 is produced by articular chondrocytes and induces proinflammatory and catabolic responses. Journal of Immunology, 162(2), pp.1096–1100.

Van Osch, G.J.V.M. et al., 2009. Cartilage repair: past and future--lessons for regenerative medicine. Journal of Cellular and Molecular Medicine, 13(5), pp.792–810.

Oussedik, S., Tsitskaris, K. & Parker, D., 2015. Treatment of Articular Cartilage Lesions of the Knee by Microfracture or Autologous Chondrocyte Implantation: A Systematic Review. Arthroscopy: The Journal of Arthroscopic and Related Surgery, 31(4), pp.732–744. Available at: http://linkinghub.elsevier.com/retrieve/pii/S0749806314009414.

Oyen, M.L., 2014. Mechanical characterisation of hydrogel materials. International Materials Reviews, 59(1), pp.44–59. Available at: http://www.maneyonline.com/doi/full/10.1179/1743280413Y.0000000022.

Palmer, R.M.J. et al., 1993. Induction of Nitric Oxide Synthase in Human Chondrocytes. Biochemical and Biophysical Research Communications, 193(1), pp.398–405. Available at: http://www.sciencedirect.com/science/article/pii/S0006291X83716372.

Park, H. et al., 2009. Effect of swelling ratio of injectable hydrogel composites on chondrogenic differentiation of encapsulated rabbit marrow mesenchymal stem cells in vitro. Biomacromolecules, 10(3), pp.541–546.

Park, Y. et al., 2004. Bovine primary chondrocyte culture in synthetic matrix metalloproteinase-sensitive poly(ethylene glycol)-based hydrogels as a scaffold for cartilage repair. Tissue Engineering, 10(3-4), pp.515–522.

Pedley, D.G., Skelly, P.J. & Tighe, B.J., 1980. Hydrogels in Biomedical Applications. The British Polymer Journal, 12(September), pp.99–110.

Peppas, N.A. & Benner, R.E., 1980. Proposed method of intracordal injection and gelation of poly (vinyl alcohol) solution in vocal cords: Polymer considerations. Biomaterials, 1(3), pp.158–162.

Perdisa, F. et al., 2015. Review Article Adipose-Derived Mesenchymal Stem Cells for the Treatment of Articular Cartilage : A Systematic Review on Preclinical and Clinical Evidence. Stem Cells International.

Pestka, J.M. et al., 2011. In vitro cell quality of articular chondrocytes assigned for autologous implantation in dependence of specific patient characteristics. Archives of Orthopaedic and Trauma Surgery, 131(6), pp.779–789.

Poole, A. R., 1995. Imbalances of anabolism and catabolism of cartilage matrix components in osteoarthritis. Osteoarthritic disorders, pp.247-260.

Poole, A.R. et al., 1996. Contents and distributions of the proteoglycans decorin and biglycan in normal and osteoarthritic human articular cartilage. Journal of Orthopaedic Research, 14(5), pp.681–689.

Poole, C.A., 1997. Articular cartilage chondrons: form, function and failure. Journal of Anatomy, 191, pp.1–13.

Poole, C.A., Flint, M.H. & Beaumont, B.W., 1984. Morphological and functional interrelationships of articular cartilage matrices. Journal of Anatomy, 138(1), pp.113–138.

Pottenger, L.A. et al., 1982. Influence of cartilage particle size and proteoglycan aggregation on immobilization of proteoglycans. Journal of Biological Chemistry, 257(19), pp.11479–11485.

Qiu, W. et al., 2000. Outgrowth of chondrocytes from human articular cartilage explants and expression of alpha-smooth muscle actin. Wound Repair and Regeneration, 8(5), pp.383–391.

Rehman, J. et al., 2004. Secretion of Angiogenic and Antiapoptotic Factors by Human Adipose Stromal Cells. Circulation, 109(10), pp.1292–1298.

Reyes, C.D. & García, A.J., 2003. Engineering integrin-specific surfaces with a triple-helical collagen-mimetic peptide. Journal of Biomedical Materials Research - Part A, 65(4), pp.511–523.

Roughley, P.J. & Lee, E.R., 1994. Cartilage Proteoglycans: Structure and Potential Functions. Microscopy Research and Technique, 397(28), pp.385–397.

Ruetze, M. & Richter, W., 2014. Adipose-derived stromal cells for osteoarticular repair: trophic function versus stem cell activity. Expert reviews in molecular medicine, 16(May), p.e9. Available at: http://www.pubmedcentral.nih.gov/articlerender.fcgi?artid=4017835&tool=pmcentrez&rendertype=abstract.

Ruoslahti, E. & Pierschbacher, M.D., 1987. New perspectives in cell adhesion: RGD and integrins. Science, 238(4826), pp.491–497.

Salinas, C.N. & Anseth, K.S., 2008a. The enhancement of chondrogenic differentiation of human mesenchymal stem cells by enzymatically regulated RGD functionalities. Biomaterials, 29(15), pp.2370–2377.

Salinas, C.N. & Anseth, K.S., 2008b. The influence of the RGD peptide motif and its contextual presentation in PEG gels on human mesenchymal stem cell viability. Journal of Tissue Engineering and Regenerative Medicineedicine, 2, pp.296–304.

Schiltz, J.R., Mayne, R. & Holtzer, H., 1973. The Synthesis of Collagen and Glycosaminoglycans by Dedifferentiated Chondroblasts in Culture. Differentiation, 1(2), pp.97–108. Available at: http://dx.doi.org/10.1111/j.1432-0436.1973.tb00106.x.

Schüettler, K.F. et al., 2013. Repair of a chondral defect using a cell free scaffold in a young patient - a case report of successful scaffold transformation and colonisation. BMC Surgery.

Schulze-Tanzil, G. et al., 2002. Redifferentiation of dedifferentiated human chondrocytes in high-density cultures. Cell and Tissue Research, 308(3), pp.371–379.

Schumacher, B.L. et al., 1994. A novel proteoglycan synthesized and secreted by chondrocytes of the superficial zone of articular cartilage. Archives of biochemistry and biophysics, 311(1), pp.144–152.

Secretan, C., Bagnall, K.M. & Jomha, N.M., 2010. Effects of introducing cultured human chondrocytes into a human articular cartilage explant model. Cell and Tissue Research, 339, pp.421–427.

Seol, D. et al., 2012. Chondrogenic progenitor cells respond to cartilage injury. Arthritis and Rheumatism, 64(11), pp.3626–3637.

Seol, D. et al., 2014. Effect of Short-Term Enzymatic Treatment on Cell Migration and Cartilage Regeneration: In Vitro Organ Culture of Bovine Articular Cartilage. Tissue Engineering, 20(13), pp.1807–1814.

Setton, L.A., Zhu, W. & Mow, V.C., 1993. The biphasic poroviscoelastic behavior of articular cartilage: role of the surface zone in governing the compressive behavior. Journal of Biomechanics, 26(4-5), pp.581–592.

Seung, H.H. et al., 2008. Histological and biomechanical properties of regenerated articular cartilage using chondrogenic bone marrow stromal cells with a PLGA scaffold in vivo. Journal of Biomedical Materials Research - Part A, 87(4), pp.850–861.

Shakibaei, M., Csaki, C. & Mobasheri, A., 2008. Diverse roles of integrin receptors in articular cartilage.,

Shapiro, F., Koide, S. & Glimcher, M.J., 1993. Cell origin and differentiation in the repair of full-thickness defects of articular cartilage. The Journal of Bone and Joint Surgery. American Volume, 75(4), pp.532–553.

Shimizu, M. et al., 1997. Chondrocyte migration to fibronectin, type I collagen, and type II collagen. Cell Structure and Function, 22(3), pp.309–315.

Shin, H., Temenoff, J.S. & Mikos, A.G., 2003. In Vitro Cytotoxicity of Unsaturated Oligo [poly (ethylene glycol) fumarate] Macromers and Their Cross-Linked Hydrogels. Biomacromolecules, 4, pp.552–560.

Shin, H.J. et al., 2006. Electrospun PLGA nanofiber scaffolds for articular cartilage reconstruction: mechanical stability, degradation and cellular responses under mechanical stimulation in vitro. Journal of Biomaterials Science. Polymer Edition, 17(1- 2), pp.103–119.

Da Silva Meirelles, L. et al., 2009. Mechanisms involved in the therapeutic properties of mesenchymal stem cells. Cytokine and Growth Factor Reviews, 20(5-6), pp.419–427.

Simha, N.K., Carlson, C.S. & Lewis, J.L., 2004. Evaluation of fracture toughness of cartilage by micropenetration. Journal of Materials Science: Materials in Medicine, 15(5), pp.631–639.

Sims, C.D. et al., 1996. Injectable cartilage using polyethylene oxide polymer substrates. Plastic and Reconstructive Surgery, 98(5), pp.843–850.

Sittinger, M. et al., 1996. Resorbable polyesters in cartilage engineering: Affinity and biocompatibility of polymer fiber structures to chondrocytes. Journal of Biomedical Materials Research, 33(2), pp.57–63.

Skalnikova, H. et al., 2011. Mapping of the secretome of primary isolates of mammalian cells, stem cells and derived cell lines. Proteomics, 11(4), pp.691–708.

Smith Callahan, L.A. et al., 2013. Maximizing phenotype constraint and extracellular matrix production in primary human chondrocytes using arginine-glycine-aspartate concentration gradient hydrogels. Acta Biomaterialia, 9(7), pp.7420–7428. Available at: http://dx.doi.org/10.1016/j.actbio.2013.04.005.

Solheim, E. et al., 2010. Microfracture treatment of single or multiple articular cartilage defects of the knee: A 5-year median follow-up of 110 patients. Knee Surgery, Sports Traumatology, Arthroscopy, 18(4), pp.504–508.

Söntjens, S.H.M. et al., 2006. Biodendrimer-based hydrogel scaffolds for cartilage tissue repair. Biomacromolecules, 7(1), pp.310–316.

Spiller, K.L., Maher, S.A. & Lowman, A.M., 2011. Hydrogels for the repair of articular cartilage defects. Tissue Engineering Part B, Reviews, 17(4), pp.281–299.

Stadler, J. et al., 1991. Articular chondrocytes synthesize nitric oxide in response to cytokines and lipopolysaccharide. Journal of Immunology, 147(11), pp.3915–3920.

Steadman, J.R. et al., 1999. Die technik der mikrofrakturierung zur behandlung von kompletten knorpeldefekten im kniegelenk. Orthopade, 28(1), pp.26–32.

Steadman, J.R. et al., 2003. Outcomes of microfracture for traumatic chondral defects of the knee: Average 11-year follow-up. Arthroscopy: The Journal of Arthroscopic and Related Surgery, 19(5), pp.477–484.

Stockwell, RA., 1979. Biology of cartilage cells. Cambridge: Cambridge University Press
Strachan, R.K. et al., 1992. Arthroscopic Lavage and Debridement for Osteoarthritis of the Knee. Journal of Bone and Joint Surgery, 74-B, pp.534–537.

Strioga, M. et al., 2012. Same or Not the Same? Comparison of Adipose Tissue-Derived Versus Bone Marrow-Derived Mesenchymal Stem and Stromal Cells. Stem Cells and Development, 21(14), pp.2724–2752.

Suggs, L.J. et al., 1998. In vitro cytotoxicity and in vivo biocompatibility of poly (propylene fumarate-co-ethylene glycol) hydrogels.

Sukarto, A. et al., 2012. Co-delivery of adipose-derived stem cells and growth factor-loaded microspheres in RGD-grafted N-methacrylate glycol chitosan gels for focal chondral repair. Biomacromolecules, 13, pp.2490–2502.

Swann, D.A. et al., 1981. The lubricating activity of synovial fluid glycoproteins. Arthritis and Rheumatism, 24(1), pp.22–30.

Temenoff, J.S. et al., 2002. Effect of poly(ethylene glycol) molecular weight on tensile and swelling properties of oligo(poly(ethylene glycol) fumarate) hydrogels for cartilage tissue engineering. Journal of Biomedical Materials Research, 59(3), pp.429–437.

Temenoff, J.S. et al., 2004. Thermally cross-linked oligo(poly(ethylene glycol) fumarate) hydrogels support osteogenic differentiation of encapsulated marrow stromal cells in vitro. Biomacromolecules, 5(1), pp.5–10.

Temenoff, J.S. & Mikos, A.G., 2000. Review: tissue engineering for regeneration of articular cartilage. Biomaterials, 21(5), pp.431–40. Available at: http://www.ncbi.nlm.nih.gov/pubmed/10674807.

Tögel, F. et al., 2007. Vasculotropic, paracrine actions of infused mesenchymal stem cells are important to the recovery from acute kidney injury. American journal of physiology. Renal physiology, 292(5), pp.F1626–F1635.

Tuncel, A. & Cicek, H., 1998. Immobilization of a -Chymotrypsin in Thermally Reversible Isopropylacrylamide-Hydroxyethylmethacrylate Copolymer Gel. Journal of Polymer Science: Part A: Polymer Chemistry, 36, pp.543–552.

Ude, C.C. et al., 2014. Cartilage regeneration by chondrogenic induced adult stem cells in osteoarthritic sheep model. PLoS ONE, 9(6).

Varghese, S. et al., 2008. Chondroitin sulfate based niches for chondrogenic differentiation of mesenchymal stem cells. Matrix Biology, 27(1), pp.12–21.

Vinardell, T. et al., 2010. Composition-function Relations of Cartilaginous Tissues Engineered from Chondrocytes and Mesenchymal Stem Cells Isolated from Bone Marrow and Infrapatellar Fat Pad. Journal of Tissue Engineering and Regenerative Medicine, (January), pp.1–7.

Wakitani, S. et al., 2002. Human autologous culture expanded bone marrow-mesenchymal cell transplantation for repair of cartilage defects in osteoarthritic knees. Osteoarthritis and Cartilage, 10(3), pp.199–206.

Wakitani, S. et al., 1994. Mesenchymal cell-based repair of large, full-thickness defects of articular cartilage. The Journal of Bone and Joint Surgery. American Volume, 76(4), pp.579–592.

Wang, D.-A. et al., 2007. Multifunctional chondroitin sulphate for cartilage tissue-biomaterial integration. Nature Materials, 6(5), pp.385–392.

Wang, L.F., Shen, S.S. & Lu, S.C., 2003. Synthesis and characterization of chondroitin sulfate-methacrylate hydrogels. Carbohydrate Polymers, 52(4), pp.389–396.

Wang, M. et al., 2006. Human progenitor cells from bone marrow or adipose tissue produce VEGF, HGF, and IGF-I in response to TNF by a p38 MAPK-dependent mechanism. American journal of physiology. Regulatory, integrative and comparative physiology, 291(4), pp.R880–R884.

Wichterle, O. & Lím, D., 1960. Hydrophilic Gels for Biological Use. Nature, 185(4706), pp.117–118.

Williams, C.G. et al., 2005. Variable cytocompatibility of six cell lines with photoinitiators used for polymerizing hydrogels and cell encapsulation. Biomaterials, 26(11), pp.1211–1218.

Williamson, A.K. et al., 2001. Compressive properties and function - composition relationships of developing bovine articular cartilage. Journal of Orthopaedic Research, 19, pp.1113–1121. Available at: http://dx.doi.org/10.1016/S0736-0266(01)00052-3.

Wong, M. et al., 1996. Zone-specific cell biosynthetic activity in mature bovine articular cartilage: A new method using confocal microscopic stereology and quantitative autoradiography. Journal of Orthopaedic Research, 14(3), pp.424–432.

Xiao, Y. et al., 2013. Mechanical testing of hydrogels in cartilage tissue engineering: beyond the compressive modulus. Tissue engineering.Part B, Reviews, 19(5), pp.403–412.

Zhang, C. et al., 2011. Oligo(trimethylene carbonate)-poly(ethylene glycol)-oligo(trimethylene carbonate) triblock-based hydrogels for cartilage tissue engineering. Acta Biomaterialia, 7(9), pp.3362–3369. Available at: http://dx.doi.org/10.1016/j.actbio.2011.05.024.

Zhang, Z. et al., 2006. The in vivo and in vitro degradation behavior of poly(trimethylene carbonate). Biomaterials, 27(9), pp.1741–1748.

Zhao, Y., Waldman, S. & Flynn, L., 2013. Multilineage Co-culture of Adipose-derived Stem Cells for Tissue Engineering. Journal of Tissue Engineering and Regenerative Medicine.

Zhao, Y., Waldman, S.D. & Flynn, L.E., 2012. The effect of serial passaging on the proliferation and differentiation of bovine adipose-derived stem cells. Cells Tissues Organs, 195, pp.414–427.

Zhu, J., 2010. Bioactive modification of poly(ethylene glycol) hydrogels for tissue engineering. Biomaterials, 31(17), pp.4639–4656. Available at: http://dx.doi.org/10.1016/j.biomaterials.2010.02.044.

Zhu, K. et al., 1991. Synthesis, properties, and biodegradation of poly (1, 3-trimethylene carbonate). Macromolecules, 24(8), pp.1736–1740.

Zuk, P.A. et al., 2002. Human Adipose Tissue is a Source of Multipotent Stem Cells. Molecular Biology of the Cell, 13(December), pp.4279–4295.

Zwingmann, J. et al., 2007. Chondrogenic differentiation of human articular chondrocytes differs in biodegradable PGA/PLA scaffolds. Tissue Engineering, 13(9), pp.2335–2343.

Appendix A

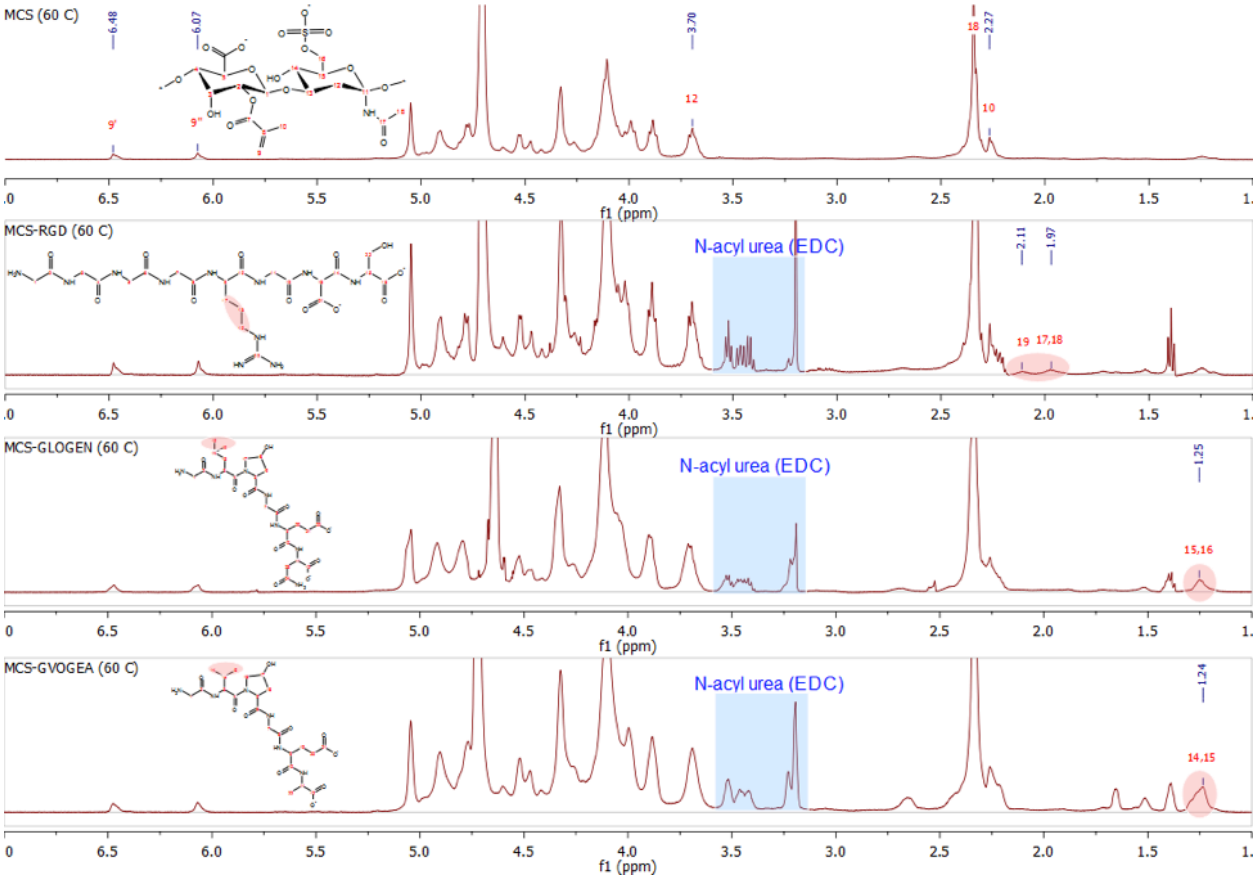

Figure 0.1: ^{1}H NMR spectra of MCS and GGGGGRGDS, GLOGEN, and GVOGEA conjugated MCS with relevant peak assignments.